

Adaptive Modulation & Coding-Based Packet Scheduling with Inter-Base Station Coordination in Fixed Cellular Broadband Wireless Networks

By

Md. Mahmudur Rahman

A thesis submitted to
the Faculty of Graduate Studies and Research
in partial fulfillment of
the requirements of the degree of
Master of Applied Science

Ottawa-Carleton Institute for Electrical and Computer Engineering
Department of Systems and Computer Engineering
Carleton University
Ottawa, Ontario

©Copyright 2004, Md. Mahmudur Rahman

The undersigned hereby recommended to the Faculty of Graduate Studies and Research acceptance of the thesis

Adaptive Modulation & Coding-Based Packet Scheduling with Inter-Base Station Coordination in Fixed Cellular Broadband Wireless Networks

Submitted by Md. Mahmudur Rahman
In partial fulfillment of the requirements for the
Degree of Master of Applied Science

Thesis Co-Supervisor
Professor Halim Yanikomeroglu

Thesis Co-Supervisor
Professor Samy A. Mahmoud

Chair, Department of Systems and Computer Engineering
Professor Rafik A. Goubran

Carleton University
May 2004

Abstract

This thesis is about packet scheduling in wireless networks. We considered a broadband cellular fixed wireless access network with an aggressive channel reuse of 1 (more specifically, the reuse is $1/6$ as each cell is composed of 6 sectors). Certain interference management/avoidance techniques have to be used when such an aggressive channel reuse scheme is employed. Towards that end, a number of packet scheduling schemes based on inter-base station (and thus, inter-sector) coordination have been proposed in the literature in recent years. One recent study [23] proposes a dynamic time slot allocation scheme which avoids concurrent transmissions in “interference groups” (the interference group for a sector is composed of those sectors which cause the most interference to the sector at hand).

In this thesis, we have first refined the scheduling discipline proposed in [23] in various ways, most notably by incorporating adaptive modulation and coding (AMC) to improve the throughput; we refer to this case as the IIS-AMC-ST (intra and inter-sector scheduling with adaptive modulation and coding: single transmission) scheme. We compared the performance of the IIS-AMC-ST scheduling discipline with that of the reference IIS-FM-ST (intra and inter-sector scheduling with fixed modulation: single transmission) discipline, and we showed that significant enhancements are achievable in net throughput, area spectral efficiency, rate of the dropped packets in the scheduler queues, and end-to-end delay. The IIS-AMC-ST scheduling discipline is the first major contribution in this thesis.

Delay is an essential factor in delay-sensitive applications as such a packet in the scheduler queue gets dropped if the delay in the queue exceeds a threshold value. Although the delay performance of the IIS-AMC-ST scheme is better than that of the reference IIS-FM-ST scheme, the orthogonal transmissions in an interference group (composed of a sector and two other sectors which cause the most interference to this sector) nevertheless cause some packets wait too long in the queues; such packets are eventually dropped. This observation is actually valid for all orthogonal scheduling disciplines proposed in the literature.

The other (and perhaps more significant) major contribution of this thesis is the development of a novel scheduling discipline called IIS-AMC-MT (intra and inter-sector scheduling with adaptive modulation and coding: multiple transmissions) which allows multiple transmissions in an interference group in a controlled manner. Basically, if the aggregate spectral efficiency is predicted to be higher when two or three sectors in the interference group transmit concurrently, then this multi-transmission mode is chosen. By this way the aggregate throughput is further increased, the end-to-end delay is further reduced, and the packet dropping rate in the scheduler queues is also further decreased in comparison to the IIS-AMC-ST scheme.

The performances of all three scheduling disciplines (IIS-FM-ST, IIS-AMC-ST, and IIS-AMC-MT) are analyzed with a realistic packet-level simulation. The effects of some system parameters, such as the user terminal directional antenna beamwidth, on the interference management are studied as well.

Since the IIS-AMC-ST discipline, and especially the IIS-AMC-MT discipline, both require some link gain information exchange across sectors (as well as sector traffic information), they might be more suitable for fixed cellular wireless applications where the link gains change very slowly. However, the concept of IIS-AMC-MT scheduling discipline is general and can be applied in mobile wireless networks as well if the required inter-BS signaling happens to be feasible.

Acknowledgement

I would like to express my heartfelt gratitude to my supervisors Prof. Halim Yanikomeroglu and Prof. Samy A. Mahmoud for their continuing support and invaluable guidance to make this thesis a successful endeavor. I extend my cordial thanks to Prof. Yanikomeroglu for his valuable time and friendly yet highly motivational professional advice that he always has offered to me. I am deeply indebted to Prof. M. Hossam Ahmed at Memorial University for his fruitful suggestions, valuable opinions and comments at different stages during the course of this thesis.

I am grateful to Mr. Narendra Mehta for his technical supports not only in buying the fastest possible computer terminal for me but also in installing and maintaining OPNET simulation tool for my research. I thank OPNET Inc. for providing educational license to carry out simulations for this thesis.

I am thankful to National Capital Institute for Telecommunications (NCIT) for funding this research partially.

Finally, I thank my wife, little daughter, friends and colleagues for their encouragements and moral supports. This thesis is lovingly dedicated to my lovely daughter Prianna Rahman who had to sacrifice a lot of her playtime for this thesis.

Table of Contents

Abstract	iii
Acknowledgement	v
Table of Contents	vi
List of Figure and Tables	viii
List of Acronyms	xi
List of Symbols	xiv
Chapter 1 INTRODUCTION	1
1.1 Thesis Motivation	2
1.2 Thesis Objectives	4
1.3 Thesis Organization	5
Chapter 2 LITERATURE REVIEW	6
2.1 Introduction	6
2.2 Scheduling	6
2.2.1 Scheduling in Wired Networks	7
2.2.2 Scheduling in Wireless Networks	9
2.2.2.1 Channel Condition Dependent Packet Scheduling	10
2.2.2.2 Fair Queuing Based Wireless Packet Scheduling	12
2.2.3 Scheduling in Fixed Broadband Wireless Access Networks	15
2.3 Network Assisted Resource Allocations	19
2.4 Adaptive Modulation and Coding	20
2.5 Summary of Review and Problem Formulation	23
Chapter 3 SYSTEM MODELS AND METHODOLOGIES	25
3.1 Introduction	25
3.2 Network Related Models	25
3.2.1 Channel Model	25
3.2.1.1 Large Scale Path Loss Model	26
3.2.1.2 Shadowing	28
3.2.1.3 Fading	28
3.2.2 Background Noise Model	34
3.2.3 Traffic Model	34
3.2.4 Delay Model	37
3.2.5 Packet Error Rate and Error Correction Model	37
3.3 Algorithm Related Models	39
3.3.1 Wraparound Interference Model	39
3.3.2 Base Station Coordination	41
3.3.3 Adaptive Modulation and Coding Modes	41
3.4 Overview on Simulated Scheduling Schemes	43
3.4.1 Implementation Issues of the Schemes	44
3.4.2 Overview on Inter-sector Schedulers and Slot	

	Allocations	47
Chapter 4	INSIGHT INTO SIMULATED SCHEDULING SCHEMES	54
	4.1 Introduction	54
	4.2 Framework for SINR Computation	54
	4.3 Base Station Information Exchange	58
	4.4 SINR Prediction	59
	4.5 Scheduling Decision	60
	4.5.1 IIS-FM-ST	60
	4.5.2 IIS-AMC-ST	60
	4.5.3 IIS-AMC-MT	61
	4.6 Effect of Out-of-Group Interferers and Compensation	66
Chapter 5	SIMULATION RESULTS AND ANALYSIS	68
	5.1 Introduction	68
	5.2 System Parameters and Performance Metrics	69
	5.3 Key Observations	71
	5.4 Results for 60 ⁰ Directional Antenna Both at Sector and User Stations	74
	5.4.1 Packet Error Rate (PER)	74
	5.4.2 Area Spectral Efficiency and Net Throughput	77
	5.4.3 50 th -Percentile End-to-End Delay and Dropped Packets	80
	5.5 Performance Results for 60 ⁰ Beamwidth Sector Antenna and 30 ⁰ Beamwidth User Antenna.....	83
	5.6 Results for 30 ⁰ Beamwidth User Antenna with Out-of-Group Interference Compensation Guards in IIS-AMC-ST and IIS-AMC-MT	89
	5.7 Exclusive Comparison between IIS-AMC-ST and IIS-AMC-MT.....	97
Chapter 6	CONCLUSIONS AND FUTURE WORKS	104
	6.1 Summary on Findings	104
	6.2 Thesis Contributions	105
	6.3 Recommendation for Future Works	106
References		108
Appendix A	Finding Wraparound Interference Positions.....	112
Appendix B	Link Budget Calculation	118
Appendix C	Additional Curves for the System with Propagation Exponent of 3.7.....	120

List of Figures and Tables

Figure 2.1	Staggered resource allocation	16
Figure 2.2	Enhanced staggered resource allocation	18
Figure 3.1	Rounded Doppler power spectral density	29
Figure 3.2	Instantaneous power of fading envelope	31
Figure 3.3	Comparison of CDF of envelope power of simulated and theoretical Rayleigh fading	32
Figure 3.4	Time correlation of the fading samples	33
Figure 3.5	2IRP video traffic model	35
Figure 3.6	State diagram of interrupted renewal process	35
Table 3.1	Traffic model parameters of the video stream	36
Figure 3.7	Calculation of segmented SINR in a packet	38
Figure 3.8	Simulated nine-cell network	40
Figure 3.9	Wraparound interferer positions for users in BS1, BS2 and BS3	40
Figure 3.10	Adaptive modulation and coding modes	42
Table 3.2	Lookup table for adaptive modulation and coding modes	43
Figure 3.11	Block diagram of intra and inter-sector scheduling	45
Figure 3.12	Group-wise orthogonal slot allocations	46
Figure 3.13	Decision instant and decision region in IIS-AMC-MT	47
Figure 3.14	Flow diagram of inter-sector scheduler in IIS-FM-ST	49
Figure 3.15	Flow diagram of inter-sector scheduler in IIS-AMC-ST	51
Figure 3.16	Flow diagram of inter-sector scheduler in IIS-AMC-MT	53
Figure 4.1	Link gains to desired user	56
Table 5.1	System parameters	69
Figure 5.1	Probability mass function (PMF) of AMC modes used by IIS-AMC-ST and IIS-AMC-MT	72
Figure 5.2	Percentage of one, two, and three transmissions per group in IIS-AMC-MT	73
Figure 5.3	Packet error rate in different schemes	

	(60 ⁰ sector antenna and 60 ⁰ user antenna)	74
Figure 5.4	Probability mass function of number of out-of-group interferers appear per packet at loading 4 users per sector	75
Figure 5.5	Probability mass function of number of out-of-group interferers appear per packet at loading 16 users per sector	77
Figure 5.6	Area spectral efficiency in different schemes (60 ⁰ sector antenna and 60 ⁰ user antenna)	78
Figure 5.7	Net throughput in different schemes (60 ⁰ sector antenna and 60 ⁰ user antenna)	79
Figure 5.8	50 th -Percentile End-to-End packet delay in different schemes (60 ⁰ sector antenna and 60 ⁰ user antenna)	80
Figure 5.9	Dropped packets by scheduler in different schemes (60 ⁰ sector antenna and 60 ⁰ user antenna)	83
Figure 5.10	Packet error rate comparison for 60 ⁰ and 30 ⁰ beamwidth user antenna	84
Figure 5.11	Area spectral efficiency improvements for 30 ⁰ beamwidth user antenna	85
Figure 5.12	Comparison of multiple transmission decisions in IIS-AMC-MT for 60 ⁰ and 30 ⁰ beamwidth user antennas	86
Figure 5.13	Net throughput improvements for 30 ⁰ beamwidth user antenna	87
Figure 5.14	ETE delay improvements in IIS-AMC-MT due to 30 ⁰ beamwidth user antenna	88
Figure 5.15	Packet dropping improvements in IIS-AMC-MT for 30 ⁰ beamwidth user antenna	89
Table 5.2	Out-of-group interference compensation guard	90
Figure 5.16	Packet error rate improvements due to out-of-group interference compensation for adaptive modulation schemes	91
Figure 5.17	Effect of out-of-group interference compensation on area spectral efficiency	92
Figure 5.18	Effect of compensation guard on AMC mode selections in IIS-AMC-ST (24 users per sector)	93
Figure 5.19	Effect of compensation guard on AMC mode selections in IIS-AMC-MT (24 users per sector)	94

Figure 5.20	Effect of out-of-group interference compensation on net throughput	95
Figure 5.21	Effect of out-of-group interference compensation on dropped packets	96
Figure 5.22	Effect of out-of-group interference compensation on packet delay	97
Figure 5.23	CDF of received interference in IIS-AMC-MT (for $n = 3.0$ and $n = 3.7$) (12 users/sector; 60^0 sector and 30^0 user antennas; no compensation)....	98
Figure 5.24	Packet error rates in IIS-AMC-ST and IIS-AMC-MT for $n = 3.7$	100
Figure 5.25	Area spectral efficiency in IIS-AMC-ST and IIS-AMC-MT for $n = 3.7$	101
Figure 5.26	Net throughput in IIS-AMC-ST and IIS-AMC-MT for $n = 3.7$	101
Figure 5.27	ETE delay in IIS-AMC-ST and IIS-AMC-MT for $n = 3.7$	102
Figure 5.28	Queue dropped packets in IIS-AMC-ST and IIS-AMC-MT for $n = 3.7$	103
Figure A.1	Finding BS7 interferer location for users in BS3	113
Figure A.2	Wraparound interferer positions for users in BS3	114
Figure A.3	2-Tier interference pattern for users in BS10 (60^0 directional user antenna)	115
Figure A.4	2-Tier interference pattern for users in BS10 (30^0 directional user antenna)	116
Figure B.1	Packet error rate for a user at cell boundary against simulation time (no interference is present)	119
Figure C.1	Percentage of multiple transmission decisions in IIS-AMC-MT ($n = 3.7$)	120
Figure C.2	PMF of AMC modes in IIS-AMC-ST and IIS-AMC-MT (12 users per sector, $n = 3.7$)	120

List of Acronyms

ACK	Acknowledgement
ADSL	Asymmetric Digital Subscriber Loop
AMC	Adaptive Modulation and Coding
ASE	Area Spectral Efficiency
AWGN	Additive White Gaussian Noise
BER	Bit Error Rate
BICM	Bit-Interleaved Coded Modulation
BPSK	Binary Phase Shift Keying
BS	Base Station
CBQ	Class Based Queuing
CDF	Cumulative Distribution Function
CDPA	Capture Division Packet Access
CIF-Q	Channel-condition Independent Fair Queuing
CSDPS	Channel State Dependent Packet Scheduling
CSI	Channel State Information
dB	decibel
dBW	dB watts
DCA	Dynamic Channel Allocation
DRR	Deficit Round Robin
EDF	Earliest Deadline First
ESRA	Enhanced Staggered Resource Allocation
ETE	End-to-End
ETF	Earliest Timestamp First
FBWA	Fixed Broadband Wireless Access
FCFS	First Come First Serve
FDD	Frequency Division Duplex
FEC	Forward Error Correction
FFQ	Fluid Fair Queuing
GHz	Gigahertz

GPS	Generalized Processor Sharing
HFC	Hybrid Fiber-Coax
HOL	Head of Line
Hz	Hertz
IEEE	Institute of Electrical and Electronics Engineers
IFFT	Inverse Fast Fourier Transform
IG	In-Group
IIS-AMC-MT	Intra and Inter-sector Scheduling with AMC: Multiple Transmissions
IIS-AMC-ST	Intra and Inter-sector Scheduling with AMC: Single Transmission
IIS-FM-ST	Intra and Inter-sector Scheduling with Fixed Modulation: Single Transmission
IPP	Interrupted Poisson Process
IRP	Interrupted Renewal Process
IWFQ	Idealized Wireless Fair Queuing
LAN	Local Area Network
LQF	Longest Queue First
LSM	Link Status Monitor
MAC	Medium Access Control
MHz	Megahertz
M-QAM	M-arry Quadrature Amplitude Modulation
NF	Noise Figure
OG	Out-of-Group
PDF	Probability Density Function
PER	Packet Error Rate
PL	Path Loss
PMF	Probability Mass Function
PSD	Power Spectral Density
QoS	Quality of Service
QPSK	Quadrature Phase Shift Keying
QRA-IA	Quasi-static Resource Allocation with Interference Avoidance
RR	Round Robin

SCFQ	Self-Clocked Fair Queuing
SFQ	Start-time Fair Queuing
SINR	Signal to Interference plus Noise Ratio
SNR	Signal to Noise Ratio
SRA	Staggered Resource Allocation
TCP	Transport Control Protocol
TDMA	Time Division Multiple Access
T-R	Transmitter to Receiver
WF ² Q	Worst-case Fair Weighted Fair Queuing
WFQ	Weighted Fair Queuing
WRR	Weighted Round Robin

List of symbols

\bar{p}	Average envelope power of received signal
P_N^i	Average thermal noise power at user i
L_p^i	Length of user i 's packet
G_J^i	Link gain from user i to interferer sector J
G_I^i	Link gain from user i to own sector I
t_d^i	Packet transmission delay for user i 's packet
$\gamma_{(i)}$	SINR in segment i of a packet
π	Constant, 3.141592654
α	Parameter used for graceful degradation
ρ	Pareto parameter for location
β	Pareto parameter for shape
Λ	Traffic arrival rate
λ	Wavelength
$\phi(l)$	Compensation guard in dB as a function of loading l
β_1	Pareto parameter for ON time distribution
β_2	Pareto parameter for OFF time distribution
η_I	Modulation efficiency (bps/Hz) of sector I 's transmission
$\mu_{off \rightarrow on}$	State transition rate from OFF to ON
$\mu_{on \rightarrow off}$	State transition rate from ON to OFF
ΔPL_f	Frequency correction factor in path-loss calculation
ΔPL_h	Receiver antenna height correction factor in path-loss calculation
A	Set of all active flows
B	Channel bandwidth
C	Boltzman's constant
d	Propagation distance
d_0	Reference distance
f	Operating frequency
f_m	Maximum Doppler frequency
F_p	CDF of envelope power

f_p	PDF of envelope power
h_r	Receiver antenna height
Lag_i	Measure of service session i received
L_p	Packet length
L_{pq}	Packet length for q^{th} packet
M	M-ary modulation
N	Number of samples to represent Doppler spectrum
n	Propagation exponent
$N_{b(i)}$	Number of bits in error in segment i
N_e	Number of bit errors in a packet
p	Instantaneous power of Rayleigh envelope
P_I	Transmit power of base station I
PL	Path loss in dB
PL_{fs}	Free space path loss
$Pr_{b(i)}$	Probability of bit error in segment i
Pr_{off}	Probability being OFF state
Pr_{on}	Probability being ON state
r	Rayleigh variable
r_c	Coding rate
r_s	Symbol rate
S	Real system
$S(f)$	Power spectral density
S'	Reference ideal system
SR_i	Service rate for session i
T	Ambient temperature
t_{aq}	Arrival time of q^{th} packet
T_c	Coherence time
t_d	Packet transmission delay
T_{fd}	Fading samples simulation time
T_{off}	Mean dwell time on OFF state
T_{on}	Mean dwell time on ON state
w	Scheduler selected sector

X_σ	Log-normal shadow variable
x_1	In-phase component of Rayleigh variable
x_2	Quadrature phase component of Rayleigh variable
Γ_w	Overall spectral efficiency for concurrent transmission of w sectors

Chapter 1

Introduction

Fixed broadband wireless access (FBWA) [1, 2] is a promising alternative to existing copper line *asymmetric digital subscriber loop* (ADSL) [3, 4] or *hybrid fiber-coaxial* (HFC) [5] cable broadband services that has drawn tremendous attention recently in research and industry. The remarkable advantage of FBWA is its ability to provide access without extensive installation of copper or fiber infrastructures. However, efficient system planning and resource allocation policies are warranted for such systems, because in addition to the challenges posed by the dynamic nature of wireless links, interference resulting from aggressive frequency reuse is a major design concern in FBWA.

We propose two novel scheduling schemes that consider interference management issues, integrate adaptive modulation and coding (AMC), and take channel state based scheduling decisions to enhance network performance. We name these two schemes as **IIS-AMC-ST** (intra and inter-sector scheduling with adaptive modulation and coding: single transmission) and **IIS-AMC-MT** (intra and inter-sector scheduling with adaptive modulation and coding: multiple transmissions). A group of base stations that are dominant interferers for each other's downlink transmissions form an *interferer group*, and exchange traffic and link related information to facilitate scheduling operations. Therefore, inter-base station signaling is an essential part in these schemes. IIS-AMC-MT permits simultaneous multiple packet transmissions in an interferer group, while transmissions in IIS-AMC-ST are orthogonal in time. The performance results of these schemes are compared with the results obtained from a reference scheduling scheme that

uses fixed modulation, namely **IIS-FM-ST** (intra and inter-sector scheduling with fixed modulation: single transmission), which is adapted from [23].

1.1 Thesis Motivation

Scheduling techniques designed for wired networks [6-10] are not suitable for wireless systems as wireless channel quality varies in time, frequency and locations due to fading, shadowing, noise etc. Consequently, unlike wired media, the capacity of wireless channels is variable. Wireless scheduling techniques have emerged as versions of wireline scheduling schemes tailored to cope with wireless link variability [12-14, 16, 17]. Scheduling in fixed broadband wireless networks require further attention to manage interference as these systems are highly prone to co-channel interference resulting from dense reuse of frequency. Therefore, it is common to consider the issues of interference management as an integral part of scheduling techniques in FBWA networks [19, 20, 22-25]. A very effective means of managing interference is to employ coordinated transmissions among dominant interferers achieved by inter-BS signaling [23-25, 27]. The main idea of these schemes is to schedule traffic in such a way that it avoids dominant interferers. M.H. Ahmed et al. [23-25] have proposed intra and inter-sector scheduling techniques in fixed broadband wireless access networks, where a group (termed as *interferer group*) of BSs exchanges traffic related information; coordinated inter-sector scheduling is performed so that transmissions in an interferer group are orthogonal in time. At any instant, the arrival times of the *head of the line* (HOL) packets of in-group sectors are compared by the inter-sector scheduler and the service opportunity is given to the sector which has the earliest arrival time. Base station coordination in these schemes successfully reduces co-channel interference and improves packet error

rates while sacrificing packet delay as only one BS among the *interferer group* transmits at any instant.

Packet delay is an important *quality of service* (QoS) parameter for a variety of delay-sensitive applications which is directly related to the throughput for a given traffic rate. Therefore, improving throughput and delay in an orthogonal scheduling scheme is essential. The benefits of integration of AMC with scheduling decisions in IIS-AMC-ST are expected to provide enhanced throughput and delay performance in comparison to IIS-FM-ST. The inter-sector scheduler in IIS-AMC-ST gives service opportunity to the sector having the best link to the user intending to receive its HOL packet. The performances can further be enhanced when controlled multiple transmissions in the interferer group are permitted as in IIS-AMC-MT. If the aggregate throughput of simultaneous transmissions (from two or three sectors) is predicted to be higher than single transmission, multiple transmissions will take place.

Improving packet delay has another significance besides QoS, which is related to the queue management issues. Packets that wait too long in the transmitter queue not only become useless (especially for real-time traffic) for users when received but also overflow the transmitter queue. Therefore, it is common to drop severely delayed packets to avoid queue overflow as well as to save resources by not transmitting these packets susceptible to be useless to the receiver. The decreased packet delay in IIS-AMC-ST is expected to provide fewer packet drops from the transmitter queue in comparison to IIS-FM-ST. IIS-AMC-MT would be able to reduce the packet dropping rates further because of its enhanced delay performance than that of IIS-AMC-ST.

1.2 Thesis Objectives

The primary objective of this thesis is to introduce novel scheduling techniques that take channel state dependent scheduling decisions and integrate AMC to provide enhanced throughput, spectral efficiency, packet delay, and packet dropping rate in traditional orthogonal packet scheduling schemes designed for FBWA networks.

We summarize the objectives of this thesis as below:

1. To integrate AMC with scheduling techniques and observe network performance improvements in terms of throughput, area spectral efficiency, end-to-end packet delay, and packet dropping rate.
2. To observe the performance enhancements when concurrent transmissions in the interferer group are allowed (if found to be more efficient than single transmission) instead of conservative interference avoidance approaches.
3. To introduce novel scheduling decision algorithms that utilize link state information from inter-BS signaling in IIS-AMC-ST and IIS-AMC-MT.
4. To observe the impact of out-of-group interference on network performance by varying the beamwidth of directional user antennas, and by considering out-of-group interference compensation guard in the scheduling decision process (discussed in Chapter 4).

1.3 Thesis Organization

Chapter 2 presents discussions on relevant literature associated with various aspects of this thesis. Scheduling, AMC, and inter-BS signaling are three building blocks of the research carried out in this thesis. A summary of these discussions is given at the end of Chapter 2 followed by problem formulation. We present various models and sub-models in Chapter 3. These models are categorized into two major classes such as network related models and algorithm related models. Network related models include propagation, traffic, delay and packet error rate models etc. Wrap-around interference, adaptive modulation and inter-BS signaling are modeled under the category of algorithm related models. An overview on the simulated scheduling schemes is given at the end of Chapter 3. We look deeper into the scheduling schemes in Chapter 4, where some intuitive analytical discussions for all simulated schemes are sketched. In Chapter 5, performance of the simulation schemes are presented and compared to quantify the benefits of integration of AMC with scheduling, and also to observe performance enhancements when in-group interferers are allowed to transmit simultaneously. Chapter 6 concludes the thesis and points out relevant future research that can be done by extending the ideas and schemes developed in this thesis.

Chapter 2

Literature Review

2.1 Introduction

In this chapter of the thesis, overview on literature relevant to various aspects of this study, such as wireless scheduling (specially, in fixed broadband wireless access networks), BS information exchange, and AMC is presented.

To cope with the variability of link quality, wireless scheduling demands some special considerations to achieve *fairness* compared to traditional scheduling in wired media. A brief review on wired and wireless scheduling followed by scheduling techniques proposed for fixed broadband wireless networks are provided in Section 2.2. Network assisted resource allocation using inter-BS signaling has been an attractive approach to optimize the available resources in the network. Literature review on inter-BS signaling is presented in Section 2.3. Adaptive modulation and coding is an appealing means to improve network throughput efficiency in any wireless systems. A few key literatures on AMC are surveyed in Section 2.4. Section 2.5 summarizes the review and sketches foundations for the problems that are addressed in this thesis.

2.2 Scheduling

Scheduling, in general, is a term that must be addressed when a multiplexed resource is shared among many entities. More specifically, in telecommunications, scheduling is used to allocate different resources to different users according to user demands or classes. The aim of a scheduling algorithm is to assure performance guarantee of the system such as delay and throughput, and fairness among different services so that the

available resources are utilized efficiently. Scheduler looks at three basic management decisions; i) which packets to serve (transmit), ii) when to transmit, and iii) which packet to discard in case of buffer overflow or excessive delay. These three decisions in turn affect major network performance parameters such as throughput, end-to-end delay and loss rate.

However, wireless scheduling has to be different from the scheduling techniques used in wired networks because of their difference in channel characteristics.

2.2.1 Scheduling in Wired Networks

The simplest scheduling is *First Come First Serve* (FCFS) discipline. In this case, incoming packets are tagged according to their arrival time and inserted into the tail of the service queue. When the server is free, the packet with earliest arrival time is taken from the queue and served. This discipline is easy to implement as it requires a single service queue. Arriving packets can be inserted into the queue at the tail and served from the head of the queue.

The main weakness of FCFS is that, a misbehaving source with an unusually higher rate may cause excessive delay for other sources sharing same resources. Another limitation is that FCFS can not differentiate between sources and all sources are treated equally although sometimes it might be necessary to expedite some users over others. If the data rates for all users are similar and all users belong to same service class, then FCFS is a good choice to implement, that ensure fairness among all users.

The *Round Robin* (RR) is another type of scheduling techniques where a misbehaving source can not harm other sources. Each source has different service queue and the server visits each non-empty queue in turn. The *Weighted Round Robin* (WRR) is proposed by M. Katevenis et al. in [6]. This is a variation of basic RR, and it guarantees services of different sources with different rates, by serving required portions according to their weights. The server of weighted round robin should have knowledge of the mean packet size of the source to allocate the bandwidth fairly.

M. Shreedhar and G. Verghese modeled another discipline in [7] named *Deficit Round Robin* (DRR) that can handle variable packet size without knowing the mean packet size of the source. The server visits each source's queue and serves one *quantum* worth of bits from each source at every turn. The packet at the head of the queue will only be served when the packet size is no larger than the quantum size, else the packet will not be served and one quantum worth of bits will be added to source's *deficit counter*. When that packet size is less than or equal to the sum of the deficit counter and quantum size, the packet will be served.

Weighted Fair Queuing (WFQ) is a pioneer fair queuing packet scheduling scheme proposed by A. Demers et al. [8] that ensures end-to-end delay and fairness among different sources. WFQ emulates *Generalized Processor Sharing* (GPS) or *Fluid Fair Queuing* (FFQ) in the sense that for every arriving packet a *finish number* is computed that represents the time required to finish serving the packet using GPS discipline. This finish number is a priority tag that determines the service order of the packet. The nice feature of this fair queuing scheme is that it provides real-time performance guarantee which is the key requirement for guaranteed service connections. J.C.R Bennett and H.

Zhang proposed *Worst-case-Fair-WFQ* (WF²Q) [9], another packet fair scheduling algorithm, that gives a better fairness bound than that of WFQ with equal end-to-end worst case delay, thus it is a closer emulation of FFQ. In addition to *finish time* this also takes *start time* to compute the service priority of packets. Both WFQ and WF²Q use reference time from a parallel reference FFQ system, which requires computational overhead. To alleviate such computational burden *Self-Clocked Fair Queuing* (SCFQ) was proposed by S. J. Golestani in [10], where an internally generated *virtual time* is used to determine service priority. The author showed that the end-to-end delay for SCFQ was bounded and comparable to that of any other packet fair queuing schemes, while the computation complexity was greatly reduced.

A comprehensive overview on various scheduling disciplines for packet networks can be found in [11] authored by H. Zhang.

2.2.2 Scheduling in Wireless Networks

The scheduling disciplines discussed above are not directly applicable to wireless networks as wireless channel characteristics are completely different than that of wired channel posing following concerns:

1. Wireless media is more prone to errors and the errors usually occur in bursts.
2. Wireless channel capacity is variable and location dependent because of interference, fading and shadowing.
3. Wireless bandwidth is scarce.
4. Mobility of users gives more dynamics and variability in the system (in case of mobile networks).

5. Power constraint for mobile terminals (in case of mobile networks)

Any scheduling algorithm designed for wireless system should consider the above factors to achieve service guarantees and fairness. The literature on wireless scheduling techniques can be categorized into the following classes:

- Channel condition dependent packet scheduling
- Fair queuing based wireless packet scheduling

2.2.2.1 Channel Condition Dependent Packet Scheduling

As errors in wireless networks occur in bursts, link layer packet retransmission attempts become unsuccessful, and these result in poor utilization of wireless channel. One remedy to alleviate this problem is to defer the transmissions of a weak link until it gets better. Scheduling techniques that address this issue are called *channel state dependent packet scheduling* (CSDPS) techniques. One of the earliest studies by P. Bhagwat et al. [12] showed that CSDPS can improve the throughput significantly compared to a simple FCFS discipline. This study has been carried out on a wireless LAN system. An entity, named *link status monitor* (LSM) is defined that is responsible to monitor the link between the BS and each mobile terminal. LSM detects burst error when the *medium access control* (MAC) layer *acknowledgement* (ACK) is not received for any mobile terminal. LSM marks the queue, and packets from that queue will not be transmitted for a period of estimated burst error time. The authors simulated CSDPS for three scheduling policies, i.e., *Round Robin* (RR), *Earliest Timestamp First* (ETF), and *Longest Queue*

First (LQF). Results show that 10-15% improvement in link utilization can be obtained using CSDPS.

An experimental evaluation of CSDPS has been investigated in [13] by S. Desilva and S.R. Das, where CSDPS is implemented in a commercial wireless LAN (IEEE 802.11). The outcomes of this experiment are as follows: better overall bandwidth usage by saving the bandwidth that would otherwise be wasted on dropped packets and 20-50% faster TCP session compared to FCFS queue without CSDPS.

While above CSDPS improves network throughput, it does not provide fairness among different users. Due to variability of the link quality some users transmission will have to be deferred for certain amount of time. During this time other users with good links will be given opportunity to use resources while they might have already enjoyed more than their fair share. To resolve this issue a *class-based queuing* (CBQ) is combined with CSDPS in [14] by C. Fragouli et al. CBQ is a hierarchical link sharing model proposed in [15] which ensures that users of a particular class of service receive their allocated fair service in a predefined time. CBQ does accounting of the amount of service received by a certain class in a certain time period. A particular class that receives more than its allocated share is marked as a *satisfied* class, and a class that suffers persistent backlog is tagged as an *unsatisfied* class. CBQ prohibits a satisfied class to receive services, and rather a satisfied class will have to sacrifice their services to the unsatisfied class. In [14], the CBQ part deals with the fairness issue while CSDPS takes care the link variability of the wireless channel.

2.2.2.2 Fair Queuing Based Wireless Packet Scheduling

Fair queuing model such as WFQ and its variants are not directly applicable to wireless systems as mentioned earlier. *Idealized Wireless Fair Queuing* (IWFQ) is proposed by S. Lu et al. [16] and adapted from wired WFQ by taking wireless channel quality and capacity variations into account. An IWFQ model is defined which works in parallel with a reference error free WFQ service system. Packet priority (such as *finish time*) is calculated with respect to ideal WFQ systems and packets are transmitted from IWFQ queue according to the priorities. At any time, the service received by a flow in the IWFQ system is compared with that of the error free system. A queue is marked as *leading*, *lagging*, or *in sync* if its size is smaller than, larger than, or the same as the size of the error free system, respectively. When a packet with smallest finish time can not be transmitted because of the bad link, the packet from another queue with next smallest finish time will be transmitted. The finish time tags are not changed after packet arrival; therefore a deferred queue that loses its service opportunity will have packets with smaller finish times, compared with other queue's packets. When the link recovers from error state, its packets will get priority in getting services. Therefore, IWFQ assures compensation guarantee for a recovered link. IWFQ defines bounded compensation for lagging sessions such that summation of compensation for all sessions does not exceed a predefined number of bits. Also, the amount of service a leading session sacrifice is bounded. Therefore, the compensation for lagging sessions and sacrifice for leading sessions are bounded. This scheme provides fairness and QoS guarantee, but it has a weakness point. The service priority is given to the packets with smallest finish times; when a session is being compensated for its previously lagged status all other error free

sessions will not be served at all. As a result, a lagging session might receive compensation at a rate independent of its allocated share, which violates the semantics that a larger guaranteed rate should imply better QoS.

Another wireless fair queuing algorithm that works in parallel with an ideal WFQ system is termed as *channel-condition independent packet fair queuing* (CIF-Q) studied in [17] by T.S.E. Ng et al., which is very similar to IWFQ. Start-time Fair Queuing (SFQ) has been chosen as an ideal system to which CIF-Q is compared to compute the priorities for the arriving packets for different flows. CIF-Q emphasizes on fairness issue and states guidelines for designing a fairness mechanism in wireless scheduling. The objectives of the CIF-Q are as follows:

1. Delay bound and throughput guarantees: Delay bound and throughput should be guaranteed and should not be affected by other lagging sessions that are in error state.
2. Long term fairness: When an errored session exits from error it should be able gain its lost service as long as it has enough service demand.
3. Short term fairness: During any time interval, the difference in services between any two backlogged, leading or satisfied sessions should be bounded.
4. Graceful degradation: A leading backlogged session should be guaranteed to receive at least a minimum fraction of its service it would receive in an error free system, during any time interval while it is error free.

Similar to IWFQ in CIF-Q, the error-prone real system (S) is associated with an ideal reference system (S'). Arrived packets are inserted into the queues of S and S' . Packet

priorities are determined using SFQ in S^r and packets are transmitted from S . When there is no link error in S , chosen packet in S^r is served both in S and S^r . When there is a link error, real packet in S can not be served, but the virtual packet in S^r is served and corresponding flow's virtual time is updated in S^r . A parameter lag is defined that keeps track the difference in service between S and S^r . An active session i is called *lagging*, *leading* or *satisfied* when lag_i is positive, negative, or zero, respectively. The algorithm maintains the following for all active sessions:

$$\sum_{i \in A} lag_i = 0$$

where A is the set of all active flows. To assure graceful degradation, a leading flow receives service at a minimal rate which is determined by a configurable parameter α . A leading session i is allowed to continue to receive service at a rate of $\alpha \times SR_i$, where SR_i is the allocated service. The remaining share of the service rate should be given up for lagging sessions.

In particular, the following four rules must be followed to achieve four objectives of this algorithm.

1. Scheduler schedules the packet based on smallest *virtual start time*. A packet is chosen in S^r and corresponding packet from S is transmitted unless one of the following happens.
 - a. The link the packet to be transmitted over is on error
 - b. The packet belongs to a leading session that has already received service of more than $\alpha \times SR_i$.

2. Lagging sessions always have higher priorities to receive services either from given up portions from leading sessions or from a session that is not able to transmit because of link condition.
3. Lagging sessions receive compensations according to their service rates.
4. If all lagging sessions are in error the service is distributed among non-lagging sessions according to their service rates.

CIF-Q provides wonderful fairness guarantees. Unlike IWFQ, a lagging session does not receive unbounded service independent of its service rate.

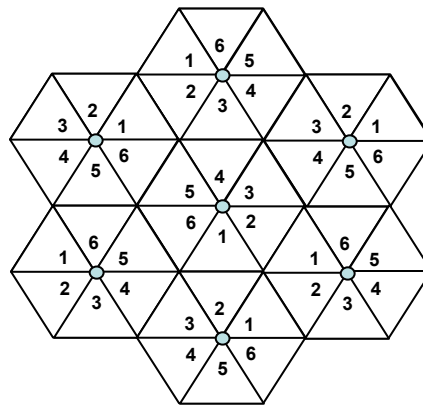
A detailed review on wireless scheduling is provided in [18] by Y. Cao and V. Li.

2.2.3 Scheduling in Fixed Broadband Wireless Access Networks

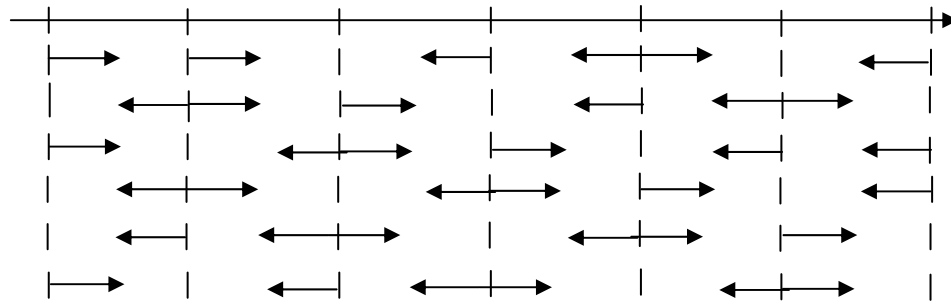
Besides fulfilling basic requirements of scheduling, interference issues must be considered for any scheduler applied to broadband wireless access networks. Several algorithms for dynamic-resource allocation are investigated in [19] by T. K. Fong et al. The method referred to as *staggered resource allocation (SRA)* shows that combination of directional antennas and SRA method is able to control the effective interference. In the scenario where frequency reuse factor of six is used, total data frame is divided into six sub-frames. Each sector is assigned a sub-frame from where it starts downlink transmission.

As shown in Figure 2.1.a, sectors are labeled by 1-6 counter-clockwise and the labeling pattern for adjacent cells differs by a 120^0 rotation. Sector 1 will start scheduling from sub-frame 1 as depicted in Figure 2.1.b. If this sector has more packets such that it needs

more than $1/6^{\text{th}}$ of the frame, it will use sub-frame 4 and then sub-frame 5 and so on. Sector 4 is just opposite to sector 1, so the idea is that after scheduling in sub-frame 1 sector 1 should schedule in sub-frame 4 in order to make the best use of the directional antennas. The assignment pattern for the next sector is “staggered” by the right rotation of one sub-frame based on the order of the previous sub-frame.



(a)



(b)

Figure 2.1: Staggered resource allocation

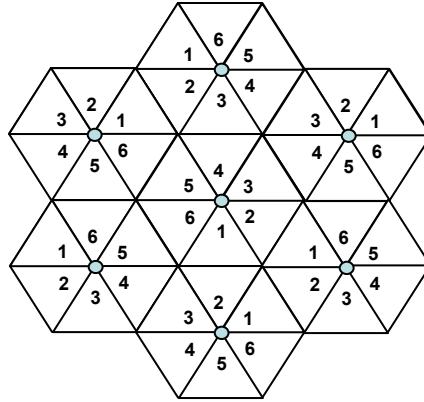
In this scheme, the intra-cell interference is avoided as long as generated traffic demand is less or equal to the capacity delivered by a sub-frame. The SRA method also helps reduce inter-cell interference. We can examine that by checking the interference caused by sector 1 of the middle cell. Sector 2 of the bottom cell and sector 3 of the top cells are

the dominant interferers for the users in sector 1 of middle cell. From the slot allocation scheme it is evident that sector 1, sector 2 and sector 3 do not transmit concurrently as long as their traffic demand is $1/3^{\text{rd}}$ of the total capacity. To reduce interference further, this method employ a rule called *left-right* rule. From Figure 2.1.b. it is seen that sector 1 first schedules in sub-frame 1 in the right direction and then sub-frame 4 in the left direction. If sector 4 does not have enough packets to send them all in sub-frame 1, concurrent transmissions do not occur as long as sector 1 finishes it packets in sub-frame 1. Simulation results show that SRA method delivers a 30% throughput increase per sector while permitting a given frequency band to be reused in every sector of every cell.

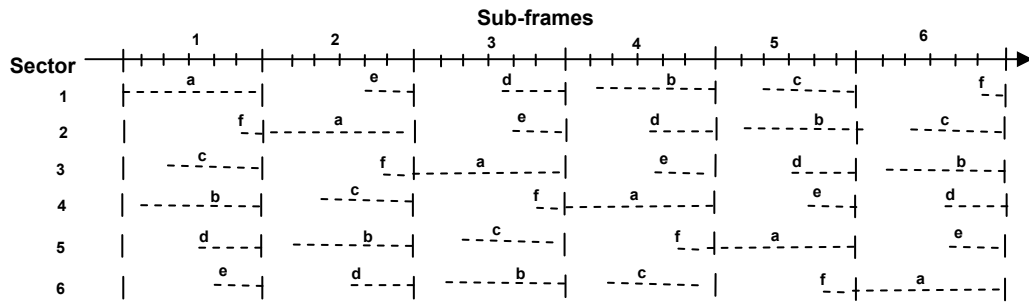
Another study similar to SRA, called as *enhanced staggered resource allocation* (ESRA), proposed by K.K. Leung and A. Srivastava in [20] to enhance the performance of SRA. This scheme basically makes use of the reception quality at the terminal to improve the throughput and the success probability of the received packets. In this method as shown in Figure 2.2, the sub-frame is further divided into six mini-frames. Terminals are classified in the ESRA method based on their ability to tolerate various degrees of concurrent transmissions according to the staggered order which depends on the T-R separation, transmit power, antenna characteristics, terrain and fading. For the layout of six sectors per cell, six levels of concurrent transmissions are defined and terminals are categorized into six classes indexed from 1 to 6.

Similar to SRA, each sector uses the sub-frames according to the staggered order, marked as **a**, **b**, **c**, **d**, **e** and **f**. However, the whole sub-frames are not available to users and only the mini-frames marked with dashed lines can be used. For example, sector 1 can use all six mini-frames in sub-frame 1, but can use only mini-frame 5 and 6 in sub-frame 2. It

should also be noted as shown in Figure 2.2.b, in mini-frame 1 no concurrent transmission is allowed and in mini-frame 2 two concurrent transmissions and so on. The idea is that different mini-frames support different degrees of concurrent transmissions. Thus a terminal classified as class 1 to 6, when transmits in the respective mini-frame would be received successfully.



(a)



(b)

Figure 2.2: Enhanced staggered resource allocation

The performance of ESRA is compared with that of Capture *Division Packet Access* (CDPA) [21] and SRA. ESRA method provides 98.64% coverage and yields maximum downlink throughput of 36.10% per sector with a packet success probability close to one.

The concept of SRA and ESRA is to identify the major sources of interference for each sector and schedule traffic accordingly to avoid them, which requires static system planning. K. Chawla and X. Qiu [22] proposed another scheme called *quasi-static*

resource allocation with interference avoidance (QRA-IA). The idea of this scheme is that every BS turns off its antenna beam for a certain portion of data frame, a terminal continually senses the interference in each frame and identify time slots during which it continually receives lower interference. The terminal feeds back information about these preferred slots to the BS and BS schedule traffics in those slots for that particular user. Simulations show that for 0.1 packet error rate (PER), 83% of the terminal can be served when QRA-IA is used, and only 50% of the terminals can be served if QRA-IA is not employed. Only first tier of interferers are considered in the simulations.

M.H. Ahmed et al. [23-25] proposed intra-sector and inter-sector scheduling schemes that takes advantage of BS coordination to avoid dominant interferers. The proposed algorithm minimizes potential dominant interferers by using orthogonality of the time slot allocation vector. Simulations show that the algorithm achieves lower PER, better throughput with a little delay penalty compared to the case when BS coordination is not used.

2.3 Network Assisted Resource Allocations

The idea behind network *assisted resource allocation* is to shift the burden of the resource allocation from air interface to network backbone infrastructure by employing information exchange mechanism among BSs. Any algorithm based on interference measurement can take advantage of inter-BS signaling to reduce over the air signaling significantly and can use the inter-BS signaling to avoid interference.

Inter-BS signaling requires that the BSs that exchange information to achieve goals should be frame synchronized and the BSs should be connected by some additional bandwidth for signaling.

A series of *dynamic channel allocation* (DCA) schemes for packet networks have been proposed in [26] by X. Qiu et al. to show improvements due to network assisted resource allocation. The simulation results show that a 25% increase of throughput can be achieved compared to conventional over the air measurement based DCA.

Time coordinated transmissions achieved by BS information exchange significantly reduce potential dominant interferers which have been shown in [23-25, 27].

2.4 Adaptive Modulation and Coding (AMC)

Spectrally efficient transmission scheme is an essential consideration to meet the increasing demands of today's fast and reliable wireless services. Adaptive modulation is an effective way to increase the spectral efficiency in a time varying wireless channel. Radio signal propagates through hostile environment which makes spectrally efficient modulation difficult. The quality of the received signal depends on a number of factors such as the distance between the transmitter and receiver, path loss exponent, log-normal shadowing, short-term fading, noise, etc. This implies that the signal to interference plus noise ratio (SINR) varies over time, frequency and/or space. For example, a Rayleigh fading channel causes intermittent reduction in the power level of the received signal, which is known as *deep fades*. During *deep fades* burst errors occur and poor bit error rate (BER) is obtained, while in between fades the received signal level is good and a better BER is obtained. Adaptive transmission is a method of combating this channel

quality fluctuation. It exploits time varying nature of the wireless channel by dynamically adjusting certain key transmission parameters such as modulation level, coding rate, transmission power level according to the channel conditions. This process is commonly referred as *adaptive modulation*; adaptive coding can similarly be implemented which results in *adaptive modulation and coding* (AMC). If necessary *power control* can further be implemented. E. Armanious [28] has investigated different link adaptation techniques for cellular fixed wireless systems. The author has showed that significant performance gain can be achieved when AMC is used in the system. The author has also shown that additional return due to power control when AMC is in place is not very significant.

The idea behind adaptive modulation is that whenever the channel is in a good condition, i.e., channel experiences high SINR, a high constellation modulation scheme with less redundant coding is used to achieve high throughput. On the other hand, when the channel is in poor condition, a lower level modulation with robust coding scheme can be used to keep the bit error rate low. The decision about selecting appropriate modulation and coding scheme is performed at the receiver side according to observed channel condition known as *channel state information* (CSI) and the decision is conveyed to the transmitter via feedback path. Therefore, it is evident that the performance of adaptive modulation scheme is dependent on the accuracy of the channel estimation at the receiver and a reliable feedback path between the transmitter and the receiver.

A.J. Goldsmith and P.P. Varaiya [29] have developed a set of formulae for the capacity limits of a channel with single user in flat fading channel for arbitrary fading distributions. The scenarios include limit imposed by Shannon's theory, attainable limit when the channel state is known to both transmitter and receiver termed as *optimal*

adaptation, and when channel is known to receiver only. Transmitter adapts its power, data rate or coding scheme in response to the channel variations. They have concluded that receiver only state information achieves equal level of capacity as the optimal adaptation case, while it demands less receiver complexity for independent and identically distributed (i.i.d.) fading. For correlated fading, not adapting at the transmitter causes considerable capacity penalty and increased complexity. Also, two suboptimal cases are considered in this study such as *channel inversion* and *truncated channel inversion*, where only power is adapted according to link state while keeping the data rate constant. These sub-optimal schemes achieve much less capacity in all fading scenarios.

Based on the results found in [29], M.S. Alouini and A.J. Goldsmith [30] have developed closed form expressions for the capacity in Nakagami fading channel for different adaptation scenarios such as rate adaptation with fixed transmit power and rate and power adaptation. The reason to use Nakagami fading model is that it is a general model which can easily be tailored as Rayleigh or Ricean model by fixing the fading parameter. It is seen that the capacity of Nakagami channels is always smaller than that of additive white Gaussian noise (AWGN) channel and converges to it as fading parameter m increases, i.e., the amount of fading decreases. It is also noticeable that power and rate adaptation policy has higher capacity over rate only adaptation for lower average *signal to noise ratio* (SNR) only and the difference disappears as SNR and/or m increases.

A.J. Goldsmith and S.-G. Chua [31] have shown that a four state trellis code on the top of adaptive *M-ary quadrature amplitude modulation* (M-QAM) scheme can provide a 3 dB gain over the uncoded scheme. They also concluded that a 20 dB gain can be achieved over a non-adaptive scheme.

2.5 Summary of Review and Problem Formulation

Scheduling techniques used in wireline networks are not applicable to wireless as wireless link quality varies with time, location, frequency etc., resulting in variable link capacity. The variable link capacity poses a problem to achieve fairness in wireless scheduling. Numerous wireless scheduling techniques based on different service disciplines are available in the literature that are basically adapted versions of wireline scheduling schemes to cope with the variability of wireless link and to provide different degrees of fairness among users. However, these wireless scheduling techniques do not address the issue of interference management which is a major design concern for fixed broadband wireless systems. Such systems are highly prone to co-channel interference because of aggressive reuse of frequency required to achieve high data rate with limited and expensive radio spectrum. A series of published works on scheduling and/or interference management schemes are found in the literature. The principal goal of these schemes is to avoid dominant interferers by different means. This implies that most of these try to avoid or minimize the number of concurrent transmissions among dominant co-channel interferers. The ESRA [20] scheme allows different degrees of concurrent transmissions based on terminal classes. But, the time slot allocation is static which might result in resource wastage especially for bursty traffic.

This thesis deals with the scheduling problem from a different perspective. Firstly, the notion of wireless link state is extended from two-state Markov to a larger number of channel states. Two-state Markov (*good or bad*) is used for most wireless packet fair queuing algorithms such as IWFQ, CIF-Q and also in various CSDPS schemes. In these

schemes, packets are not transmitted for the link which is in *bad* state. While, a larger number of states enable the scheduler to transmit packets with various modulation and/or rates according to channel conditions. Thus, in this thesis we observe the impact of integration of AMC and scheduling technique on network performances. Secondly, proposed algorithm in IIS-AMC-MT emphasizes maximizing the number of concurrent transmissions among co-channel interferers in a controlled manner as opposed to conservative schemes that only allows orthogonal transmissions. Basically, if a number of co-channel BSs transmit simultaneously, each becomes interferer for others. The idea is that if the interference levels are estimated or predicted and known to each BS transmitting concurrently, then every BS would potentially be able to transmit simultaneously with its feasible AMC mode in the presence of others being interferers. As opposed to ESRA, dynamic time slot allocations in IIS-AMC-MT provide efficient use of resources.

The proposed scheduling schemes are expected to provide throughput gain, from AMC (in IIS-AMC-ST and IIS-AMC-MT), and from multiple transmissions (in IIS-AMC-MT) in the interferer group compared with the results obtained from a scheme that uses fixed modulation and implements orthogonal transmissions in the interferer group. End-to-end packet delay is also expected to improve as queuing delay reduces with the increase of throughput (higher queue service rate) for a given packet arrival rate. A delay threshold is set for the queue such that when a waiting packet in the queue exceeds the delay threshold, it is dropped from the queue. The number of dropped packets would also be improved as queuing delay decreases by increased throughput in the schemes employing AMC with (or without) concurrent in-group transmissions.

Chapter 3

System Models and Methodologies

3.1 Introduction

Any simulation model could be divided into various sub-models that collectively conceptualize the whole simulated system. These sub-models are required to be validated in order for them to be used in the simulation accurately. In this chapter, several sub-models, categorized as *network related models* and *algorithm related models*, developed for this simulation study are discussed. Modeling radio propagation accurately is probably the most important job in designing a wireless system as network performance is fully dependent on the characteristics of the wireless channel. Propagation model is described in Section 3.2.1 followed by other network related models such as background noise model, traffic model, delay model, packet error rate models in the subsequent sections. Although a nine-cell network is implemented in this work, wrap-around interference model has been used to capture more realistic interference effects. Section 3.3 discusses wraparound interference patterns for users in different BS locations, followed by BS information exchange, AMC schemes. Finally, an overview on different simulation scenarios investigated in this thesis is provided in Section 3.4.

3.2 Network Related Models

3.2.1 Channel Model

As transmit signal propagates from transmitter to receiver the signal strength weakens. Propagation or channel models characterize the varying nature of wireless channel which has been one of the most challenging tasks of designing a radio system. Channel models

are used to predict the average received signal strength for a given transmitter-receiver (T-R) separation which is called *large-scale path-loss* model, and as well as the fluctuations of the signal strength around the average for a particular location which is termed as *small-scale fading* or *fading* model.

Large-scale path-loss depends on the distance between the transmitter and receiver as well as the operating frequency and is therefore modeled in a deterministic fashion for a given T-R distance and frequency. But, in reality, this loss is not constant, and the variations depend on the objects surrounding the receiver and the terrain of the transmission path. This location depended variation of large-scale path-loss is known as *shadowing*. Therefore, a wireless channel is characterized by three different attenuating effects *large-scale path-loss*, *fading* and *shadowing*. In the following sections, all these models are elaborated in details as they are used in the simulation study of this thesis.

3.2.1.1 Large-scale Path Loss Model

Large-scale path-loss models are empirical models established from extensive field measurements in different terrain conditions such as urban, suburban and rural. The general expression for path-loss for a T-R separation d is given by [34],

$$PL \text{ [dB]} = PL_{fs} + 10n \log_{10} \left(\frac{d}{d_0} \right), \quad (3.1)$$

where large-scale path-loss PL is expressed in dB, n is propagation exponent, and PL_{fs} is free space path-loss at reference distance d_0 . PL_{fs} is dependent on operating wavelength λ as follows,

$$PL_{fs} = 20 \log_{10} \left(\frac{4\pi d_0}{\lambda} \right). \quad (3.2)$$

There are other more elaborate path-loss models which factor in antenna height, carrier frequency and other system parameters. In this study we have used suburban model as in [32, 33] presented for fixed broadband wireless access networks. Since the simulation network is implemented in 2.5 GHz operating region and the roof-top antenna height is considered 3.0 meters, the path-loss is adjusted according to the following antenna height and frequency correction factor as follows [32, 33].

$$\Delta PL_f = 6 \log_{10}(f / 2000) \quad (3.3)$$

$$\Delta PL_h = -20 \log_{10}(h_r / 2), \quad (3.4)$$

where f is the operating frequency in MHz and h_r is the receiver antenna height in meters.

Therefore, the resulting large-scale path-loss including correction factors is given by,

$$PL \text{ [dB]} = \begin{cases} 20 \log_{10} \left(\frac{4\pi d_0}{\lambda} \right) + 10n \log_{10} \left(\frac{d}{d_0} \right) + 6 \log_{10} \left(\frac{f}{2000} \right) - 20 \log_{10} \left(\frac{h_r}{2} \right) & ; d \geq d_0 \\ 20 \log_{10} \left(\frac{4\pi d}{\lambda} \right) & ; d < d_0 \end{cases}. \quad (3.5)$$

where large-scale path-loss is given by free space path-loss when the T-R separation is less than the reference distance.

In this thesis, a terrain with moderate to low density trees is chosen so that with sufficiently high BS antenna, the resulting propagation constant n becomes 3. The cell radius is taken to be 2.0 kilometers and the reference distance at which the receiver still has free space path-loss is 10 meters. With these parameters, large-scale path-loss at the

cell boundary and at the reference distance for 2.5 GHz operating frequency would be 126.49 dB and 60.4 dB, respectively.

3.2.1.2 Shadowing

Measurements established that the large-scale path-loss such as given in (3.5) for a particular T-R separation is random and distributed log-normally around the mean value described by the path-loss formula. Therefore, path-loss including the shadowing would be,

PL [dB]

$$= \begin{cases} 20 \log_{10} \left(\frac{4\pi d_0}{\lambda} \right) + 10n \log_{10} \left(\frac{d}{d_0} \right) + 6 \log_{10} \left(\frac{f}{2000} \right) - 20 \log_{10} \left(\frac{h_r}{2} \right) + X_\sigma & ; d \geq d_0 \\ 20 \log_{10} \left(\frac{4\pi d}{\lambda} \right) + X_\sigma & ; d < d_0 \end{cases} \quad (3.6)$$

In the above, X_σ is a Gaussian distributed random variable with a mean of 0 and a standard deviation of σ . In this study we have considered independent lognormal random variables with a standard deviation of 8 dB for shadowing.

3.2.1.3 Fading

Fading is the variation of the received signal resulted from the constructive or destructive addition of multiple versions of the transmitted signal each having followed a different transmission path. This fluctuation is experienced over a short period of time and is, therefore, denoted as *small-scale fading* or *fading*. Fading is dependent on the speed of the receiver in case of mobile terminal. In *fixed broadband wireless* systems, fading mainly depends on the movements of the objects surrounding the receiver. Therefore,

fading changes very slowly in case of fixed wireless system as compared to the mobile system. Doppler frequency is a measure of the rate of changes in fading. In fixed broadband wireless, Doppler power spectral density is mainly distributed at $f = 0$ Hz forming a bell-shaped PSD, as shown in Figure 3.1, which is different from classical Clarke's model [34]. Time-correlated flat Rayleigh fading with Doppler frequency of 2.0 Hz has been considered in this study where the Doppler spectrum is given by the following equation [33].

$$S(f) = \begin{cases} 1 - 7.2f_0^2 + 0.785f_0^4 & ; |f_0| \leq 1 \\ 0 & ; |f_0| > 1 \end{cases} \quad (3.7)$$

where $f_0 = \frac{f}{f_m}$ and f_m is the maximum doppler frequency.

Correlated fading dataset is generated using Clarke and Gans model [34, 35]. The method is based on filtered Gaussian random variables, where a sequence of in-phase and quadrature components x_1 and x_2 are generated which together yield the instantaneous fading power as discussed later in this section.

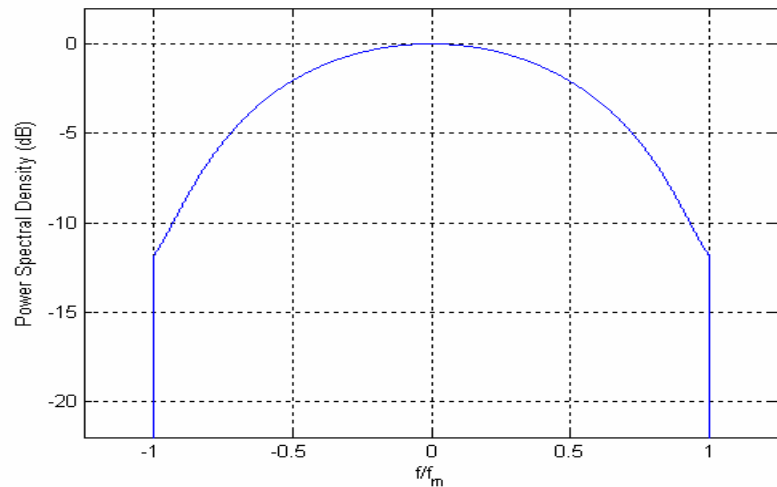


Figure 3.1: Rounded Doppler power spectral density

The fading samples are generated as per the following steps:

- The number of frequency domain points N is specified as 1024 that represents the filter response $\sqrt{S(f)}$. The maximum Doppler frequency f_m is 2.0 Hz. With these parameters, the time duration of the correlated fading waveform is,

$$T_{fd} = \frac{N-1}{2f_m}, \text{ i.e., } 256 \text{ seconds.}$$
- Complex Gaussian random variables for each of the frequency components are generated for the positive $N/2$ components. The negative half components are the complex conjugate of the positive frequency components.
- Filter response function $\sqrt{S(f)}$ is multiplied with these complex variables at specified frequency points.
- *Inverse Fast Fourier Transform* (IFFT) has been performed on the resulting data to yield a complex time series data
- All steps above are repeated to get another time series data
- These two time series data are summed up to give in-phase and quadrature component of fading dataset.

The dataset entries x_1 and x_2 are normalized so that their variance become unity.

Therefore, the Rayleigh fading variable can be given by,

$$r(ind) = \sqrt{\frac{x_1^2(ind) + x_2^2(ind)}{2}}, \quad (3.8)$$

where (ind) is the index of the discrete samples generated by the IFFT process and is limited by IFFT size (2^{20} considered in the generation of samples). It should be mentioned here that the mean value of the fading power is unity, i.e., $E[r^2(ind)] = 1$. The plot of the instantaneous fading power (in dB) is illustrated in Figure 3.2.

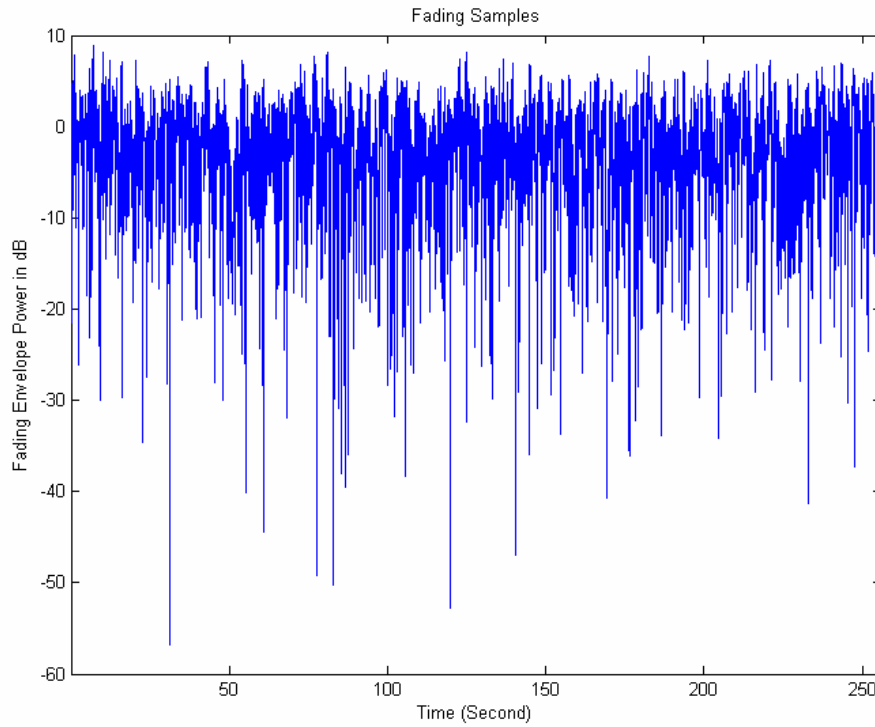


Figure 3.2: Instantaneous power of fading envelope

It should be mentioned that 2^{20} generated fading samples span over 256 seconds resulting inter-sample time 0.244 ms which is much smaller than coherence time 211 ms (shown later in this section). Therefore, the generated samples are highly time correlated.

It can be shown that if p is the instantaneous power of a Rayleigh envelope, the probability density function of p is exponentially distributed as follows,

$$f_p = \begin{cases} \frac{1}{\bar{p}} \exp\left(-\frac{p}{\bar{p}}\right) & ; p \geq 0 \\ 0 & ; p < 0 \end{cases}, \quad (3.9)$$

where the average envelope power is given by \bar{p} . The CDF of the instantaneous power is expressed by,

$$F_p = \begin{cases} 1 - \exp\left(-\frac{p}{\bar{p}}\right) & ; p \geq 0 \\ 0 & ; p < 0 \end{cases}. \quad (3.10)$$

Equation (3.10) gives the theoretical CDF of instantaneous power of a Rayleigh fading envelope. The theoretical and simulated Rayleigh CDF has been compared in Figure 3.3, and hereby validated that the simulated Rayleigh agrees well with the theoretical one.

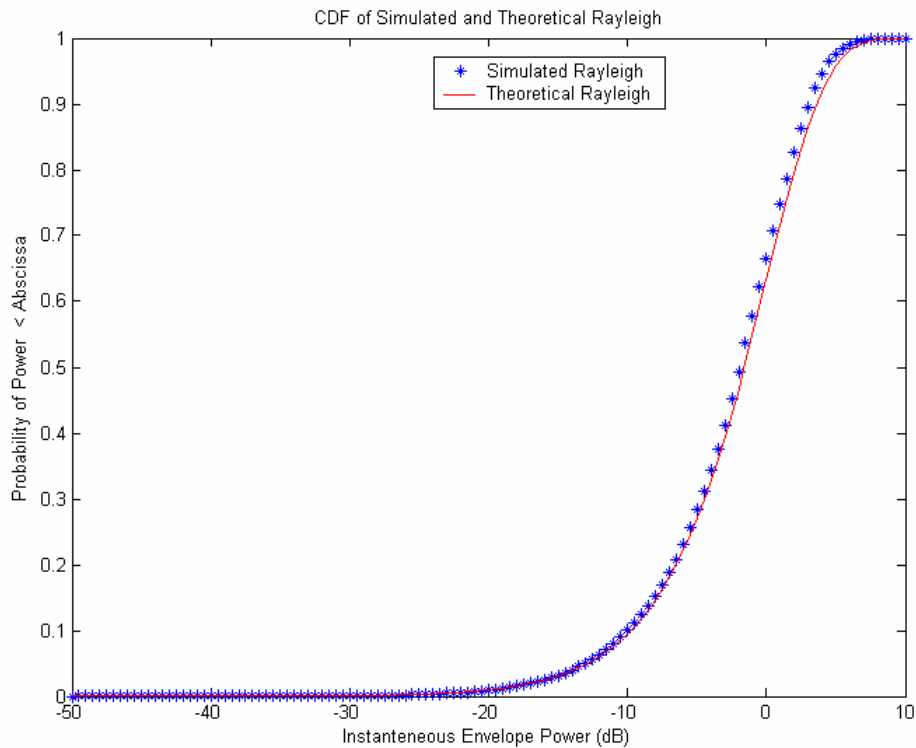


Figure 3.3: Comparison of CDF of envelope power of simulated and theoretical Rayleigh fading

Coherence time T_c is a statistical measure of the time duration over which the received signals have strong amplitude correlation and it is the time domain dual of the Doppler spread. A rule of thumb expression for time coherence can be expressed by the following relation [34]:

$$T_c = \frac{0.423}{f_m}. \quad (3.11)$$

Using maximum Doppler frequency of 2.0 Hz, T_c would be 211 ms. Figure 3.4 shows the fade duration of the fading dataset that are used in this study. It is apparent that the fade durations are larger than T_c and therefore the samples are correlated over the coherence time.

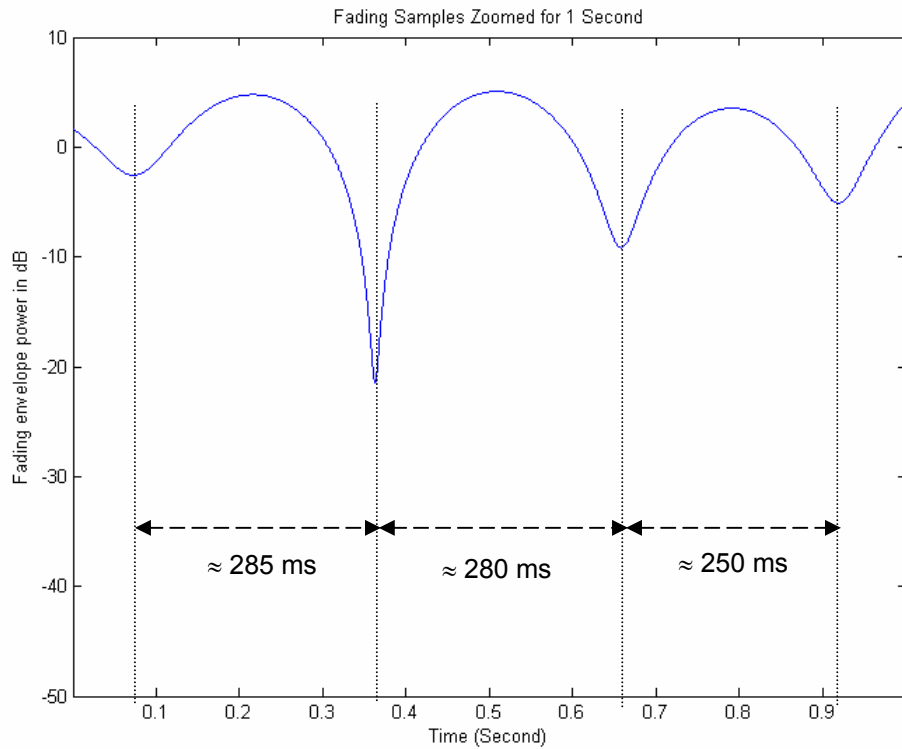


Figure 3.4: Time correlation of the fading samples

3.2.2 Background Noise Model

Thermal noise is the source of background noise at the receiver. Average thermal noise power is related to the Boltzman's constant C , ambient temperature T in degree Kelvin and channel bandwidth B in Hz according to (3.12) below.

$$P_N = 10 \log_{10}(CTB) + NF(dB). \quad (3.12)$$

With a bandwidth of 3.0 MHz and noise figure (NF) of 5 dB the average noise power is -134.06 dBW. This is an additive white Gaussian noise (AWGN) that must be considered while calculating received signal's SINR.

3.2.3 Traffic Model

Real-time video traffic is used in this study. Two *Interrupted Renewal Process* (2IRP) sources are superimposed to model user's video traffic in the downlink transmission as indicated in [36]. This is a standard model of video traffic often used in fixed broadband wireless access networks [23-25, 36]. In each of these sources, modeled traffic is bursty in that there are separate ON and OFF distribution of the source. During the OFF state the IRP process does not generate packets. During the ON state, packets are generated with exponentially distributed inter-arrival time. The mean dwell time or sojourn time in ON or OFF state is Pareto distributed. The model is shown in Figure 3.5. The IRP process is derived from *Interrupted Poisson Process* (IPP). The difference between IPP and IRP is that while the ON and OFF time for IPP is exponential distributed, they are Pareto in IRP.

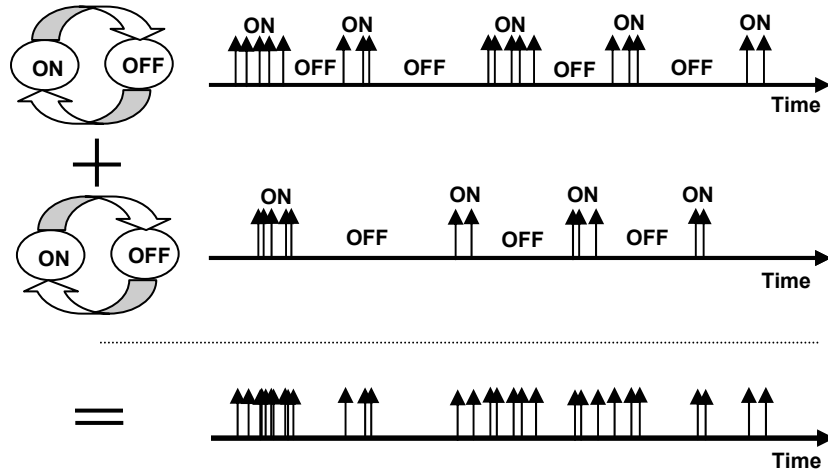


Figure 3.5: 2IRP video traffic model

To find out the generated data rate of the IRP process, we begin with a state diagram of a basic IRP process as shown in Figure 3.6. Let us assume that $\mu_{on \rightarrow off}$ is the state transition rate from ON to OFF and $\mu_{off \rightarrow on}$ is the rate from OFF to ON. The mean dwell time on the ON state is given by $T_{on} = 1/\mu_{on \rightarrow off}$ while the mean dwell time on the OFF state is $T_{off} = 1/\mu_{off \rightarrow on}$. The probability being ON and OFF state would be $Pr_{on} = T_{on}/(T_{on}+T_{off}) = \mu_{off \rightarrow on}/(\mu_{on \rightarrow off} + \mu_{off \rightarrow on})$ and $Pr_{off} = T_{off}/(T_{on}+T_{off}) = \mu_{on \rightarrow off}/(\mu_{on \rightarrow off} + \mu_{off \rightarrow on})$, respectively.

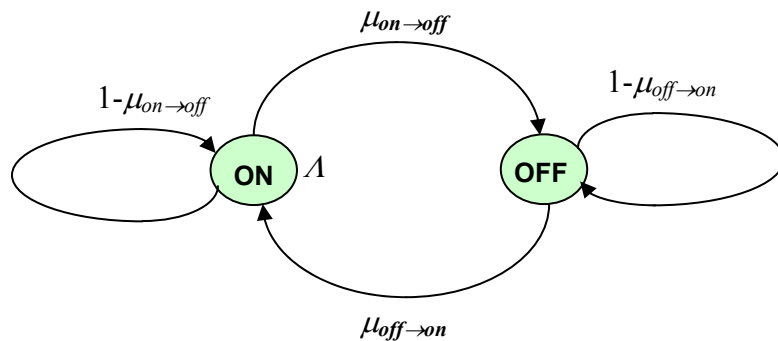


Figure 3.6: State transition diagram of IRP process

If, during the ON state process, the source generates λ packets per second on average, then the mean number of generated packets will be $\lambda \times Pr_{on}$ packets per second. The

Pareto distribution parameters for OFF and ON distributions are given in Table 3.1. If a random variable X is Pareto distributed, the probability density function of X is given by, $f_x(x) = \beta \rho^\beta / x^{\beta+1}$, $\rho \leq x < \infty$. The parameters ρ and β are called location and shape parameters, respectively. The location parameter $\rho = 1$ is considered in this model. The shape parameter β is related to the mean value as $E[x] = \beta / (\beta - 1)$ for $\beta > 1$. From the parameters in Table 3.1, it can be found that for IRP1 the mean dwell time on ON and OFF states are $T_{on} = \beta_1 / (\beta_1 - 1) = 8.143$ sec and $T_{off} = \beta_2 / (\beta_2 - 1) = 5.545$ sec, respectively. Therefore, for IRP1 the probability being ON state, $Pr_{on} = T_{on} / (T_{on} + T_{off}) = 8.143 / (8.143 + 5.545) = 0.595$. Similarly, for IRP2 the probability being ON state is given by 0.384. With these probabilities and packet arrival (exponential) rates shown in the table, IRP1 and IRP2 generate $0.595 \times 112.38 = 66.87$ and $0.384 \times 154.75 = 59.42$ packets/sec, respectively. Therefore, the average packet rate of one 2IRP generator is 126.3 packets per second.

Table 3.1: Traffic Model Parameters of the Video Stream [36]

IRP #	Packet Arrival Rate Λ (packets/sec)	Pareto parameter for ON distribution, β_1	Pareto parameter for OFF distribution, β_2
IRP1	112.38	1.14	1.22
IRP2	154.75	1.54	1.28

The length of packets is assumed to be variable and is uniformly distributed between 250 to 550 bytes. Therefore, the downlink data rate for each user is 404.16 kbps. We have considered a larger packet size ($U \sim (250, 550)$ bytes) in our study than proposed ($C \sim 188$ bytes) in [36] in order to capture greater impact of interference on packets.

3.2.4 Delay Model

Besides queuing delay, two kinds of delays are associated in a wireless packet network, namely propagation delay and transmission delay. In this study, propagation delay, which is equal to the ratio of T-R separation in meters and speed of the light in meters per second, is neglected. Packet transmission delay is defined as the time interval between the beginning of transmission of first bit and end of transmission of last bit of a packet. This time will depend on the packet size and data rate of the transmission channel. Since AMC is being used in this study the transmission delay t_d can be expressed as,

$$t_d = \frac{L_p}{\log_2 M} \cdot \frac{1}{r_s} \cdot \frac{1}{r_c}, \quad (3.13)$$

where L_p is packet size in bits, M is the modulation level used for that packet, r_s is the symbol rate of the channel and r_c is code rate used.

3.2.5 PER and Error Correction Model

When a packet is received by the user, the number of erroneous bits is calculated from the SINR pattern during the transmission time of the packet. Interferers may arrive or leave anytime during the transmission time of a packet of interest as shown in Figure 3.7.

The SINR pattern depends on the desired packet's signal received power, interferer power and the receiver noise. SINR is constant over a particular segment i ; therefore the probability of bit error in that segment is also constant. The number of erroneous bits in a segment is given by the product of the probability of the bit error and the number of bits corresponding to the segment length. The total number of bits in error in the packet can be written by the following relation.

$$N_e = \sum_{i=1}^s \Pr_{b(i)} \times N_{b(i)}, \quad (3.14)$$

where $\Pr_{b(i)}$ is the probability of bit error in packet segment i calculated from a look-up table for SINR $\gamma_{(i)}$, $N_{b(i)}$ is the number of bits reside in segment i , and s is the total number of segments in that packet with different SINR.

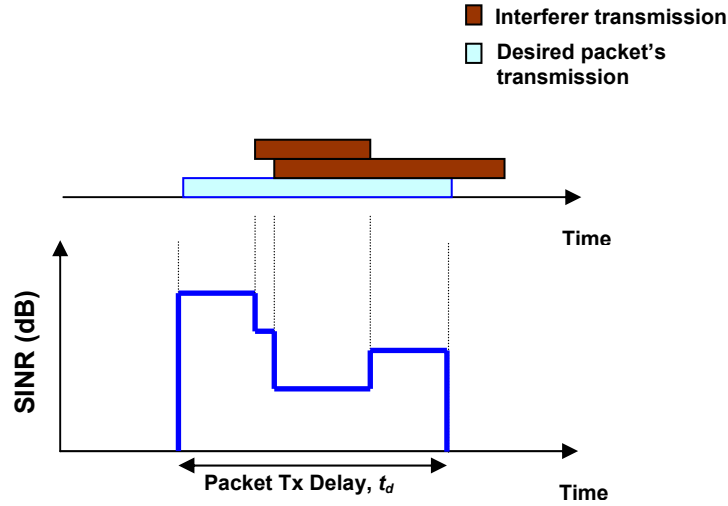


Figure 3.7: Calculation of segmented SINR in a packet

To provide a simple example, let us consider that a packet containing 300 bytes of information is received by a user with 16-QAM modulation with a coding rate of $\frac{1}{2}$. The total number of bits in that received packet would be 4800 bits including the coding bits. The transmission time t_d for this packet according to (3.13) is 4.0×10^{-4} second. Now let us assume that the packet experiences interference from only one interferer that arrives just at the middle of the desired packet's transmission time and exists through the rest of the transmission time. There will be two levels of SINR associated with the desired packet. Let us assume that SINR are 9.6 and 8.4 dB in the interference free and interfered segments, respectively. Now, the probabilities of bit error in these two segments (for 16-

QAM with a coding rate of $\frac{1}{2}$) are 3.46×10^{-5} and 7.48×10^{-4} , respectively (obtained from Figure 3.10 in Section 3.3.3). As each segment contains 2400 bits, number of errors is 0 and 2 in the interference free and interfered segment, respectively, giving a total error of 2 bits in this desired packet.

In simulations, we assume that a packet is considered to be in error if more than 1% of the total bits present in the packet are erroneous. Taking the same example above, the error threshold for this packet would be 48 bits. The received packet is considered to be correct as it has errors less than the threshold.

3.3 Algorithm Related Models and Methodologies

Base station information exchange and AMC are two integral parts of the study under investigation. In the following sections, algorithm related models such as wraparound interference model, inter-base information exchange model, adaptive modulation schemes are provided followed by the simulation scenarios implemented in this thesis.

3.3.1 Wraparound Interference Model

It is customary to consider wraparound interference while doing network simulations with limited number of cells in order to achieve more realistic interference effects that resemble to a system with larger number of virtual cells. In this thesis, the location of a particular interferer is chosen such that it gives the highest interference power among all possible positions, as discussed in Appendix A. The nine-cell network is implemented according to the layout shown in Figure 3.8. The whole available frequency band is divided into six sub-bands and each sector is assigned with a sub-band of frequencies.

The whole band is repeated in each cell such that sector 1 of each cell is assigned with the same frequency sub-band, and hence they collectively form a co-channel set. Only sector 1 of each cell is considered in the simulation¹.

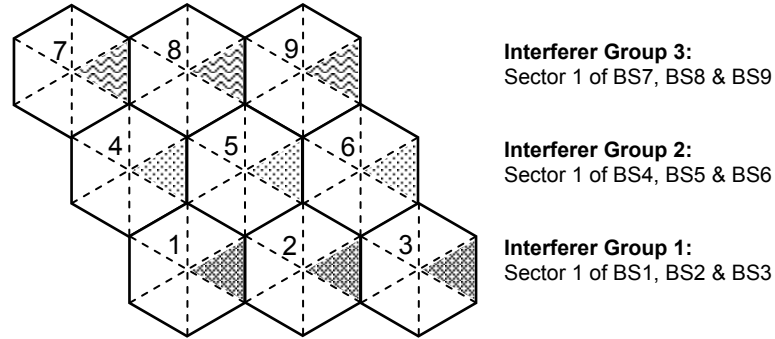


Figure 3.8: Simulated nine-cell network

The interferer locations are functions of relative positions and directivities of user and sector antennas. The detailed method of finding wraparound interferer positions is given in Appendix A. Following the method the wraparound positions for interferers on users in BS1, BS2 and BS3 are determined as shown in Figure 3.9.

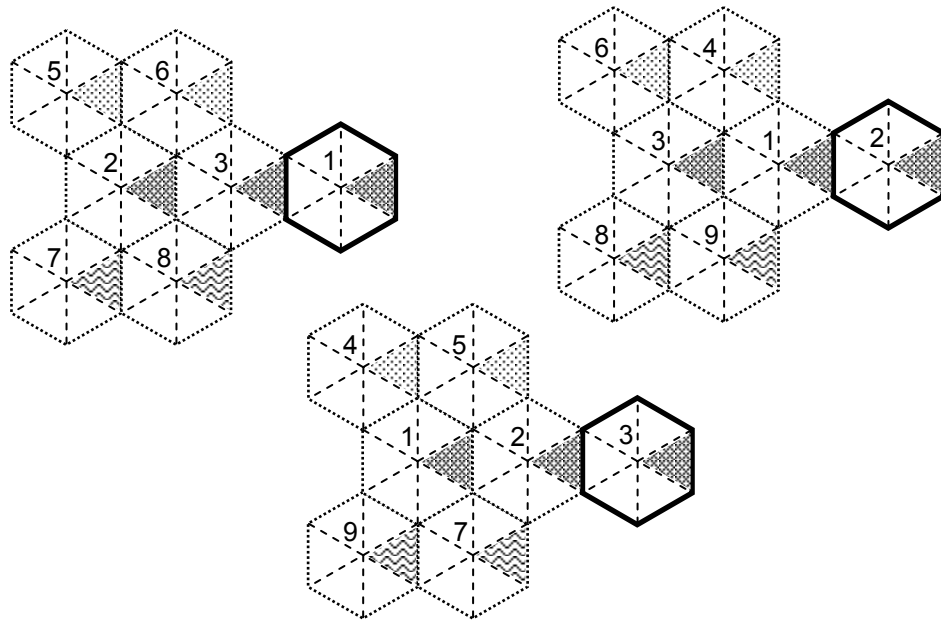


Figure 3.9: Wraparound interferer positions for users in BS1, BS2 and BS3

¹ BSx actually implies sector 1 of BSx throughout this thesis.

It should be noted that for users in BS1, two most dominant interferers arrive from BS2 and BS3, as discussed elaborately in Appendix A. So are the cases for users in BS2 and BS3. Therefore, BS1, BS2 and BS3 form an interferer group.

3.3.2 Base Station Coordination

Base stations in an interferer group are assumed to be connected for inter-BS signaling. These BSs exchange the following information with each other at the start of every data frame:

- Number of packets arrived in the previous frame.
- Downlink link gain from BS to each user. User terminal is capable of monitoring its link with its own BS as well as with other BSs in the interferer group. This information is fed back to own BS in every frame duration using uplink data frame.

3.3.3 Adaptive Modulation and Coding (AMC) Modes

Bit-interleaved Coded Modulation (BICM) has been used in this study which is known to be a good choice for a network with burst errors [37]. Different modulation levels such as QPSK, 16-QAM and 64-QAM, each with different coding rates $\{\frac{1}{2}, \frac{2}{3}, \frac{3}{4}, \frac{7}{8}$ and 1} are the possible options for AMC modes. These three modulation schemes are mandatory for downlink transmission in fixed wireless systems with BPSK and 128-QAM being optional [1]. Figure 3.10 shows bit error rate curves for these AMC modes obtained from link level simulation².

² Data for BICM modulation curves is provided by Dr. Sirikiat Lek Ariyavisitakul, Radia Communications, Norcross, GA, USA.

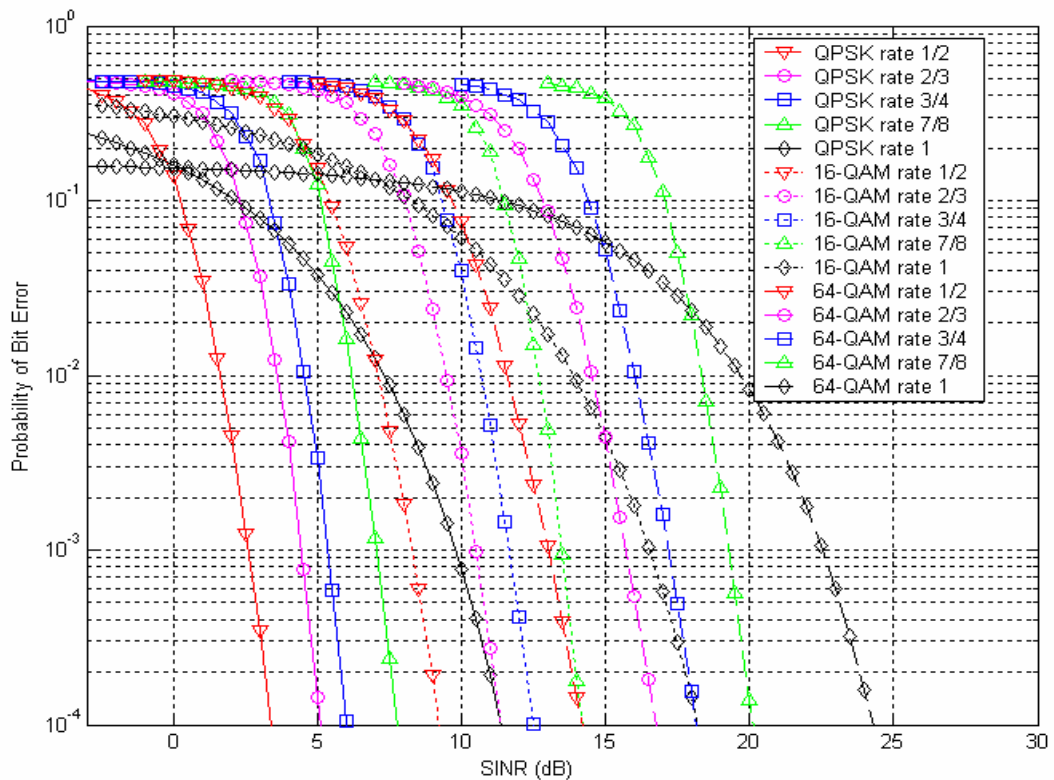


Figure 3.10: Adaptive modulation and coding modes

For a video service the maximum allowable bit error rate is 1.0×10^{-4} [23]. Using this bit error rate a look-up table, Table 3.2, is arranged which shows the AMC level to be used for particular range of SINR. Basically, a threshold based approach is to be used to select the appropriate AMC mode. For example, if the expected SINR falls between 12.5 to 14.21 dB, 16-QAM rate $\frac{3}{4}$ BICM would have to be used for that transmission.

The efficiencies of QPSK rate 1 and 16-QAM with a coding rate of $\frac{1}{2}$ schemes are both equal to 2.0. However, the SINR requirement for QPSK rate 1 is higher than that of 16-QAM rate $\frac{1}{2}$ for a bit error rate of 1.0×10^{-4} as in Figure 3.10. Therefore, QPSK with a

coding rate of 1 is not used in the simulation. For similar reasons 16-QAM with a coding rate of 1 and 64-QAM with a coding rate of $\frac{1}{2}$ modes are omitted in the simulation.

Table 3.2: Lookup table for AMC modes

SINR Range (dB)	AMC Mode	Efficiency (Bits/Sec/Hz)
$3.39 \geq \text{SINR} < 5.12$	QPSK rate $\frac{1}{2}$	1.0
$5.12 \geq \text{SINR} < 6.02$	QPSK rate $\frac{2}{3}$	1.33
$6.02 \geq \text{SINR} < 7.78$	QPSK rate $\frac{3}{4}$	1.5
$7.78 \geq \text{SINR} < 9.23$	QPSK rate $\frac{7}{8}$	1.75
$9.23 \geq \text{SINR} < 11.36$	16-QAM rate $\frac{1}{2}$	2.0
$11.36 \geq \text{SINR} < 12.50$	16-QAM rate $\frac{2}{3}$	2.67
$12.5 \geq \text{SINR} < 14.21$	16-QAM rate $\frac{3}{4}$	3.0
$14.21 \geq \text{SINR} < 16.78$	16-QAM rate $\frac{7}{8}$	3.5
$16.78 \geq \text{SINR} < 18.16$	64-QAM rate $\frac{2}{3}$	4.0
$18.16 \geq \text{SINR} < 20.13$	64-QAM rate $\frac{3}{4}$	4.5
$20.13 \geq \text{SINR} < 24.30$	64-QAM rate $\frac{7}{8}$	5.25
$\text{SINR} \geq 24.30$	64-QAM rate 1	6.0

3.4 Overview on Simulated Scheduling Schemes

The principal objectives of this study are to show benefits of integrating AMC with scheduling techniques and to quantify performance enhancements by allowing concurrent transmissions among sectors in the interferer group.

Three scheduling schemes are investigated in this study as follows:

1. Intra-sector and Inter-sector Scheduling using Fixed Modulation: Single Transmission per interferer group (**IIS-FM-ST**).

2. Intra-sector and Inter-sector Scheduling using Adaptive Modulation and Coding: Single Transmission per interferer group (**IIS-AMC-ST**).
3. Intra-sector and Inter-sector Scheduling using Adaptive Modulation and Coding: Multiple Transmissions per interferer group (**IIS-AMC-MT**). IIS-AMC-MT scheduling discipline is the most important contribution in this thesis.

IIS-FM-ST is adapted from [23] and is used as a reference scheme to show the performance gains due to adaptive modulation and concurrent transmissions proposed in this thesis. This reference scheme uses fixed modulation and does not allow interferers in the group to transmit concurrently. IIS-AMC-ST and IIS-AMC-MT take advantage of link and information and use AMC. Like IIS-FM-ST, IIS-AMC-ST is also a conservative technique that prohibits co-channel interferers in the group to transmit simultaneously. On the other hand, IIS-AMC-MT permits concurrent transmissions of interferers in the group. The benefits of using AMC can be observed by comparing IIS-FM-ST and IIS-AMC-ST. Multiple transmissions in the interferer group in a controlled fashion yield performance enhancements, which can be quantified by comparing IIS-AMC-ST and IIS-AMC-MT.

3.4.1 Implementation Issues of the Schemes

In all three scheduling schemes, it is assumed that the time slot is infinitesimally small and a packet (whose length varies between 250 to 550 bytes according to the traffic model discussed in Section 3.2.3) can take as number of time slots as required in the data frame. The reason for this assumption is that when AMC is used, a packet with variable length can take variable length in the frame, and therefore traditional *time division*

multiple access (TDMA) slot allocation with fixed time slot strategy is not applicable in such systems.

Every scheduling scheme mentioned above comprises of two independent scheduling techniques, namely *intra-sector* and *inter-sector scheduling*. Although any scheduling discipline can be used for intra-sector part such as FCFS, WRR, EDF, WFQ or its variants, for the simplicity of implementation FCFS is used for all three schemes as intra-sector scheduler. Intra-sector scheduler determines the service order of users in a sector.

Figure 3.11 shows the general structure of *intra-sector and inter-sector* schedulers for *interferer group 1* in a block diagram.

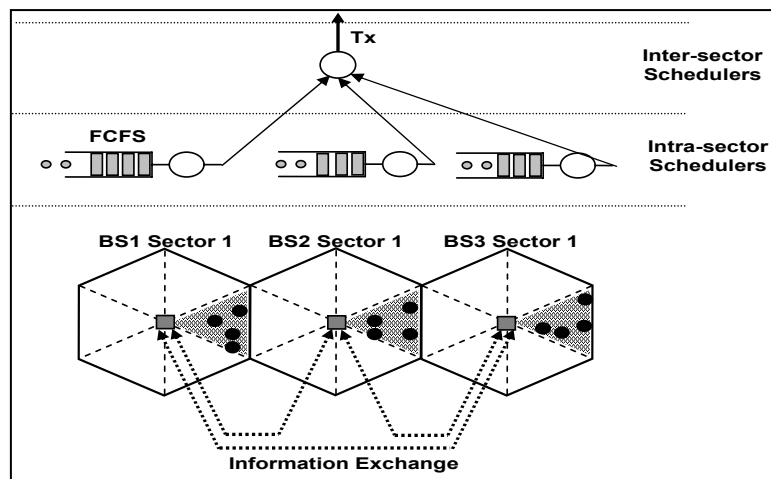


Figure 3.11: Block diagram of intra and inter-sector scheduling

For lower network loading, orthogonal slot allocations among interferer groups are implemented as illustrated in Figure 3.12. Data frame will be filled from left to right and the level of frame occupancy will depend on the degree of network loading. Packets are scheduled from the beginning of the frame in interferer group 1. In interferer group 2,

allocation starts from $1/3^{\text{rd}}$ of the frame and continues until end of the frame. If there are more packets to be scheduled, part II (rest $1/3^{\text{rd}}$ frame) will be used starting from the beginning of the frame as shown in Figure 3.12. Interferer group 3 starts allocation at $2/3^{\text{rd}}$ of the frame, and after finishing scheduling until end of the frame, it will schedule part II (rest $2/3^{\text{rd}}$) of the frame from the start of the frame.

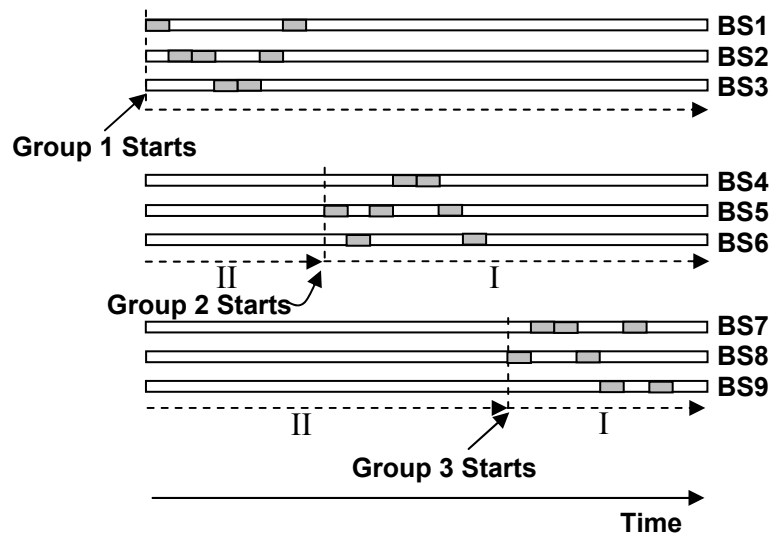


Figure 3.12: Group-wise orthogonal slot allocations
(Example shows a single transmission case)

It is easy to see that when the network is lightly loaded such that the arrived packets occupy only $1/3^{\text{rd}}$ of the total frame length for all three groups, there is no out-of-group interferer as the allocation is group-wise orthogonal. However, with increasing loading the orthogonality gradually fades away, and more and more out-of-group interferers become eminent.

As shown in Figure 3.13, *decision instant* is defined as a location in the frame, where a packet (single transmission) or packets (multiple transmissions) is or are to be scheduled from the result of a scheduling decision. The duration between decision points is regarded

as *decision region*. In single transmission cases, decision region is given by the transmission time required by the packet. In multiple transmission case, decision region is determined from the packet that takes longest time in the frame among all transmitting concurrently. Only one packet per group is transmitted during the decision region in single transmission cases, while based on decision rules one to three packets per group are transmitted simultaneously in multiple transmission case. Let us assume in IIS-AMC-MT case, two packets are eligible to transmit at a decision instant. Because of their difference in packet size and/or difference in achievable modulation and coding scheme they occupy different time portion in the frame. For instance, a packet from one BS takes 0.25 ms while the other requires 0.20 ms. Next decision instant would be 0.25 ms after the current decision instant and the decision region in between these two points is 0.25 ms.

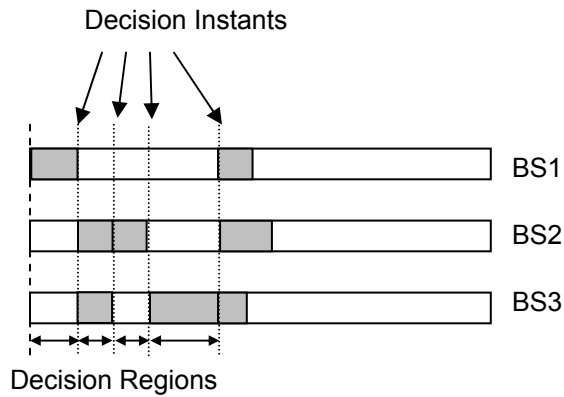


Figure 3.13: *Decision instant and decision region in IIS-AMC-MT*

3.4.2 Overview of Inter-sector Schedulers and Slot Allocations

We describe three scheduling schemes in this section and a comprehensive numeric example of IIS-AMC-MT will be presented in Chapter 4.

IIS-FM-ST

Fixed 16-QAM (*Quadrature Amplitude Modulation*) *Bit-Interleaved Coded Modulation* (BCIM) with a coding rate of $\frac{1}{2}$ is used in this scheme. Base stations in an interferer group exchange traffic related information such as the number of packets (with packet length and arrival time) arrived in previous frame duration. The scheduler checks the arrival time of all three *head-of-line* (HOL) packets and selects the candidate packet to be transmitted that has the earliest arrival time.

Basic functional blocks for this scheduler are shown in a flow diagram in Figure 3.14. This flow chart shows slot allocations in a particular frame for *interferer group 1*. It should be noted here that for BSs of group 1, packets are scheduled from the start of a frame to the end starting from left to right. However, to implement *group-wise orthogonality* as shown in Figure 3.12, BSs of groups 2 and 3 will start at the $\frac{1}{3}^{\text{rd}}$ and $\frac{2}{3}^{\text{rd}}$ of the frame, respectively, as discussed above which is not shown in the flow diagram.

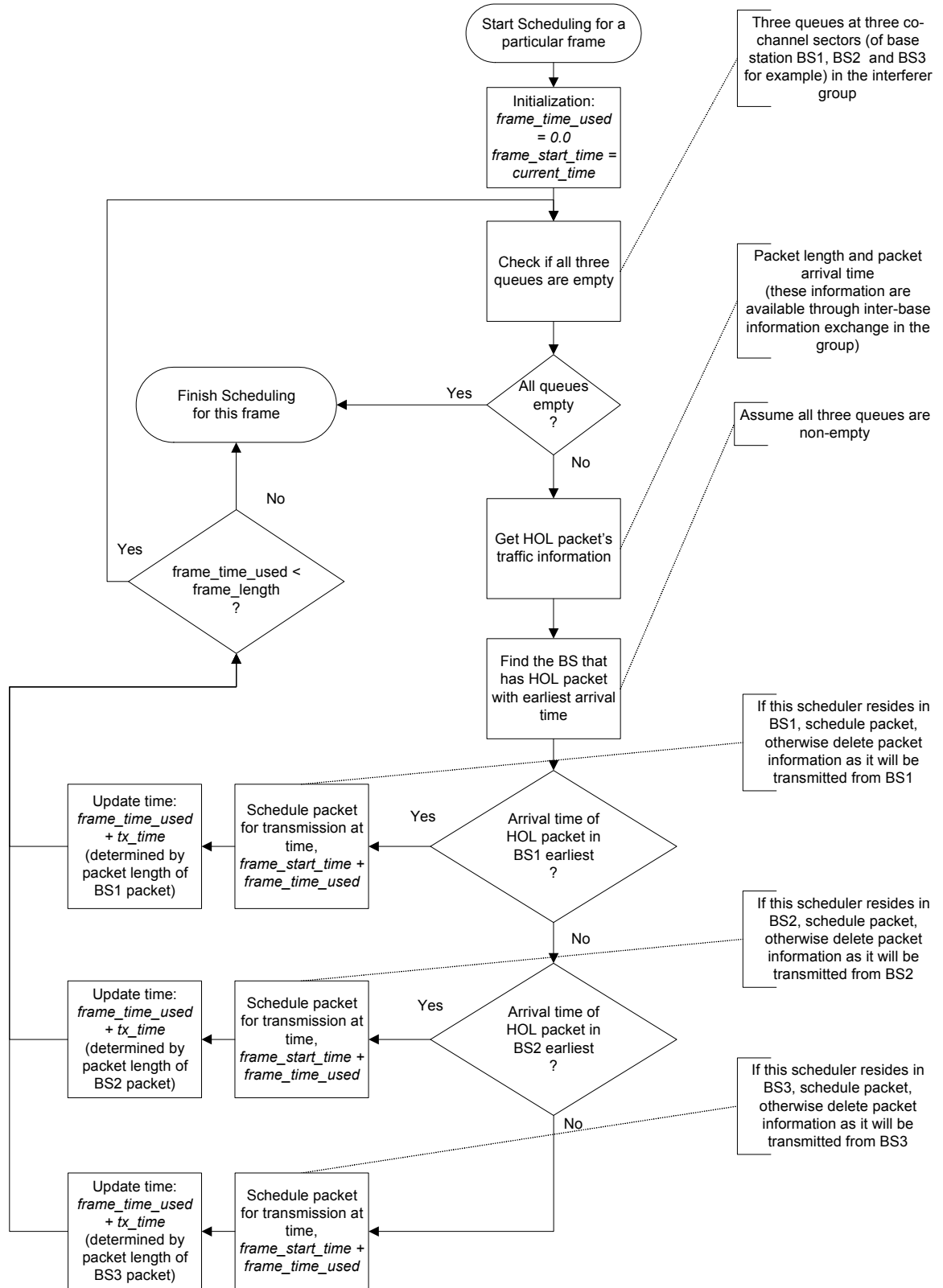


Figure 3.14: Flow diagram of inter-sector scheduler in IIS-FM-ST

IIS-AMC-ST

Like IIS-FM-ST, concurrent transmission is not permitted in this scheme. But this scheme takes channel state into account in the inter-sector scheduling. Adaptive modulation and coding is used. Base stations exchange traffic related information as well as link related information.

Figure 3.15 shows the algorithm for this scheme along with slot allocations for BSs of group 1 in a block diagram. At any decision instant, three HOL packets are compared to select the candidate packet for which the BS has the best link to user. At any time, if it happens that all three packets can not be transmitted because of their bad channel quality, *HOL blocking* occurs. To counter HOL blocking problem, the algorithm employs following rules as shown in Figure 3.15,

- Increment queue pointer so that another three packets (if all queues are non-empty at that point) which are positioned next to HOL are compared to find a candidate.
- If candidate found, schedule that packet for the current decision instant while keep the HOL packet intact at its position.
- If not, increment pointer and continue searching until a candidate can be found.

The above guidelines provide two benefits. First, HOL blocking is prevented and the resources are not wasted as the scheduler does not wait for the candidate packet's user link to come out of bad state. The position of all other packets that can not be transmitted up to the search point are kept at their original position and hence their priorities remain same, because at the next decision instant the scheduler will again look at the HOL packets and so on to select a candidate packet.

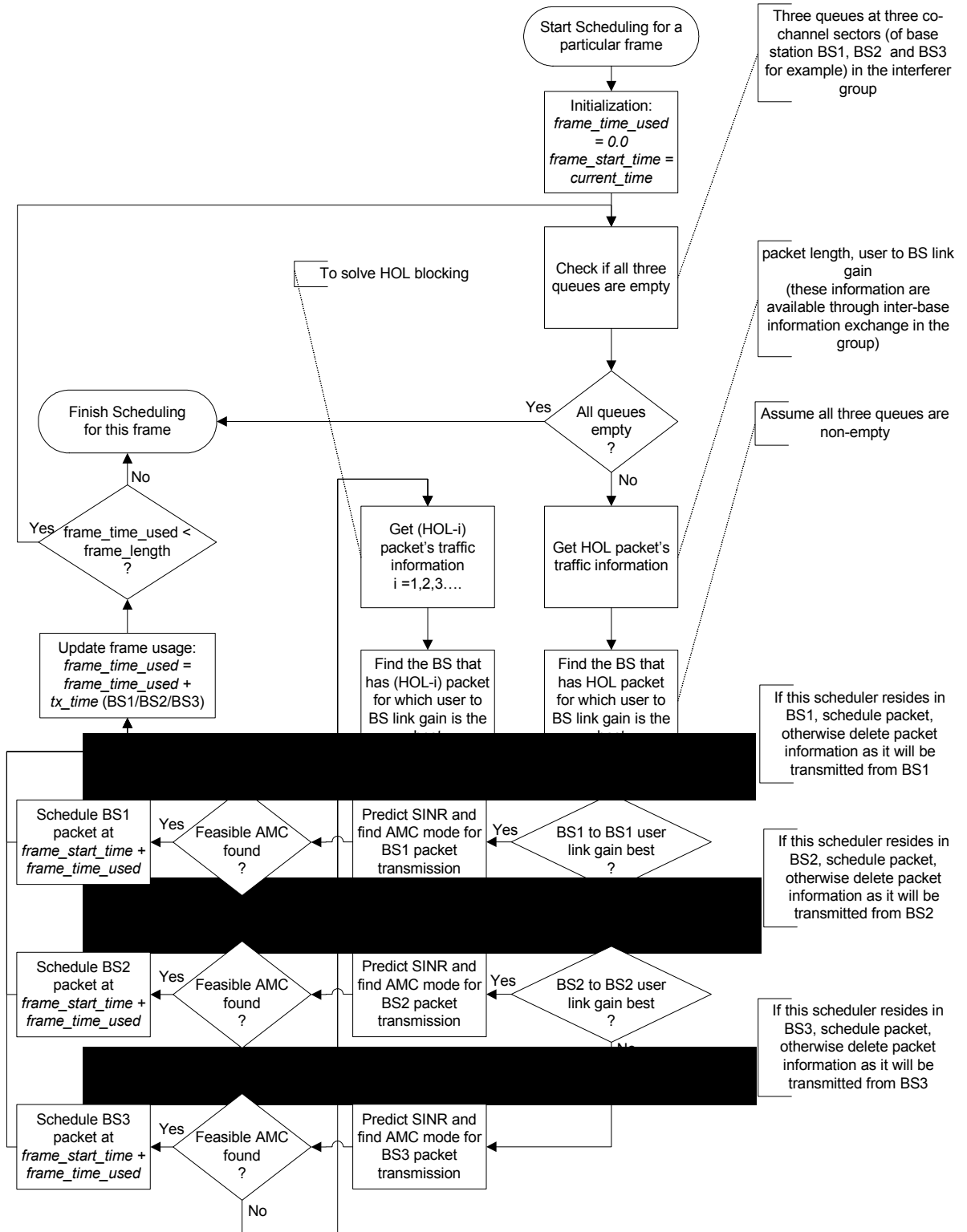


Figure 3.15: Flow diagram of inter-sector scheduler in IIS-AMC-ST

IIS-AMC-MT

This novel scheme constitutes the main contribution in this thesis; it tries to maximize number of concurrent transmission by allowing controlled interferers to transmit simultaneously in the interferer group. Base stations among interferer group exchange traffic and link related information. Inter-sector scheduler finds a combination of concurrent transmission that gives highest throughput efficiency. The basic functional block diagram of this algorithm is shown in Figure 3.16.

This scheme also employs rules discussed above to alleviate HOL blocking problems. If all three queues are non-empty, there are seven possible combinations of transmissions at a particular decision instant. For example, all three BSs transmit (1 choice) or two BSs transmit (3 choices), or only one BS transmits (3 choices). We should point out that the last three choices are the only available options in IIS-AMC-ST. The algorithm chooses multiple transmissions only when it is more efficient than best link single transmission IIS-AMC-ST. In other words, IIS-AMC-MT might decide to schedule a single packet per group if it is most efficient among all seven possibilities.

In IIS-AMC-MT, the decision region is optimized based on available HOL packets. Nevertheless, in many instances there are *holding times* when portions of frame are left empty. An approach has been taken to minimize holding time in case of IIS-AMC-MT decisions that yield multiple transmissions. Let us consider that two packets from BS1 and BS3 are to be scheduled as a result of scheduling decision in a decision region. BS1 packet occupies 0.3 ms while BS3 packet takes only 0.12 ms in the frame. The holding time for BS3 is 0.18 ms, as next decision instant will be 0.3 ms after the current decision instant. The scheduler searches BS3 queue to find a second packet that belongs to same user. If the packet fits into the holding time, the packet will be scheduled back-to-back with the originally decided packet, to utilize the holding time that otherwise be wasted.

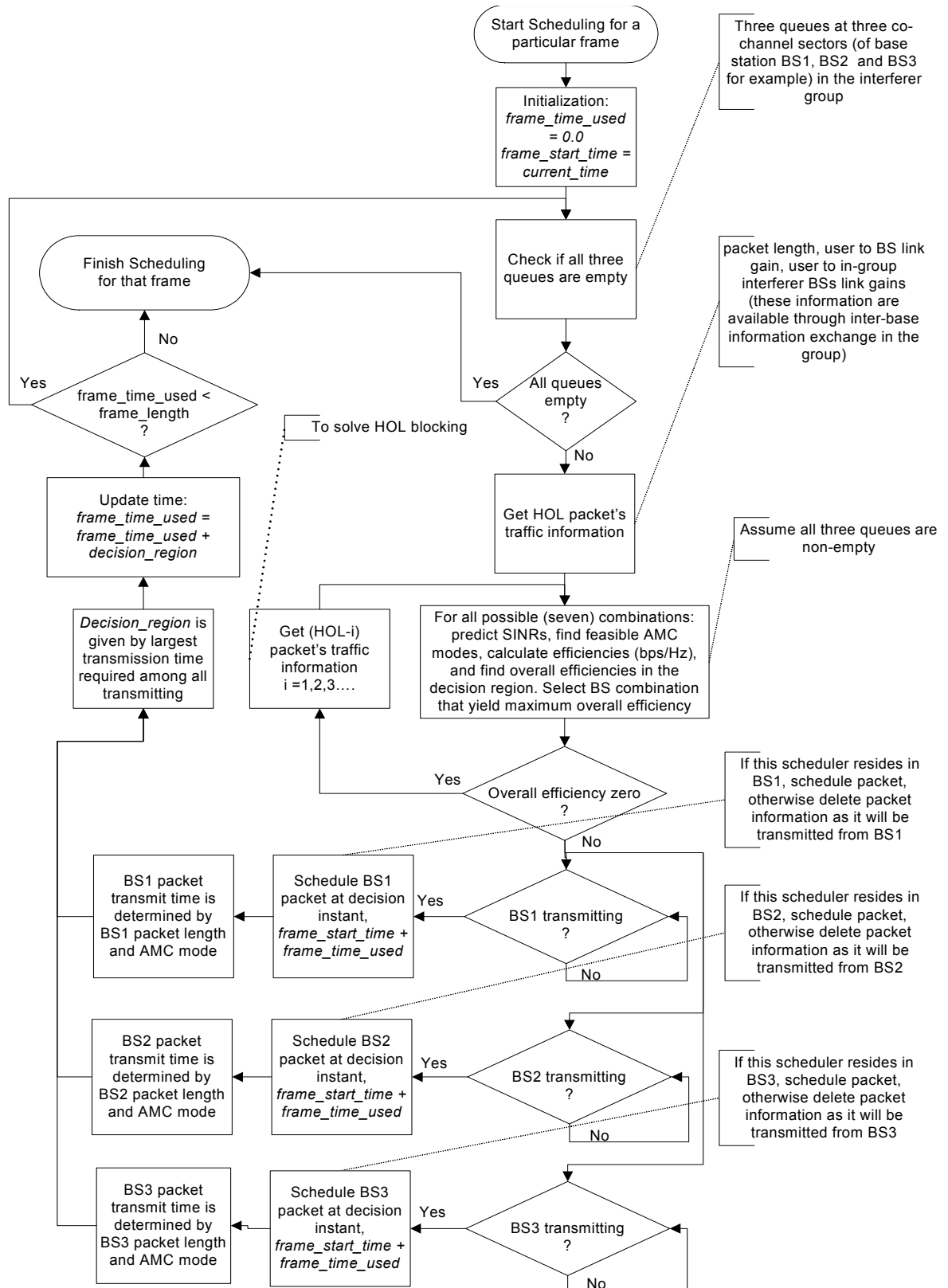


Figure 3.16: Flow diagram of inter-sector scheduler in IIS-AMC-MT

Chapter 4

Insight into Simulated Scheduling Schemes

4.1 Introduction

In this chapter, some preliminary yet crucial analyses of simulated scheduling schemes are presented. As mentioned in earlier chapters, in all three schemes, *intra-sector* scheduler uses *first-come-first-serve* (FCFS) discipline. Whenever a packet arrives for any user in the sector, it is placed at the tail of a common queue maintained for that sector. *Inter-sector* scheduler's service discipline is different for different schemes. Delay based single transmission is used for IIS-FM-ST, link quality based single transmission for IIS-AMC-ST and link quality based multiple transmissions is implemented in IIS-AMC-MT. A common framework for SINR computation, BS information exchange, SINR prediction and scheduling decision rules are discussed in the subsequent sections of this chapter. Finally, a few approaches are suggested in Section 4.6 to improve the performance of the system.

4.2 Framework for SINR Computation

We consider only downlink transmission in this thesis. Also, we assume that the transmit power is fixed for all base stations. Let us assume that users i, j , and k reside in in-group sectors I, J , and K , respectively. IG and OG represent set of in-group³ and out-of-group sectors, respectively, i.e., $IG \approx \{I, J, K\}$ and OG is the set of all BSs excluding those in IG . Let us consider again that P_I, P_J , and P_K are the transmit powers of sectors I, J , and K , respectively. Power control has not been considered and fixed transmit power has been used in this thesis, therefore $P_I = P_J = P_K$. It should be mentioned that if power control

³ Base stations in the interferer group.

were used, it would have been more beneficial for IIS-FM-ST than the schemes employing AMC. The IIS-FM-ST uses 16-QAM with coding rate of $\frac{1}{2}$, which requires a minimum SINR of 9.23 dB. Therefore, in a transmission to a user which has a good link (SINR \gg 9.23 dB), the base station would be able to reduce its power until SINR is slightly over 9.23 dB. By reducing its power base station will cause less interference to other transmissions. We should note that for 95% availability at cell boundaries, users have SINR better than 9.23 dB 95% of the time, and SINR inside the cell will almost always be much higher than 9.23 dB. Therefore, there is considerable room for power control in IIS-FM-ST. On the other hand, in IIS-AMC-ST and IIS-AMC-MT, base stations have limited room for power control. For example, if a transmission qualifies for 64-QAM with a coding rate of $\frac{3}{4}$, it requires a minimum SINR of 18.16 dB. Now, if the channel state is such that the transmission can achieve 19.0 dB, then the base station can reduce its power by 0.84 dB.

The SINR on a received packet at user i , assuming all nine BSs in the network are transmitting simultaneously, can be expressed as,

$$SINR_i = \frac{P_I G_I^i}{\sum_{\psi \in IG, \psi \neq I} P_\psi G_\psi^i + \sum_{\Theta \in OG} P_\Theta G_\Theta^i + P_N^i}, \quad (4.1)$$

where G_I^i is the link gain between the serving sector I and user i . G_ψ^i and G_Θ^i are the link gains between the interferer sectors in the group and out of group and the desired user i , respectively. These link gain parameters include the effect of antenna gain at the BS and the user's terminal as well as the propagation loss (including shadowing and fading) of the link. P_N^i is the average thermal noise power at the receiver of user i . It should be

noted that if a sector does not transmit simultaneously, its transmit power will have to be zero to calculate SINR.

Similarly, the SINRs of received packets at users j and k will be,

$$SINR_j = \frac{P_j G_j^j}{\sum_{\Psi \in IG, \Psi \neq J} P_\Psi G_\Psi^j + \sum_{\Theta \in OG} P_\Theta G_\Theta^j + P_N^j} \quad (4.2)$$

and,

$$SINR_k = \frac{P_k G_k^k}{\sum_{\Psi \in IG, \Psi \neq K} P_\Psi G_\Psi^k + \sum_{\Theta \in OG} P_\Theta G_\Theta^k + P_N^k}. \quad (4.3)$$

In reality all nine cells in the network might not transmit simultaneously. Therefore, the eligible terms those contribute to above equations will only be those that are transmitting simultaneously. A snap-shot of a multiple transmission instants are shown in the example in Figure 4.1, where the desired user i belongs to BS6. In this example, $IG \approx \{4,5,6\}$ and $OG \approx \{1,2,3,7,8,9\}$.

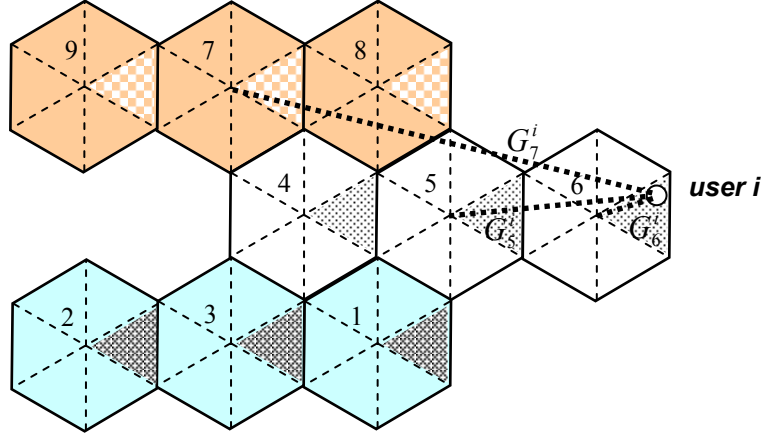


Figure 4.1: Link gain to desired user

We further assume that BS5 and BS7 are transmitting concurrently with the desired transmission from BS6 to user i . Therefore, actual SINR experienced by the received packet at user i is given by the following,

$$SINR_i = \frac{P_6 G_6^i}{P_5 G_5^i + P_7 G_7^i + P_N^i}. \quad (4.4)$$

It should be mentioned here that at any particular instant the maximum number of in-group interferers would be two while that of out of group would be six for the nine-cell network using IIS-AMC-MT scheme. In simulation, out-of-group interference from two far most sectors (BS9 and BS2 in the example) are neglected, as discussed in Appendix A.

The single transmission schemes, IIS-FM-ST and IIS-AMC-ST, do not allow the sectors in the interferer group to transmit simultaneously. Therefore, the term $\sum_{\psi \in IG, \psi \neq I} P_\psi G_\psi^i$ in (4.1) contributes nothing for these cases. Similar statement is true for (4.2) and (4.3). The SINR for single transmission cases become,

$$SINR_{ST_i} = \frac{P_I G_I^i}{\sum_{\Theta \in OG} P_\Theta G_\Theta^i + P_N^i}. \quad (4.5)$$

While the SINR for multiple transmission case such as IIS-AMC-MT remains the same as follows:

$$SINR_{MT_i} = \frac{P_I G_I^i}{\sum_{\psi \in IG, \psi \neq I} P_\psi G_\psi^i + \sum_{\Theta \in OG} P_\Theta G_\Theta^i + P_N^i}. \quad (4.6)$$

It is also worth to note that at any particular instant one sector per interferer group transmits in single transmission cases, the interference from out of group would be less in the IIS-AMC-ST scheme compared to that in IIS-AMC-MT when the network is loaded. Although IIS-AMC-MT suffers interference from own group, it would not affect the PER performance much as this interference is known from inter-BS signaling among sectors in the interferer group.

4.3 Base Station Information Exchange

BSs in an interferer group exchange traffic and link related information with each other at every frame interval. In the IIS-FM-ST scheme, BSs exchange only traffic related information such as the number of packets arrived during the period of the previous frame, the packet length and the packet arrival time. For example, BS6 will share the following information with BS4 and BS5 at every frame interval (Figure 4.1):

$$\{t_{a1}, L_1\}, \{t_{a2}, L_2\}, \dots, \{t_{aq}, L_q\} \parallel BS6.$$

In the above, q indicates the total number of packets arrived in the previous frame duration, and each tuple indicates the traffic parameters associated with each arrived packet. t_{aq} is the arrival time and L_q is the packet length of q^{th} packet in BS6. Similarly, BS4 and BS5 will share their traffic information with other two BSs.

For IIS-AMC-ST, in addition to traffic related information, link information G_I^i , G_J^j , and G_K^k are also exchanged. Sector I sends G_I^i to sector J and K , and receives G_J^j and G_K^k from J and K respectively. These are the link gains to desired user from its own sector.

In IIS-AMC-MT, additional gain values G_I^j , G_I^k , G_J^i , G_J^k , G_K^i , and G_K^j should be exchanged. These are the link gains from interferer sectors to users in I , J , or K .

These link gain parameters are monitored at the active user terminals and are reported back to serving base stations. For a user terminal that has been silent for a while, pilot signals from base stations can be used to calculate the link gains.

In fixed broadband wireless networks channel changes slowly as the shadowing does not change much in time and fading is slow as discussed in Section 3.2.1.3. Therefore, reporting channel state G does not have to be frequent and is feasible in such systems.

As BSs exchange information in the interferer group only, BSs can not predict the out of group interference.

4.4 SINR Prediction

SINR prediction is not required for IIS-FM-ST as it does not use any link state information for its scheduling decision and it does not use AMC. For the two schemes using AMC, SINR should be predicted in order to take advantage of the knowledge of the link state and employ AMC.

SINR is predicted from the exchanged link information; for IIS-AMC-ST it is given by,

$$SINR_{ST_i} \Big|_{predict} = \frac{P_I G_I^i}{P_N^i}, \quad (4.7)$$

and for IIS-AMC-MT,

$$SINR_{MT_i} \Big|_{predict} = \frac{P_I G_I^i}{\sum_{\Psi \in IG, \Psi \neq I} P_\Psi G_\Psi^i + P_N^i}. \quad (4.8)$$

As it apparent from (4.7) and (4.8), SINR predictions do not take out-of-group interference into account, therefore the estimations are optimistic. Several attempts have been made to reduce the out of group interference such as the usage of directional antennas and the employment of *group-wise orthogonal transmission* scheme etc. We

have proposed to use out-of-group interference guard to compensate this interference as will be discussed in later sections.

4.5 Scheduling Decision

4.5.1 IIS-FM-ST

As stated earlier, the decision for IIS-FM-ST is completely based on the packet arrival time. Each BS in the group is aware of the traffic information of packets in its transmission queue as well as those of other BSs in the group from exchanged information. Packets are scheduled at the start of every frame based on the arrival time. Scheduler compares the arrival time of the HOL packets of all three queues; the packet with the earliest arrival time will be chosen to be scheduled for that *decision instant*.

If I, J , and K are three BSs in the interferer group, then for a particular *decision instant*,

$$w = \arg \min_{I, J, K} (t_a^i, t_a^j, t_a^k), \quad (4.9)$$

where w is the BS that wins the service opportunity at that *decision instant*, and t_a^i , t_a^j and t_a^k are the arrival times of the HOL packets at sector I, J , and K destined to users i, j , and k , respectively.

4.5.2 IIS-AMC-ST

Service opportunity is given to the BS that has the best link to the user for its HOL packet. Base stations are aware of G_I^i , G_J^j , and G_K^k from the exchanged information. At any instant, this parameter is compared for HOL packets among all three BSs to find out the winner BS. If users i, j , and k are the candidates for HOL packets in sectors I, J , and K in the interferer group, then,

$$w = \arg \max_{I,J,K} (G_I^i, G_J^j, G_K^k). \quad (4.10)$$

Next, winner BS predicts the SINR according to (4.7). The packet is then scheduled to transmit with AMC scheme achievable with the predicted SINR for that *decision instant*.

4.5.3 IIS-AMC-MT

Service opportunity is given to a group of BSs that can transmit concurrently and yield best average spectral efficiency in the decision region. A combination of BSs is chosen to transmit at a particular decision instant based on the following relation,

$$w = \arg \max_{\text{combin}(I,J,K)} (\Gamma_{I,J,K}, \Gamma_{I,J}, \Gamma_{J,K}, \Gamma_{K,I}, \Gamma_I, \Gamma_J, \Gamma_K), \quad (4.11)$$

where w is the combination of sectors transmit concurrently and Γ_w is the aggregate spectral efficiency in bps/Hz for the combination of transmissions taking account for the *holding time*.

There are seven possibilities with three BSs as reflected in (4.11), i.e., all three Bss transmit (1 choice), two BSs transmit (3 choices), or only one BS transmits (3 choices). For each combination, first, the SINRs are predicted from exchanged information. In the case when all three BSs I , J , and K transmit concurrently to respective users i , j , and k , each reception will have two in-group interferers. Therefore, the predicted SINR for user i 's packet is,

$$SINR_{MT_i} \Big|_{\text{predict}} = \frac{P_I G_I^i}{P_J G_J^i + P_K G_K^i + P_N^i}. \quad (4.12)$$

Similarly, for BS J and K ,

$$SINR_{MT_j} \Big|_{predict} = \frac{P_j G_J^j}{P_I G_I^j + P_K G_K^j + P_N^j} \quad (4.13)$$

and,

$$SINR_{MT_k} \Big|_{predict} = \frac{P_k G_K^k}{P_I G_I^k + P_J G_J^k + P_N^k}. \quad (4.14)$$

Similarly, for the three two-transmission combinations, each reception will experience one in-group interferer and SINRs will be predicted accordingly. In three single-transmission combinations, there is no in-group interferer and the SINRs will be predicted correspondingly.

From these predicted SINRs, the achievable AMC modes, and respective spectral efficiency can be obtained from Table 3.2 for each link. Finally, the aggregate spectral efficiency in the decision region is calculated for each possible combination. Service opportunity is granted to the group of BSs that gives highest aggregate spectral efficiency as shown in (4.11).

Let us give an example of an IIS-AMC-MT decision instant which has been taken from simulation. In this example, the queues for BSs I , J , and K are non-empty. The following information for HOL packets (destined for users i , j , and k) is available at each BS:

$$\begin{aligned} G_I^i &= 4.048685e-012 \rightarrow \text{Link gain from sector } I \text{ to user } i \\ G_J^j &= 6.549013e-011 \rightarrow \text{Link gain from sector } J \text{ to user } j \\ G_K^k &= 4.210742e-013 \rightarrow \text{Link gain from sector } K \text{ to user } k \\ G_J^i &= 3.131048e-013 \rightarrow \text{Link gain from sector } J \text{ to user } i \\ G_K^i &= 3.223645e-014 \rightarrow \text{Link gain from sector } K \text{ to user } i \\ G_I^j &= 8.627985e-013 \rightarrow \text{Link gain from sector } I \text{ to user } j \end{aligned}$$

$G_K^j = 7.286561e-014 \rightarrow$ Link gain from sector K to user j

$G_I^k = 9.832234e-015 \rightarrow$ Link gain from sector I to user k

$G_J^k = 3.793328e-014 \rightarrow$ Link gain from sector J to user k

$L_p^i = 2504 \rightarrow$ Packet length of sector I 's HOL packet

$L_p^j = 3376 \rightarrow$ Packet length of sector J 's HOL packet

$L_p^k = 4248 \rightarrow$ Packet length of sector K 's HOL packet

Using these available information IIS-AMC-MT scheduler makes a decision of transmissions (which combination) that optimize the throughput efficiency for the decision region. There are seven possible combinations as follows:

Combination 1: I, J and K transmit

When all three transmit simultaneously each user receives interference from the other two in-group BSs. Therefore, predicted SINR as per (4.12)-(4.14) are as follows:

$$SINR_i = 10.47 \text{ dB}$$

$$SINR_j = 18.39 \text{ dB}$$

$$SINR_k = 8.07 \text{ dB}$$

With above SINRs sectors $I, J,$ and K can transmit their packets with the following AMC modes (from Table 3.2):

$$AMC_I = 8 \text{ (16-QAM with a coding rate of } \frac{1}{2}\text{),}$$

$$AMC_J = 3 \text{ (64-QAM with a coding rate of } \frac{3}{4}\text{),}$$

$$AMC_K = 9 \text{ (QPSK with a coding rate of } \frac{7}{8}\text{).}$$

With these AMC modes and respective packet size, transmission times of these packets would be (obtained using (3.13)):

$$t_d^i = 0.000417 \text{ sec,}$$

$$t_d^j = 0.000250 \text{ sec,}$$

$$t_d^k = 0.000809 \text{ sec.}$$

The longest of the above times defines the decision region as follows:

$$t_r = 0.000809 \text{ sec.}$$

Now for the achieved AMC modes, the spectral efficiencies of individual sectors are given as:

$$\eta_I = 2.00 \text{ bps/Hz}$$

$$\eta_J = 4.50 \text{ bps/Hz}$$

$$\eta_K = 1.75 \text{ bps/Hz}$$

The aggregate spectral efficiency for all three transmissions is given by,

$$\Gamma_{I,J,K} = \eta_I \times \frac{t_d^i}{t_r} + \eta_J \times \frac{t_d^j}{t_r} + \eta_K \times \frac{t_d^k}{t_r}, \text{ which yields,}$$

$$\Gamma_{I,J,K} = 4.17 \text{ bps/Hz}$$

In a similar way, scheduler finds the aggregate spectral efficiency for all other combinations as described below.

Combination 2: I and J transmit

$$SINR_i = 10.88 \text{ dB}$$

$$SINR_j = 18.71 \text{ dB}$$

$$AMC_I = 8 \text{ (16-QAM with a coding rate of } \frac{1}{2}\text{)}$$

$$AMC_J = 3 \text{ (64-QAM with a coding rate of } \frac{3}{4}\text{)}$$

$$t_d^i = 0.000417 \text{ sec}$$

$$t_d^j = 0.000250 \text{ sec}$$

$$t_r = 0.000417 \text{ sec}$$

$$\eta_I = 2.00 \text{ bps/Hz and } \eta_J = 4.50 \text{ bps/Hz}$$

$$\Gamma_{I,J} = 4.70 \text{ bps/Hz}$$

Combination 3: J and K transmit

$$SINR_j = 28.58 \text{ dB}$$

$$SINR_k = 8.78 \text{ dB}$$

$$AMC_J = 1 \text{ (64-QAM with a coding rate of } 1\text{)}$$

$$AMC_K = 9 \text{ (QPSK with a coding rate of } \frac{7}{8}\text{)}$$

$$t_d^j = 0.000188 \text{ sec}$$

$$t_d^k = 0.000809 \text{ sec}$$

$$t_r = 0.000809 \text{ sec}$$

$$\eta_J = 6.00 \text{ bps/Hz and } \eta_K = 1.75 \text{ bps/Hz}$$

$$\Gamma_{J,K} = 3.14 \text{ bps/Hz}$$

Combination 4: I and K transmit

$$SINR_i = 19.08 \text{ dB}$$

$$SINR_k = 11.82 \text{ dB}$$

$$AMC_I = 3 \text{ (64-QAM with a coding rate of } \frac{3}{4}\text{)}$$

$$AMC_K = 7 \text{ (16-QAM with a coding rate of } \frac{2}{3}\text{)}$$

$$t_d^i = 0.000185 \text{ sec}$$

$$t_d^k = 0.000531 \text{ sec}$$

$$t_r = 0.000531 \text{ sec}$$

$$\eta_I = 4.50 \text{ bps/Hz and } \eta_K = 2.67 \text{ bps/Hz}$$

$$\Gamma_{I,K} = 4.24 \text{ bps/Hz}$$

Combination 5: I transmits

$$SINR_i = 23.56 \text{ dB}$$

$$AMC_I = 2 \text{ (64-QAM with a coding rate of } \frac{7}{8}\text{)}$$

$$\Gamma_I = \eta_I = 5.26 \text{ bps/Hz}$$

Combination 6: J transmits

$$SINR_j = 35.64 \text{ dB}$$

$$AMC_J = 1 \text{ (64-QAM with a coding rate of } 1\text{)}$$

$$\Gamma_J = \eta_J = 6.00$$

Combination 7: K transmits

$$SINR_k = 13.73 \text{ dB}$$

$$AMC_K = 6 \text{ (16-QAM with a coding rate of } \frac{3}{4}\text{)}$$

$$\Gamma_K = \eta_K = 3.00$$

Now, the scheduler will decide the winning combination as per (4.11), which would be ‘combination 6’ for this example as it yields the highest aggregate spectral efficiency.

4.6 Effect of Out-of-Group Interferers and Compensation

In the prediction of SINR as per (4.7) and (4.8), out of group interference has been neglected. As the network is interference-limited due to its small cell size and low propagation exponent, out of group interferers are occasionally strong and may have considerable impact on the performance of the network. An approach has been made to reduce this interference by employing *group-wise orthogonal* transmission as discussed in Chapter 3, which is effective only for lighter network loading. The in-group interference does not exist in IIS-AMC-ST and is known in IIS-AMC-MT. Therefore, the difference between predicted SINR and actual SINR is a function of the out of group interferers in both cases.

Lower beamwidth user antenna will help reduce this interference. In simulations, network performance metrics for different schemes are obtained with 60° directional receiver antennas. To observe the effect of receiver antenna beamwidth, a second set of simulations has been performed with 30° directional user antenna. Better performances are expected in the later case, because the intensity of the out of group interferers will be less as each receiver antenna is pointing towards its own BS. This improvement is expected in all three scheduling schemes.

In another approach, for adaptive modulation cases, an amount of compensation guard is considered for the out of group interferers while making prediction of the SINR instead of neglecting it completely. Let us denote that 50-th percentile of the error between the

actual and predicted SINR is $\phi(l)$ (in dB), which is a function of network loading l . The predicted SINR without any correction factor is always optimistic and the effect of overestimated SINR would result in higher packet error rates. In this thesis, the values of $\phi(l)$ can be generated from simulations. First, a set of SINRs for different loading are noted in the presence of out-of-group interferers. Then, a second set is generated where the out-of-group interferers are neglected. Now, the difference of the 50th-percentile SINR (in dB) of these two sets gives $\phi(l)$.

This $\phi(l)$ set is used in decision making processes in the scheduling schemes employing AMC. The amount of error $\phi(l)$ (in dB) would have to be subtracted from the predicted SINR (in dB) given by (4.7) and (4.8) to obtain the expected SINR for IIS-AMC-ST and IIS-AMC-MT as follows,

$$SINR_{ST_i} \Big|_{\text{expected}} = 10 \log_{10} \left(\frac{P_I G_I^i}{P_N^i} \right) - \phi(l) \quad (4.15)$$

and

$$SINR_{MT_i} \Big|_{\text{expected}} = 10 \log_{10} \left(\frac{P_I G_I^i}{\sum_{\Psi \in IG, \Psi \neq I} P_\Psi G_\Psi^i + P_N^i} \right) - \phi(l). \quad (4.16)$$

It should be noted here that the effect of out-of-group interference can not be compensated totally as $\phi(l)$ is a variable for particular network loading that changes from packet to packet. Nevertheless, employing this guard will improve PER performance of the scheduling schemes employing AMC. However, the larger the guard, the lower the throughput will be as scheduler will choose the AMC modes conservatively.

Chapter 5

Simulation Results and Analysis

5.1 Introduction

In this chapter, collected statistics based on the simulation models and schemes developed in the previous chapters are presented and analyzed critically. The main objective of these simulations is to evaluate the described scheduling schemes and quantify the benefits of integrating AMC with scheduling techniques. Another major goal is to determine performance gain that can be achieved by allowing concurrent transmissions of in-group interferers. Section 5.2 summarizes system parameters and defines the performance metrics observed during the course of simulations. In Section 5.3, we present some key observations that unveil the potential of benefits for using AMC, and concurrent transmissions of in-group sectors. Results are structured primarily according to three different simulation scenarios as discussed in Chapter 4.

First, in Section 5.4, we present basic results for three scheduling schemes, i.e., IIS-FM-ST, IIS-AMC-ST, and IIS-AMC-MT, obtained by using 60° directional antennas both at sector and user stations. Results are compared to evaluate performance gain due to integration of AMC with scheduling and/or concurrent transmissions of in-group sectors. Secondly in Section 5.5, to observe the impact of out-of-group interferers on network performance, we use 30° directional user antenna instead of 60° . The results obtained in this case are compared with the first set and the performance enhancements resulted from narrower beamwidth user antenna are observed. As discussed in Chapter 4, in the above two sets of results, SINR predicted from available in-group link information is optimistic that might result in high packet error rate for scheduling schemes that employ AMC.

Therefore, in the third set of results, we first determine the out-of-group interference compensation amount $\phi(l)$, which varies with network loading. Scheduler subtracts $\phi(l)$ from the predicted SINR to find expected SINR. Packet error rate in adaptive modulation cases are expected to improve, as the scheduler takes out-of-group interferers in account while making scheduling decisions. Performance results with this out-of-group interference compensation are discussed in Section 5.6. Finally, in Section 5.7 we present comparative analysis between IIS-AMC-ST and IIS-AMC-MT in a less interference limited scenario.

5.2 System Parameters and Performance Metrics

The system parameters used in simulations are listed in Table 5.1. A detailed calculation of link budget is enclosed in Appendix B.

Table 5.1: System Parameters

Hexagonal six-sectored cell radius (km)	2.0
Propagation exponent, n	3.0 & 3.7
Fixed transmit power (Watts)	2.2 ($n = 3.0$) & 50.0 ($n = 3.7$)
Sector antenna (60° beamwidth) gain (dB)	20 (front 10, back -10)
User antenna (60° and 30° beamwidth) gain (dB)	10 (front 5, back -5)
Transmission direction	Downlink
Uplink-downlink duplexing	FDD
Multiple access	TDMA
Frequency reuse factor	1/6
Carrier frequency, f (GHz)	2.5
Channel bandwidth, B (MHz)	3.0
Time correlated Rayleigh fading: max. Doppler freq., f_m (Hz)	2.0
Independent lognormal shadowing: standard deviation (dB)	8.0
Noise power, P_N (dBW)	-134.06
Frame length (ms)	5.0
Data rate per user (kbps)	404.16
Simulation tool	OPNET Modeler 9.1 with wireless module

Scheduling schemes are evaluated in terms of the essential network performance parameters such as *packet error rate* (PER), *net throughput*, *area spectral efficiency* (ASE), *dropped packet* and *end-to-end* (ETE) *packet delay*. These performance metrics are functions of network loading, therefore these parameters are observed against the number of users per sector. Number of users per sector is varied from 4 to 24 in all simulation schemes and scenarios.

PER is calculated as the ratio of the number of erroneous packets to the number of total packets received during the simulation period. The net throughput is expressed as number of packets received correctly per frame per sector. Area spectral efficiency is a measure of resource utilization, which is expressed here as bits (correctly received information bits) per second per Hz per sector. Packet is dropped by the scheduler when delay exceeds 195 ms. The delay constraint is 200 ms with a 5 ms safety margin provided to ensure that every packet received by the user meets delay requirement. We express dropped packets in packets per frame per sector. End-to-end packet delay is a quality measure of service that is observed in ms as 50th-percentile end-to-end (ETE) packet delay. The 50th-percentile ETE packet delay is the median value of ETE packet delay. This delay is the summation of queuing delay and packet transmission delay. The delay measure does not include the delays of the dropped packets in the queue at transmitter side.

Simulation schemes in all scenarios have been run with the same *seed* value to preserve similar randomness in the results so that the presented results for different schemes are comparable by their trends. The network is executed with different scheduling schemes and scenarios in real-time, and the statistics are taken over long enough time duration

until the observed parameters converge. It should be noted that *shadowing* for a particular user does not change over simulation time as the user is fixed. At any loading, a set of shadowing values is assigned for all users (randomly placed) in the network. During the course of simulation time neither location of user nor the shadowing value is changed. For any particular user, fading is correlated and changes over time. Therefore, performed simulation is Monte-Carlo in the time axis, but not for user locations and shadowing. However, statistics are collected in all nine cells in the network and there is some averaging with respect to the user locations.

5.3 Key Observations

Before going into detailed discussion about performances, let us first have a glimpse into some important observations that exhibit potential for enormous throughput gain in AMC and/or multiple transmission cases.

Figure 5.1 shows the probability mass function (PMF) of adaptive AMC modes used by IIS-AMC-ST and IIS-AMC-MT. These results are obtained from simulation using same power budget (see Appendix B) used for IIS-FM-ST. Although, the PMFs are obtained for a network loading of 12 users per sector, they are nearly invariant with loading. We observe from the Figure that IIS-AMC-ST is capable of using the highest AMC mode, i.e., 64-QAM with coding rate of 1, 75% of the time. And, IIS-AMC-MT can use 64-QAM with coding rate of 1 63% of the time. 64-QAM with coding rate of 1 corresponds to spectral efficiency of 6.0 bps/Hz. IIS-FM-ST always uses 16-QAM with a coding rate of $\frac{1}{2}$ that translates into efficiency of 2.0 bps/Hz. Thus, adaptive modulation schemes show tremendous potential to achieve throughput and efficiency gain.

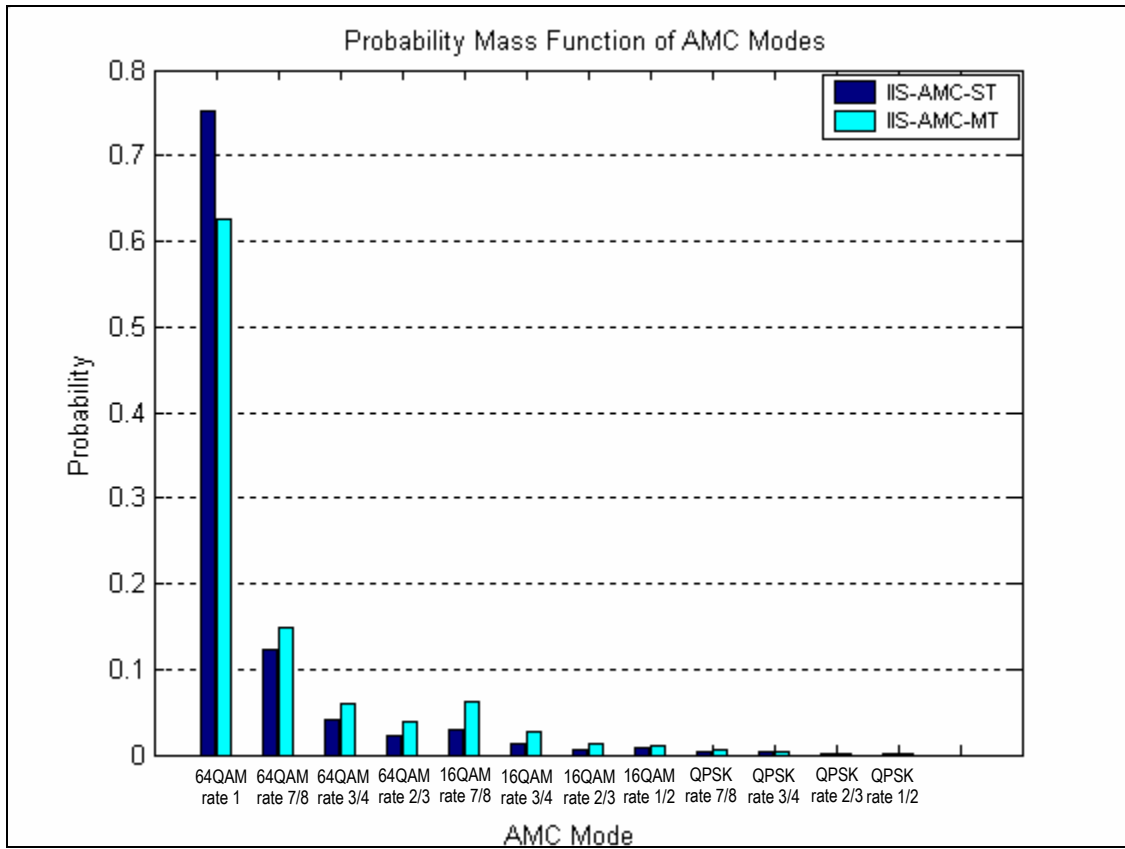


Figure 5.1: Probability mass function (PMF) of AMC modes used by IIS-AMC-ST and IIS-AMC-MT (60° sector antenna, 60° user antenna, 12 users/sector)

It can be recalled that IIS-AMC-MT scheme is designed to increase the network throughput and efficiency, and decrease delay. In IIS-AMC-MT, scheduler decides for either one transmission or two transmissions, or three transmissions, based on the aggregate spectral efficiency achieved for that decision region. Figure 5.2 shows plots of percentage of IIS-AMC-MT scheduler decisions that settle for one transmission, two transmissions, and three transmissions at different network loading.

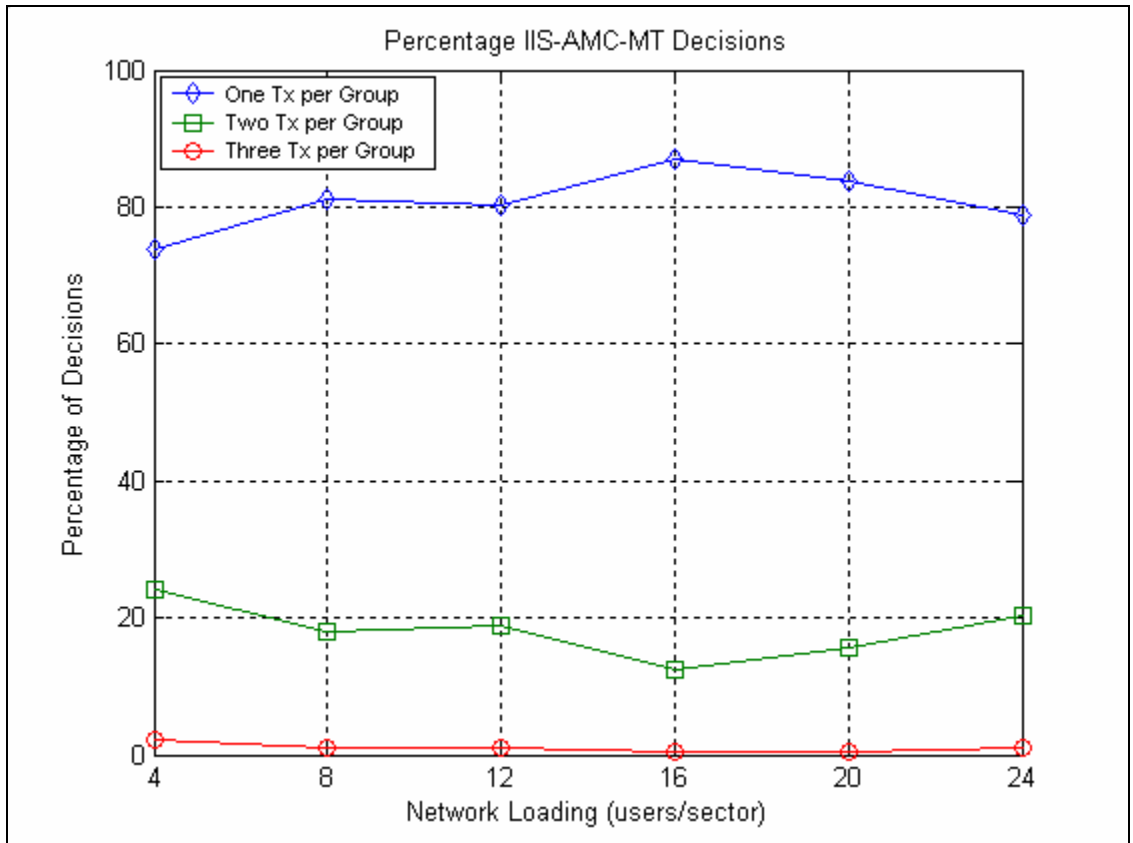


Figure 5.2: Percentage of one, two and three transmissions per group in IIS-AMC-MT

We observe in Figure 5.2 that around 75-85% of the decisions converge into single transmissions, while around 14-24% decisions yield two transmissions, and the remaining 1% are the case when all three in the group are decided to transmit concurrently. Although when multiple transmissions are used AMC modes are selected conservatively as can be seen in Figure 5.1, nevertheless IIS-AMC-MT scheme is expected to show better overall performance resulted from multiple transmission decisions in comparison to IIS-AMC-ST.

5.4 Results for 60° Beamwidth Antennas both at Sector and User Stations

5.4.1 Packet Error Rate (PER)

Figure 5.3 compares packet error rate in different scheduling schemes.

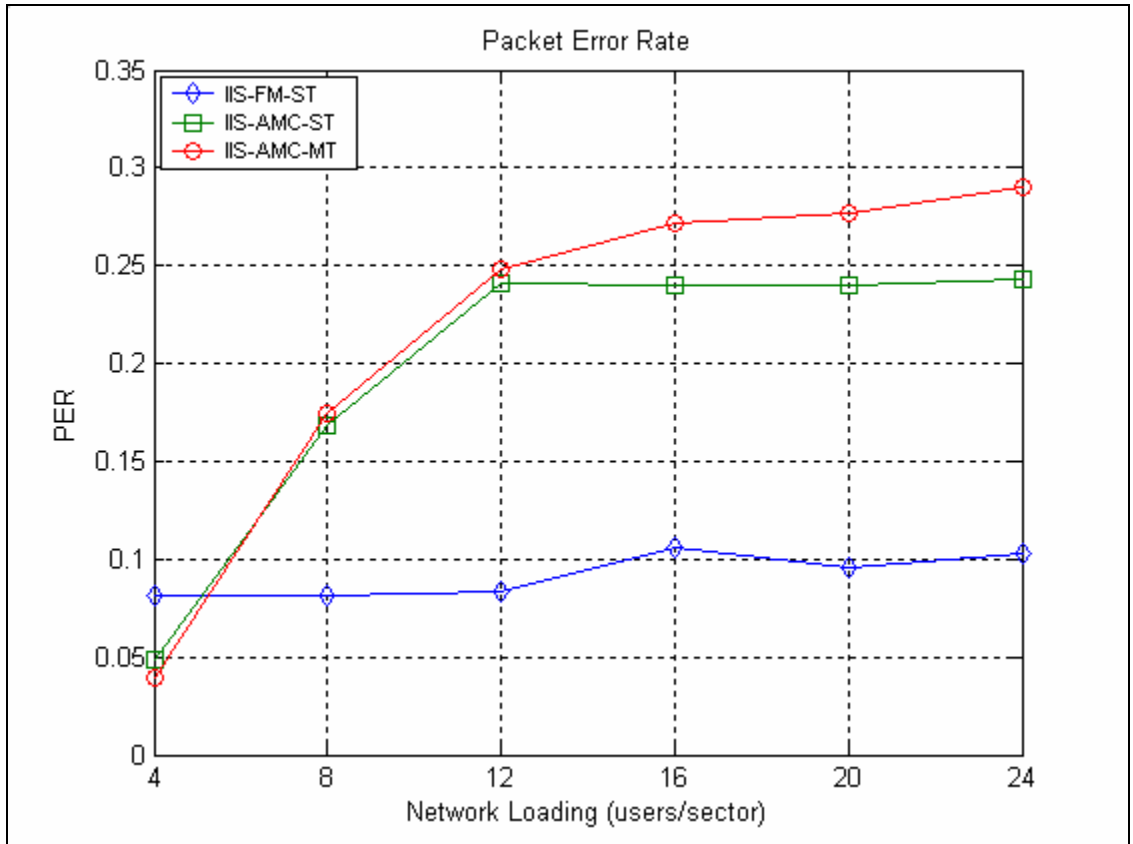


Figure 5.3: Packet error rate in different schemes

For network loading of 4 users per sector, packet error rate in IIS-FM-ST, IIS-AMC-ST and IIS-AMC-MT are 0.08, 0.05 and 0.04, respectively. Because of group-wise orthogonal allocations, effect of out of group interferers is least prominent in IIS-AMC-MT; concurrent in-group transmissions and, AMC enable packets to be allocated in the frame with less frame occupancy. IIS-FM-ST requires largest frame occupancy at this loading, and hence experiences highest number of out-of-group interferers resulting high

PER. This can be clarified more by examining Figure 5.4 which shows the PMF of number of out-of-group interferers in different schemes at this loading. These interferers appear and leave at random time during desired packet's life. In the Figure, the numbers in x-axis do not imply that they appear simultaneously. Nevertheless, it is a measure of intensity of interference that we can use to explain packet error rate at any network loading.

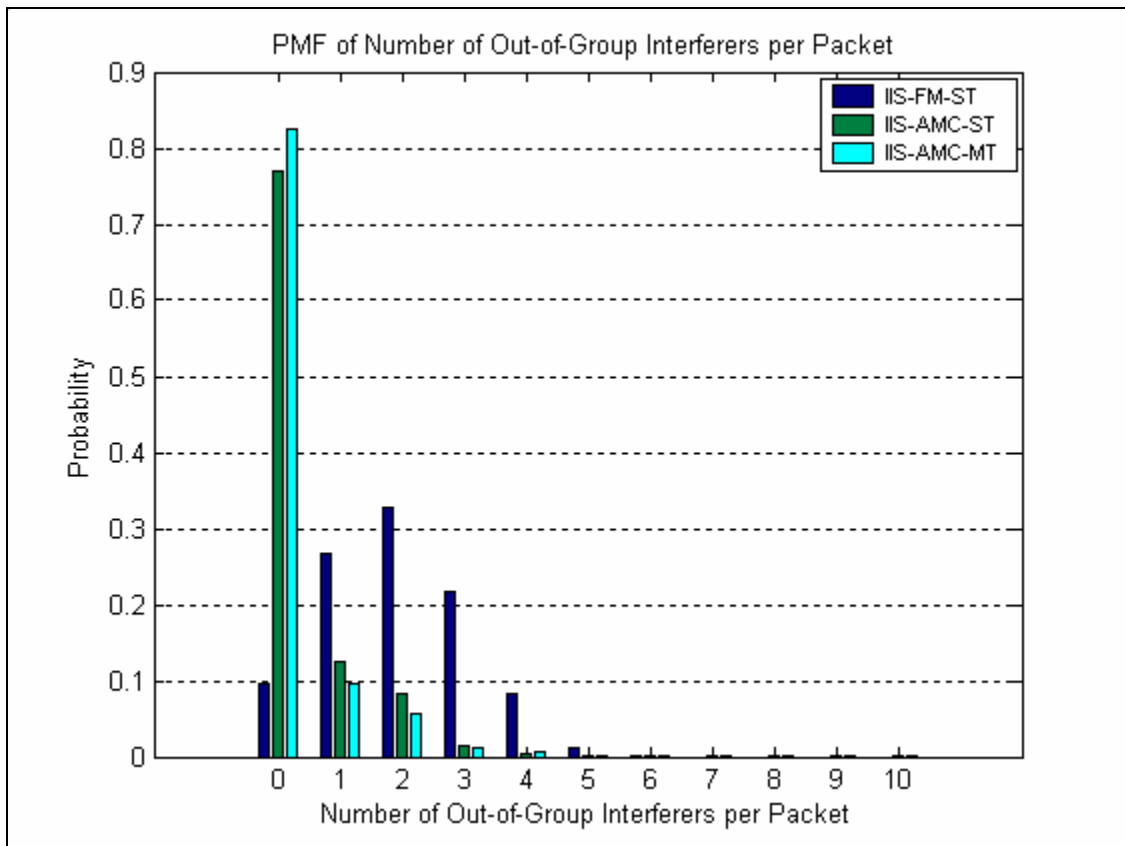


Figure: 5.4: Probability mass function of the number of out-of-group interferers appear per packet at loading of 4 users per sector

The impact of orthogonal slot allocations is also observed the PMF shown in Figure 5.4. It is found that 84.4% packets do not experience any out-of-group interferers in IIS-

AMC-MT, while this number is 77% for IIS-AMC-ST and, 9.5% in IIS-FM-ST. In IIS-FM-ST, the probability that a packet experiences one or more out-of-group interferers is much higher compared to IIS-AMC-ST or IIS-AMC-MT. This is the reason why the PER in IIS-FM-ST is much higher than those for schemes employing AMC. Also, as IIS-FM-ST scheduler does not take channel state into account, high packet error rate is expected in this case.

As loading increases, number of out-of-group interferers increases in adaptive modulation cases and PER increases with loading. From Figure 5.3 we see that PER in IIS-FM-ST does not increase much with loading because frames are pretty much saturated starting from loading 4-5 users per sector (explained more in later sections). Beyond that loading, packets are mostly discarded by the scheduler because of excessive delay. Therefore, the pattern of arriving interference does not change which in essence results almost steady PER beyond the loading of 4-5 users per sector.

At loadings of 8 and 12 users per sector, packet error rates for IIS-AMC-ST and IIS-AMC-MT are pretty close to each other. The effect of group-wise orthogonal slot allocations starts to diminish during these loadings and perhaps completely disappeared at 16 users per sector loading resulting considerably higher PER in IIS-AMC-MT. This can be explained again from the out-of-group interferers at this loading as shown in Figure 5.5. As the benefits of group-wise orthogonality are not present at this loading level, the increase in out-of-group interferers are causing very low probability of receiving packets with no out-of-group interferers in IIS-AMC-MT. Also, the probability of having packets with three or more interferers is much higher in IIS-AMC-MT that results in higher packet error rate than that of IIS-AMC-ST.

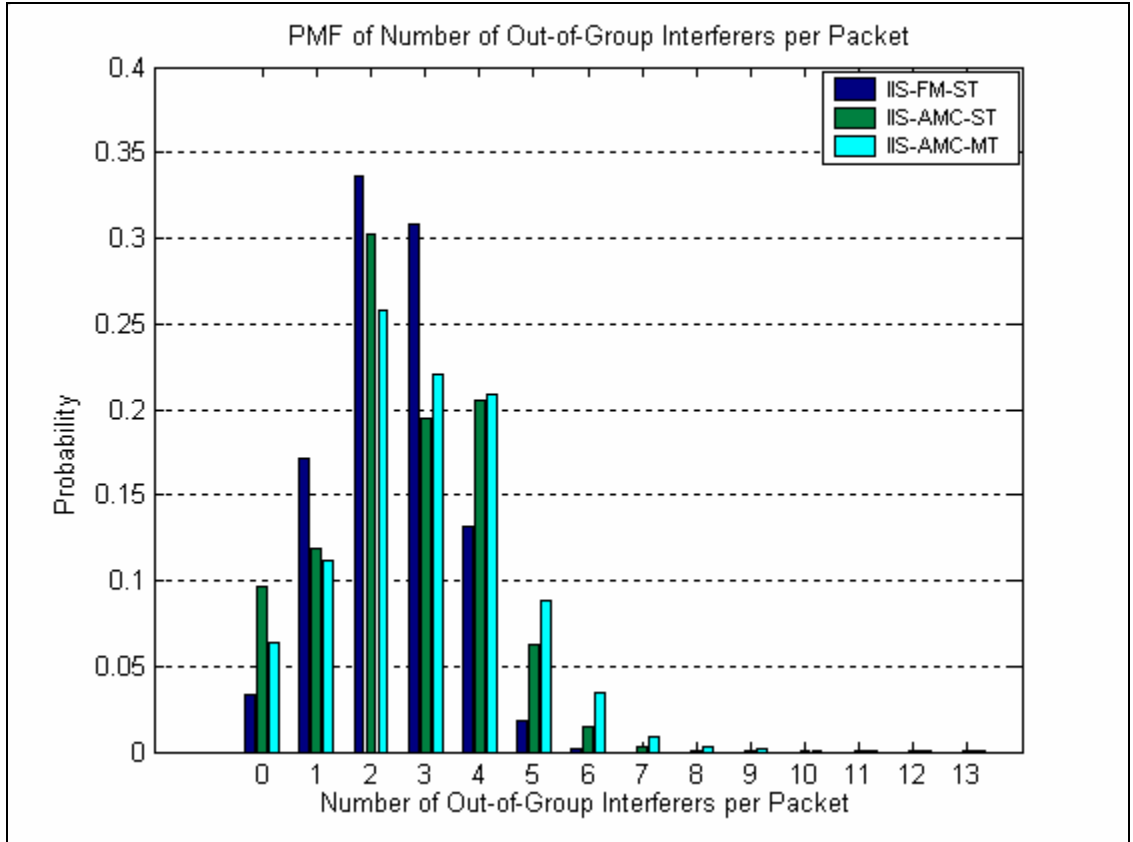


Figure: 5.5 Probability mass function of the number of out-of-group interferers appear per packet at loading of 16 users per sector

5.4.2 Area Spectral Efficiency and Net Throughput

Both schemes employing AMC provide much higher area spectral efficiency and hence net throughput compared to the fixed modulation case. This throughput gain is the result of the fact that these schemes are using higher level of AMC modes as shown in Figure 5.1. Figures 5.6 and 5.7 show area spectral efficiency and net throughput curves for different scheduling schemes.

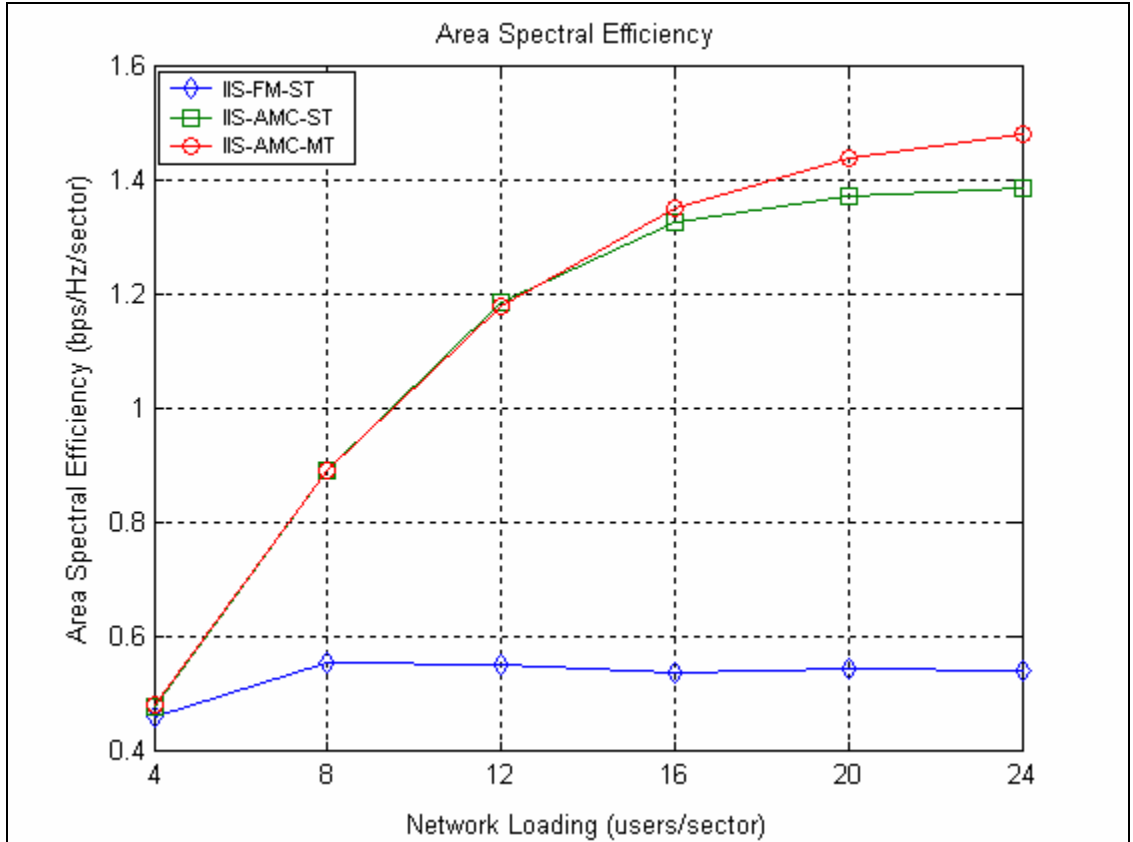


Figure 5.6: Area spectral efficiency in different schemes

In Figure 5.6, we see that the area spectral efficiency is around 0.54 bps per Hz per sector in IIS-FM-ST, and almost unchanged with increasing network loading. This is due to the fact that no matter how high the offered traffic is, the network is able to serve according to its capacity. The excess traffic that is not served will wait in the queue and will be dropped eventually when the delay of the packet grows beyond threshold. At 24 users per sector network loading, the area spectral efficiencies for IIS-FM-ST, IIS-AMC-ST and IIS-AMC-MT are 0.54, 1.39 and 1.48, respectively. The gain due to AMC translates into 157% efficiency gain if we compare the IIS-FM-ST and IIS-AMC-ST. Multiple in-group transmissions yield 6.5% more efficiency if we compare IIS-AMC-ST with IIS-AMC-MT at loading value of 24 users per sector.

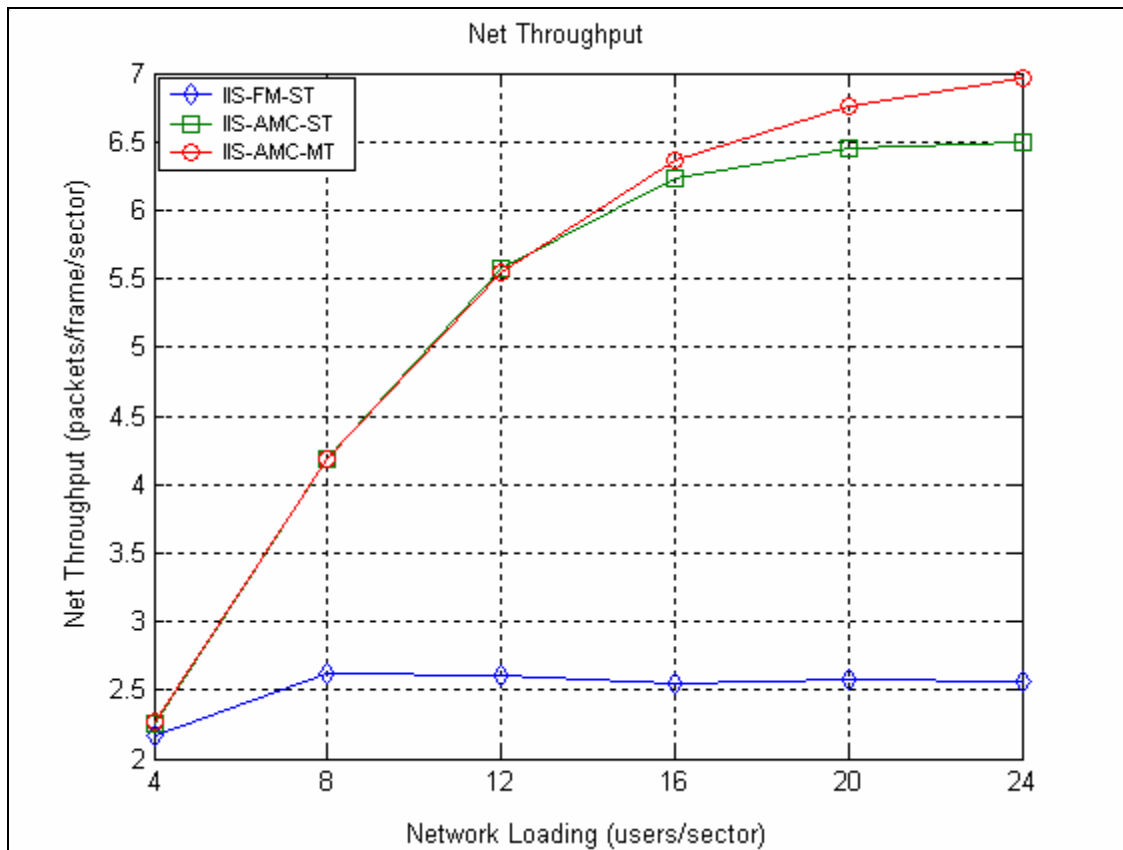


Figure 5.7: Net throughput in different schemes

A similar analysis and comments are applicable for the net throughput curves in Figure 5.7. Until 12 users per sector, area spectral efficiency and net throughput are comparable in IIS-AMC-ST and IIS-AMC-MT. This is because the throughputs in both cases are pretty much limited by the generated traffic. At these loadings, arrived packets are served and sector queues do not grow. As a result, packets are not dropped until 12 users per sector. Beyond this, IIS-AMC-ST queues start to grow, and more and more packets are dropped making it less efficient than IIS-AMC-MT.

5.4.3 50th-percentile End-to-End Delay and Dropped Packets

Figure 5.8 shows the 50th-percentile ETE packet delay for different schemes. If the packet arrival rate is higher than the serving rate, queue length grows. Scheduler drops packet from the queue if its delay exceeds the *drop threshold* value 195 ms.

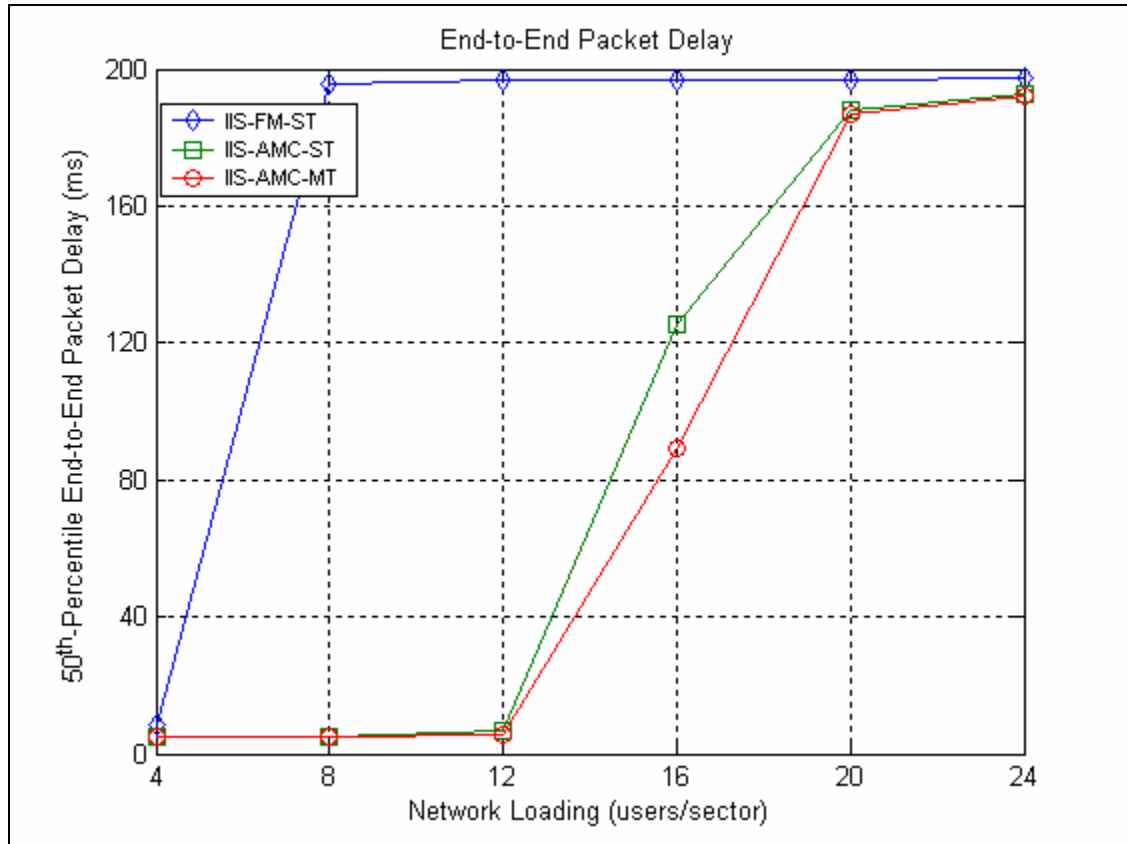


Figure 5.8: 50th-Percentile end-to-end packet delay in different schemes

Let us make some rough calculations of the maximum number of users the network can support so that sector queues do not grow. Each user generates 126.3 packets per second (2IRP process in Section 3.2.3), i.e., the number of packets arrive per frame per user is 0.6315, where the frame length is 5 ms. Now, in IIS-FM-ST the average packet service time is 0.533 ms (average packet length: 400 bytes, modulation: 16-QAM with a coding

rate of $\frac{1}{2}$) in the frame. Since concurrent transmissions are not permitted in this case, each sector can effectively use only $\frac{1}{3}$ rd of the frame on average. Therefore, the maximum numbers of supported packets by a sector during each frame length is $(5/3)/0.533 = 3.13$, which translates into $3.13/0.63 = 4.95$ users per sector. Beyond that, the queue will grow and packet will suffer excessive ETE delay. For this reason, we observe a sharp rise in delay at 8 users per sector loading in IIS-FM-ST. Adaptive modulation cases use more efficient modulation schemes and therefore are capable of serving larger number of packets in each frame.

We can find the maximum number of supported users in each sector in adaptive modulation cases with the help of Figures 5.1 and 5.2. For IIS-AMC-ST, the probability that a packet uses 64-QAM with a coding rate of 1 is 0.75, 64-QAM with a coding rate of $\frac{7}{8}$ is 0.13, 64-QAM with a coding rate of $\frac{3}{4}$ is 0.04, and so on. Using these probabilities and average packet transmission times for corresponding modulations, we can find the average time that a packet occupies in a frame, which is 0.197 ms. Now, this is also a single transmission case and each sector can use $\frac{1}{3}$ rd of a frame on average. Therefore, each frame can support $(5/3)/0.197 = 8.46$ packets from each sector. Thus, a maximum of $8.46/0.63 = 13.4$ users per sector can be supported in IIS-AMC-ST without incurring significant packet delays. This is why a sharp rise in delay is observed at 16 users per sector in IIS-AMC-ST.

In IIS-AMC-MT again with the help of Figures 5.1 and 5.2, we can find that a packet takes 0.205 ms on average in a frame. Roughly, 18% of the time two transmissions per group occurs which gives additional 12% effective frame time per sector. Therefore, IIS-AMC-MT gets 12% more effective frame time than that of IIS-AMC-ST. And, frame can

support $(5/3)*1.12/0.205 = 9.11$ packets from each sector, which translates into $9.11/0.63 = 14.5$ users per sector. The IIS-AMC-MT queues grow after this loading value which is larger than that of IIS-AMC-ST. For this reason, IIS-AMC-MT delay will always be lower in comparison to the packet delay of IIS-AMC-ST for a given loading.

Similar analysis is valid for the dropped packet curves shown in Figure 5.9. Similar to delay performance, we observe that IIS-AMC-MT is the best scheme in terms of dropped packets, while IIS-FM-ST is the worst and IIS-AMC-ST being in between these two. It should be mentioned that for any loading the packet generation rate per sector (offered load) must be equal to the packet dropping rate per sector plus packet transmission rate (packets in the air) in a sector. For instance in Figure 5.9, the packet dropping rate for IIS-AMC-MT scheme is 5.75 packets per frame per sector at a loading of 24 users per sector. For the same loading, the packet error rate and the net throughput are 0.29 and 6.95 packets per frame per sector, respectively (obtained from Figure 5.3 and 5.7, respectively); these values yield a transmission rate of $6.95/(1-0.29) = 9.78$ packets per frame per sector. It is observed from simulation that the generation rate at this loading is 15.5 packets per frame per sector which agrees with the summation ($9.78 + 5.75 = 15.5$) of packet transmission rate and packet dropping rate. We also point out that the theoretical generation rate at this loading is expected to be $0.6315 \times 24 = 15.2$ packets per frame per sector. The small discrepancy (15.2 and 15.5) in generation rate is due to statistical variation of simulation.

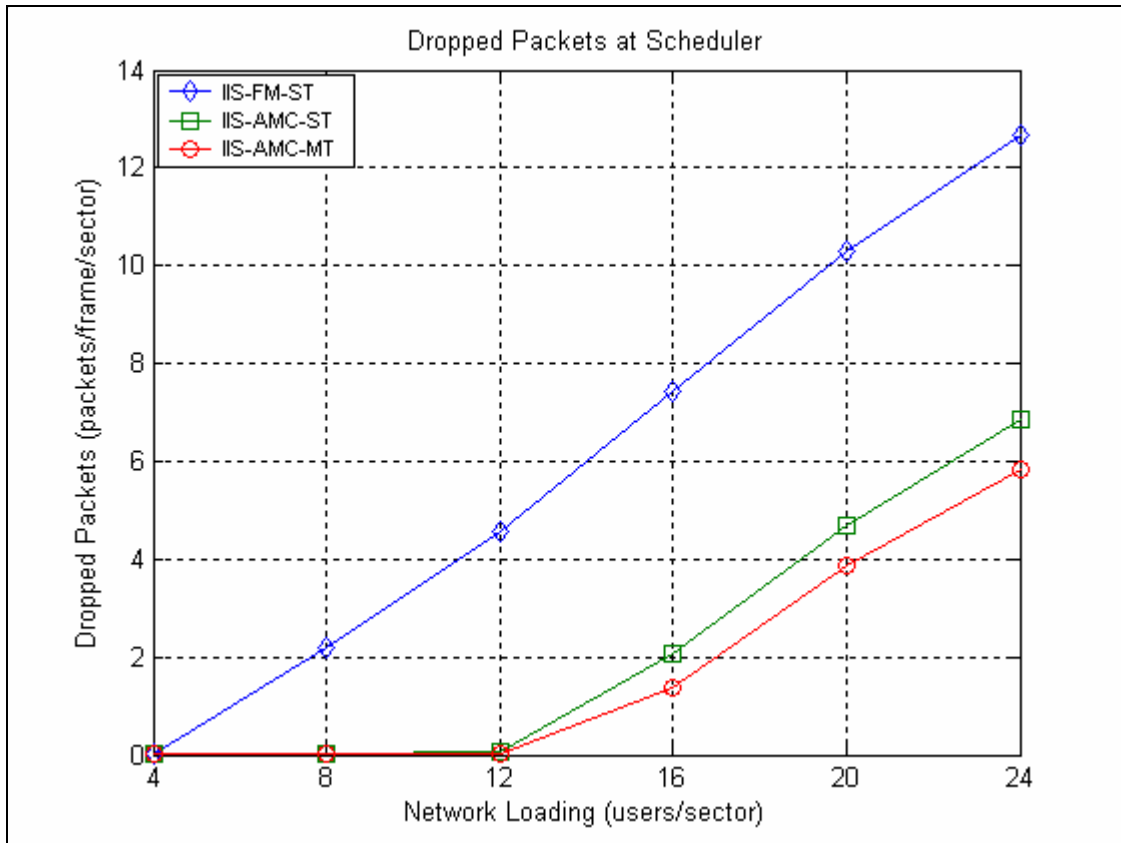


Figure 5.9: Dropped packets by scheduler in different schemes

5.5 Performance Results for 60° Beamwidth Sector Antenna and 30° Beamwidth User Antenna

We compare the packet error rates for 30° and 60° beamwidth directional user antennas in all schemes. Because of the narrower beamwidth, the effect of out-of-group interference is less when 30° beamwidth directional user antennas are employed, and hence PERs in all schemes improve as shown in Figure 5.10. It is seen that around 20-25% PERs improvements are realized by using 30° directional user antennas instead of 60° .

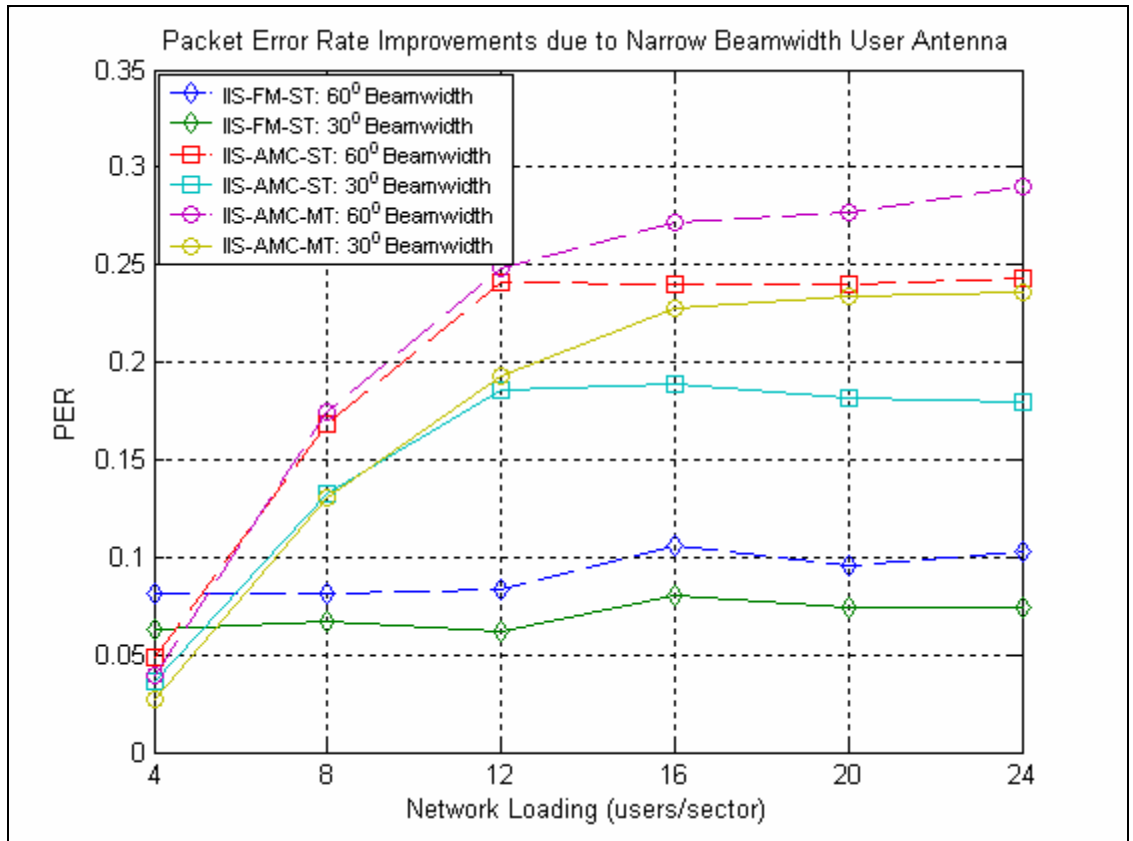


Figure 5.10: Packet error rate comparison for 30° and 60° beamwidth user antenna

These improvements in PER translate into higher spectral efficiencies and net throughput. Figure 5.11 compares area spectral efficiencies. We observe from the plots that at 24 users per sector loading the following improvements in area spectral efficiencies are obtained: around 8% in IIS-FM-ST, 9% in IIS-AMC-ST, and 15.5% improvements in IIS-AMC-MT. The reason for greater improvements in IIS-AMC-MT is its scheduling decision process that is aware of in-group interference. More specifically in IIS-AMC-MT, for 60° beamwidth directional user antenna, in-group interferers always face desired user's antenna front lobe. But, because user antennas are pointing towards their own sectors, in-group interferers might also see desired user's antenna side lobe when 30° beamwidth antenna is used. As a result, average in-group interference will be less when

30° directional user antenna is used which in-turn results in more multiple transmission decisions as shown in Figure 5.12. This figure shows percentage of two transmission decisions in IIS-AMC-MT for 60° and 30° antenna beamwidth. We observe that 4-9% more decisions for two transmissions are obtained with narrower antenna beamwidth, and this brings greater spectral efficiency improvements in this case.

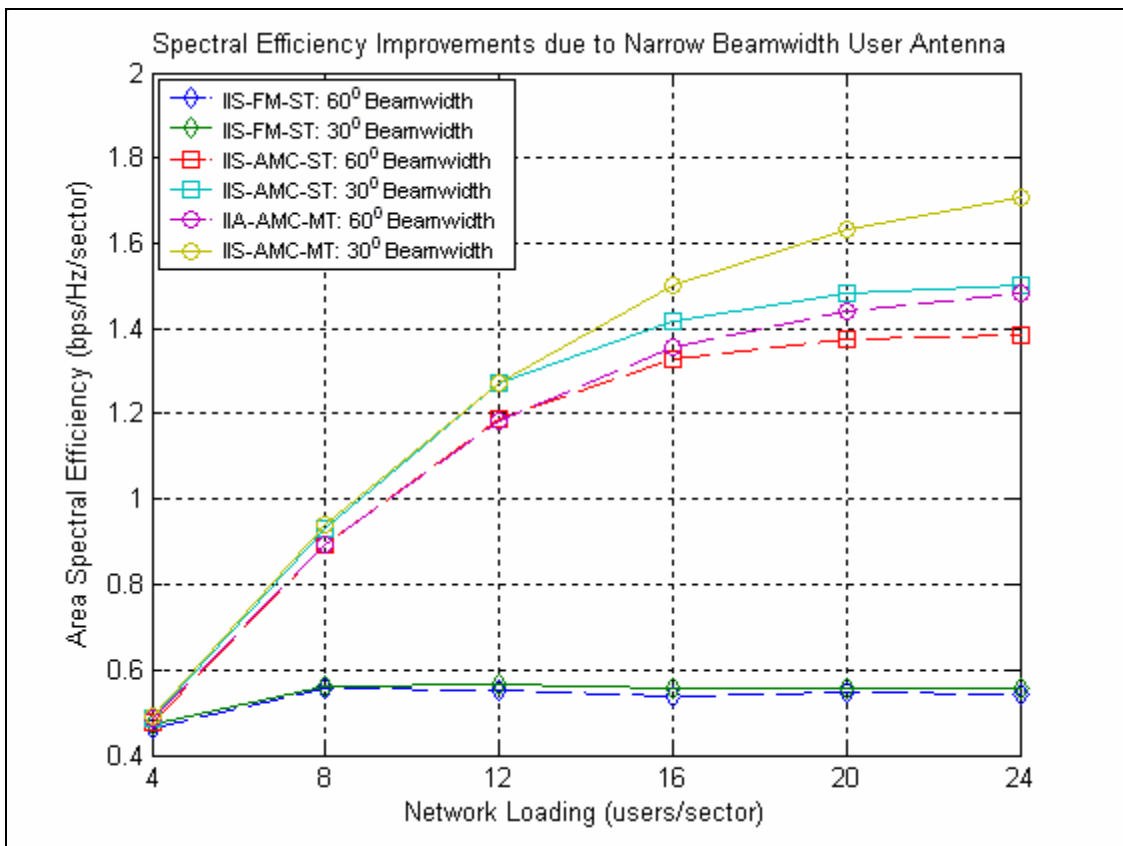


Figure 5.11: Area spectral efficiency improvements for 30° beamwidth user antenna

The net throughput also improves because of narrower user antenna beamwidth as illustrated in Figure 5.13. The reason for greater improvements in IIS-AMC-MT is again the decision process that has knowledge of the reduced in-group interference.

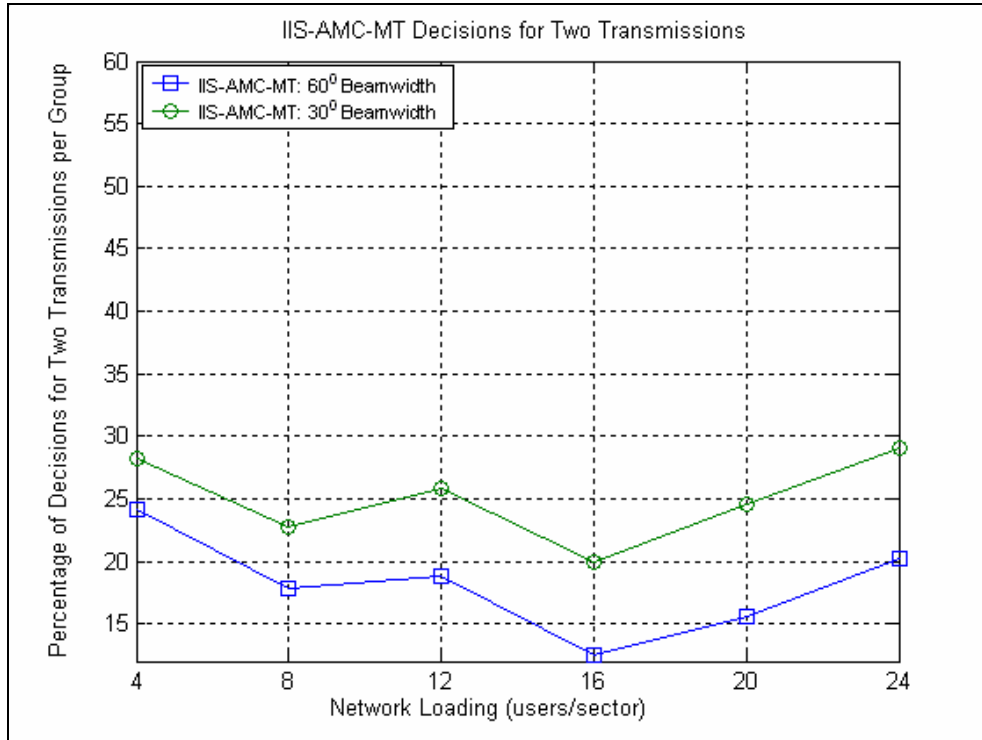


Figure 5.12: More multiple transmission decisions for 30° beamwidth user antenna

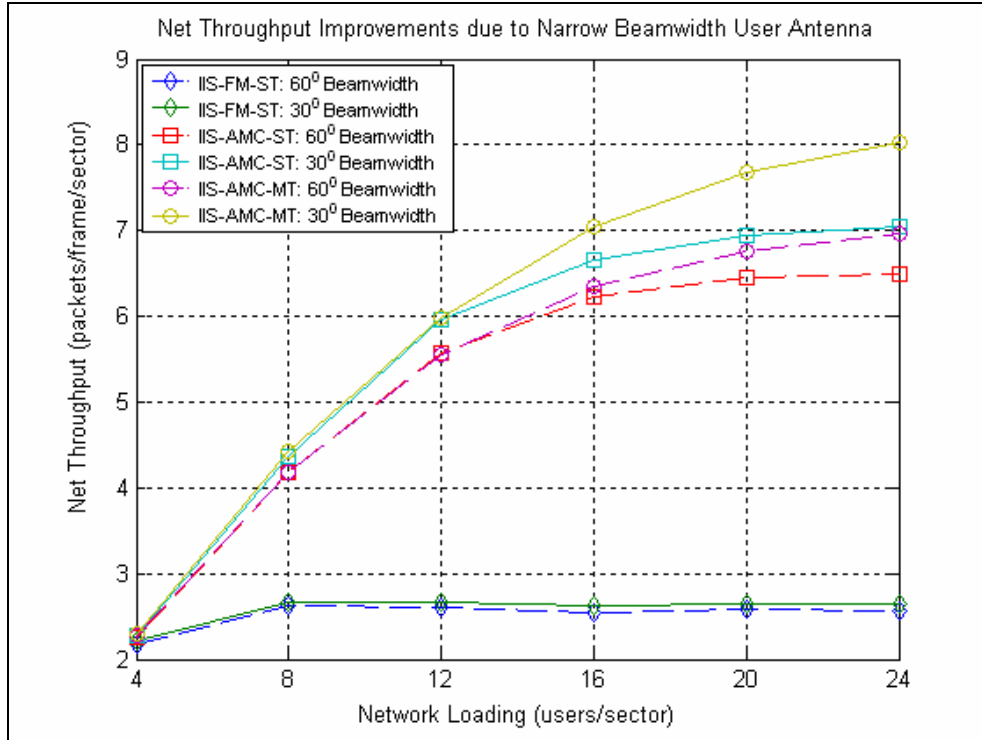


Figure 5.13: Net throughput improvements for 30° beamwidth user antenna

Changing beamwidth does not affect IIS-FM-ST and IIS-AMC-ST decision processes, i.e., service rates of queues remain unchanged. ETE packet delay performances are not changed in these cases. However, the delay performance in IIS-AMC-MT is different as shown in Figure 5.14. As stated before, because less in-group interference yields more multiple transmission decisions, more packets can be served in a given time period. As a result, IIS-AMC-MT queuing delay improves when 30° user antenna is used which translates into reduced ETE delay.

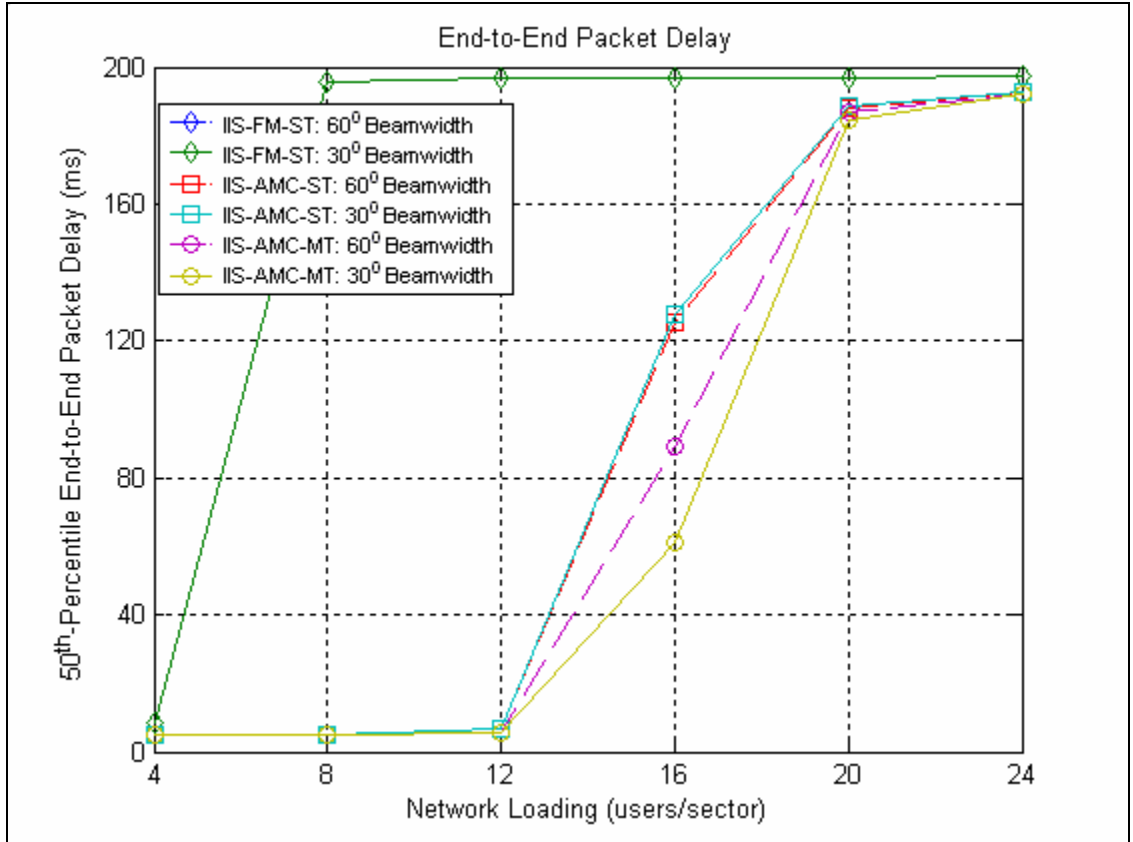


Figure 5.14: ETE delay improvements in IIS-AMC-MT for 30° beamwidth user antenna

As illustrated in Figure 5.15, improvements in packet delay provide lesser packet droppings in IIS-AMC-MT when 30° user antennas are used. The packet droppings in IIS-FM-ST and IIS-AMC-MT do not change in the cases with 30° beamwidth user antennas.

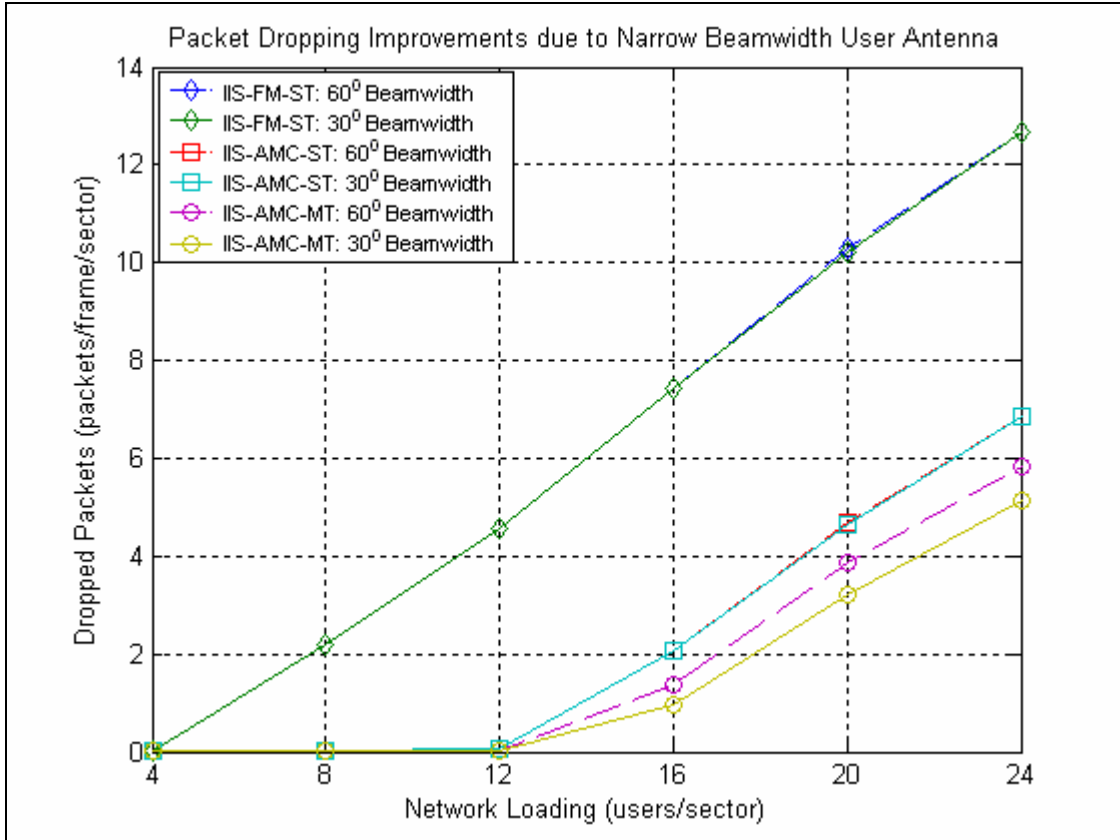


Figure 5.15: Packet dropping improvements in IIS-AMC-MT for 30° beamwidth user antenna

5.6 Results for 30° User Antenna with Out-of-Group Interference Compensation Guards in IIS-AMC-ST and IIS-AMC-MT

Out-of-group interference compensation guard is defined as the difference between expected SINR and estimated SINR based on the link information exchanged among in-group sector. As discussed in Chapter 4, this guard protects transmissions in schemes employing AMC to some extent by taking care of unknown out-of-group interference.

Table 5.2 shows the compensation guard required for different network loading in scheduling schemes employing AMC. The compensation guards are obtained from

simulation. Out-of-group interference increases with increasing loading. Therefore, the amount of compensation needed also increases with network loading.

Table 5.2: Out-of-group interference compensation guard

Network Loading (users/sector)	Compensation in IIS-AMC-ST (dB)	Compensation in IIS-AMC-MT (dB)
4	0.71	0.12
8	2.06	1.53
12	3.03	2.32
16	3.42	3.47
20	3.55	4.32
24	3.76	4.35

It is seen from the Table 5.2 that compensation required for IIS-AMC-MT is lower than that of IIS-AMC-ST for lighter network loadings. After 12 users per sector, IIS-AMC-MT requires higher guard. This is again primarily due to group-wise orthogonal allocations that work well for lower loading in avoiding out-of-group interferers.

Figure 5.16 depicts PER improvements in IIS-AMC-ST and IIS-AMC-MT when out-of-group interference compensation guard is used. Compensation guard does not have any impact on IIS-FM-ST performance. All figures in this section include IIS-FM-ST plot for comparison purposes only.

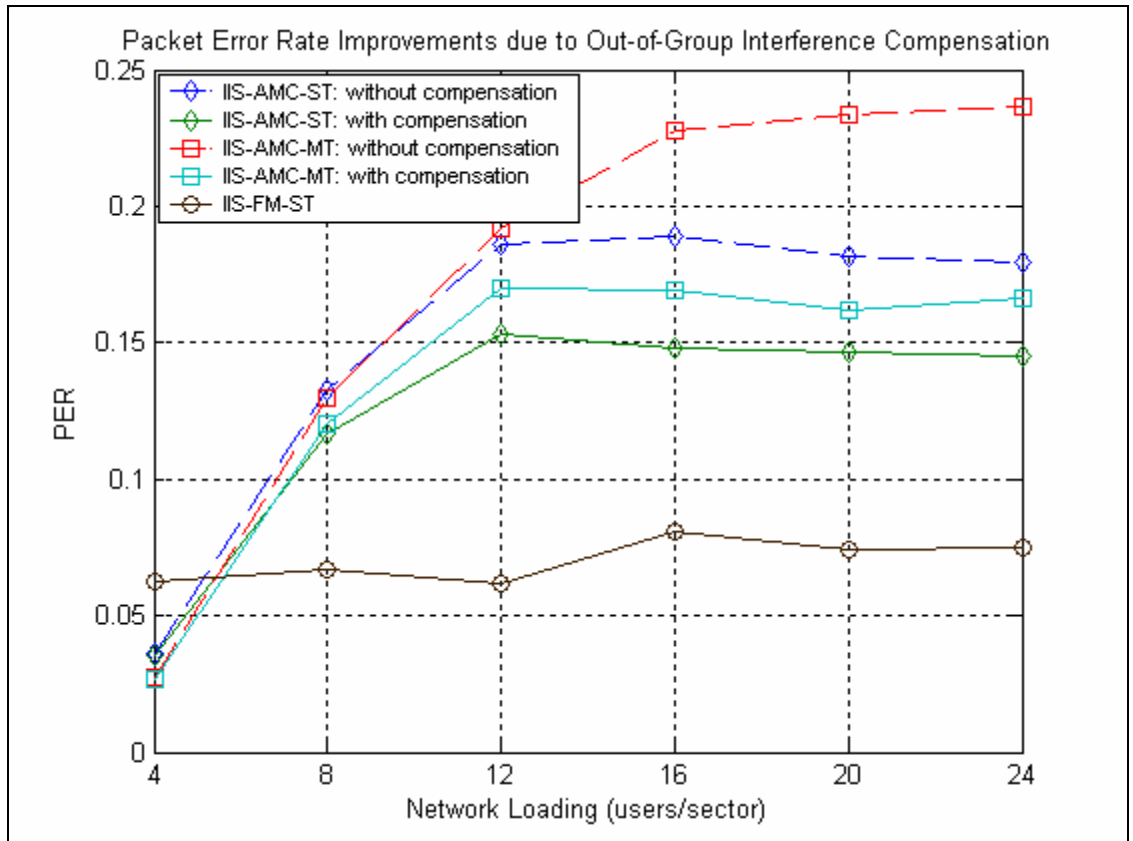


Figure 5.16: Packet error rate improvements due to out-of-group interference compensation for adaptive modulation schemes

We observe from the figure that when network loading is 24 users per sector, PER reduces from 0.24 to 0.17, and 0.18 to 0.145, in IIS-AMC-MT and IIS-AMC-ST, respectively. Improved PER has two-fold advantages. First, it contributes to better network throughput and spectral efficiency. Secondly, it relaxes the upper layer jobs by reducing the number of retransmission required.

Figure 5.17 shows the effect of compensation guard on area spectral efficiency.

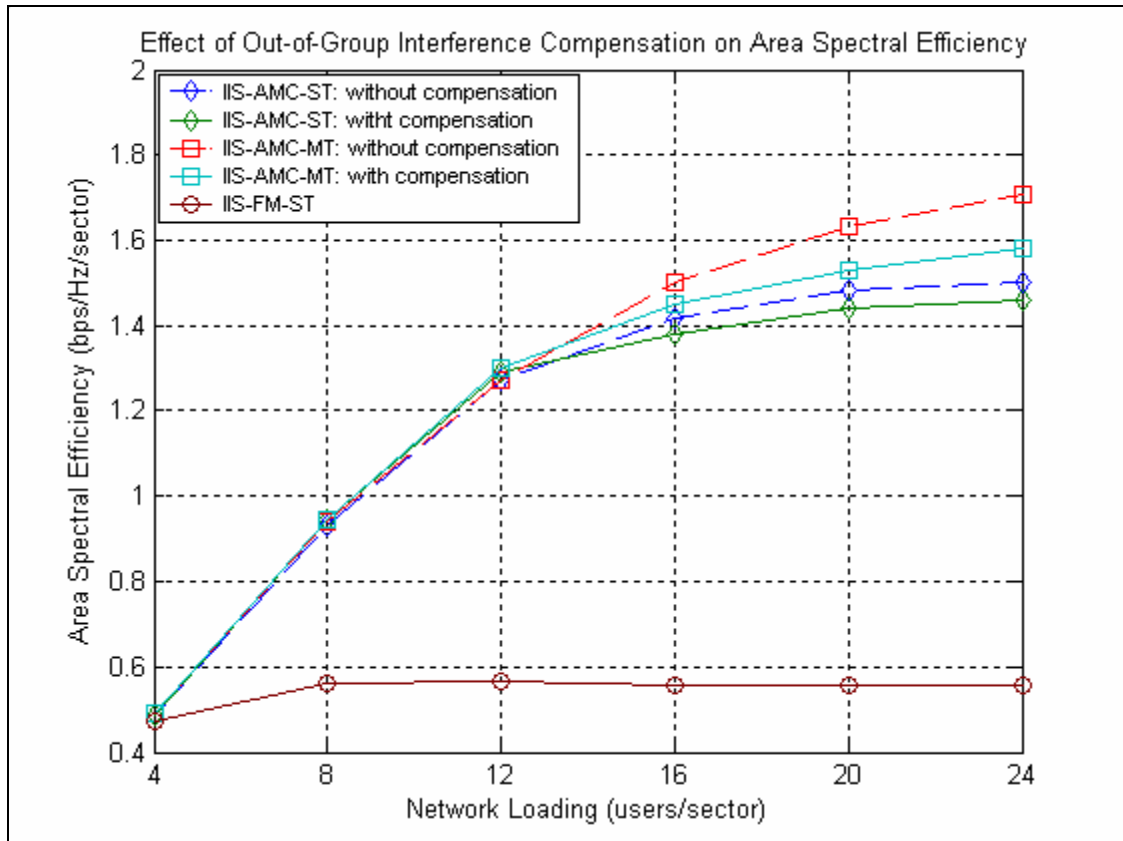


Figure 5.17: Effect of out-of-group compensation on area spectral efficiency

It is observed that compensation deteriorates spectral efficiency. In one hand, improvements in PER contributes towards higher area spectral efficiency. But, on the other hand, because of the compensation guards AMC modes are chosen conservatively which leads to reduced efficiency. Figure 5.18 and Figure 5.19 show the effect of compensation guard on AMC mode selections in IIS-AMC-ST and IIS-AMC-MT, respectively, for a loading of 24 users per sector. We see that the usage of 64-QAM with coding rate of 1 mode are reduced around 10-12% in both Figures. The combined effect of PER improvements and lower AMC modes eventually degrades spectral efficiency.

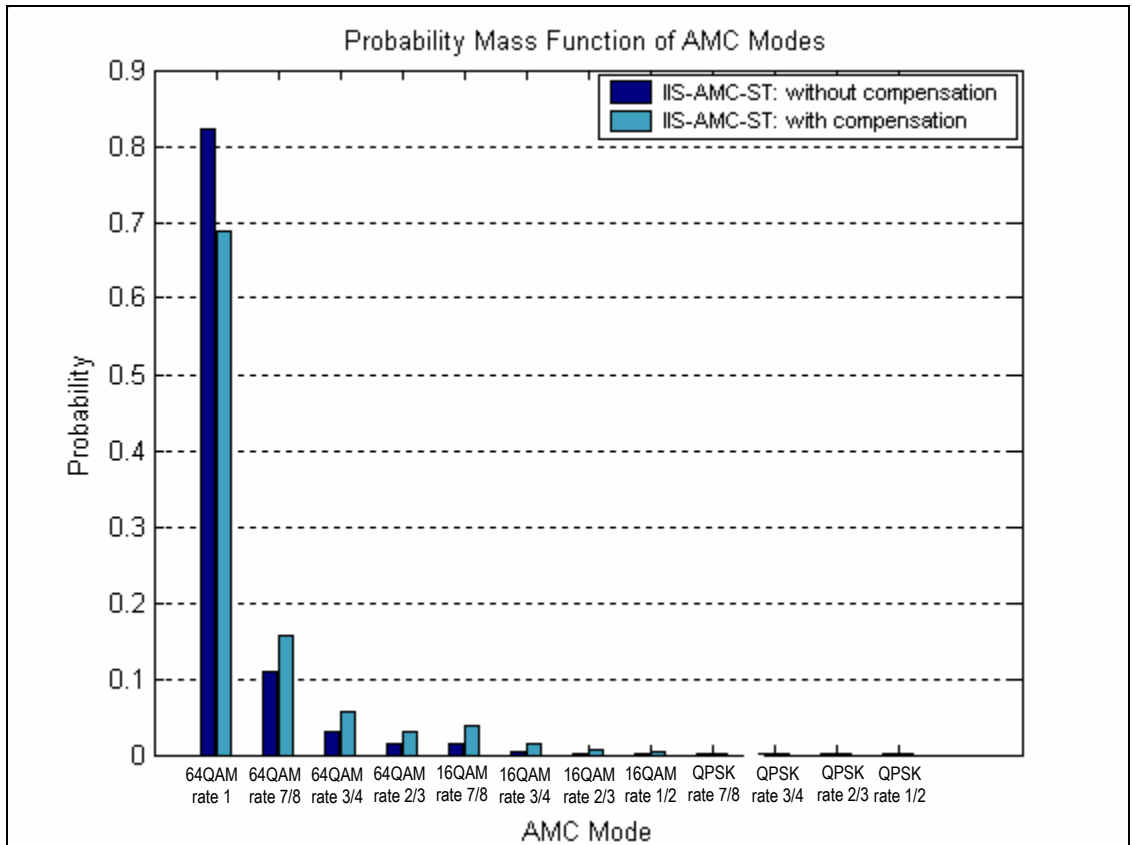


Figure 5.18: Effect of compensation guard on AMC mode selections in IIS-AMC-ST (24 users per sector)

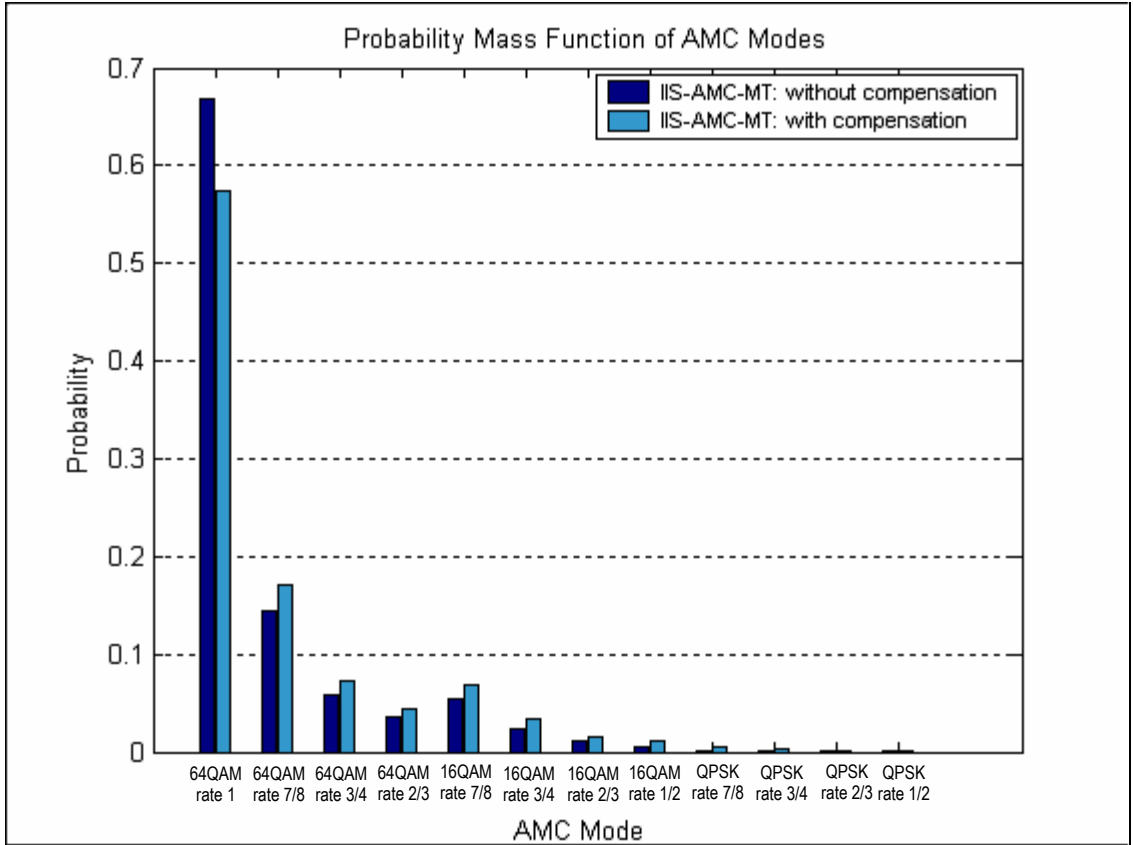


Figure 5.19: Effect of compensation guard on AMC mode selections in IIS-AMC-MT (24 users per sector)

The effect of compensation on net throughput is also worsening as expected which is illustrated in Figure 5.20. As explained before, the gain due to PER improvements is superseded by the dominant deteriorating effect of conservative AMC mode selection decisions in the schedulers of IIS-AMC-ST and IIS-AMC-MT. As a result, the net throughput degrades when out-of-group interference compensation guard is used.

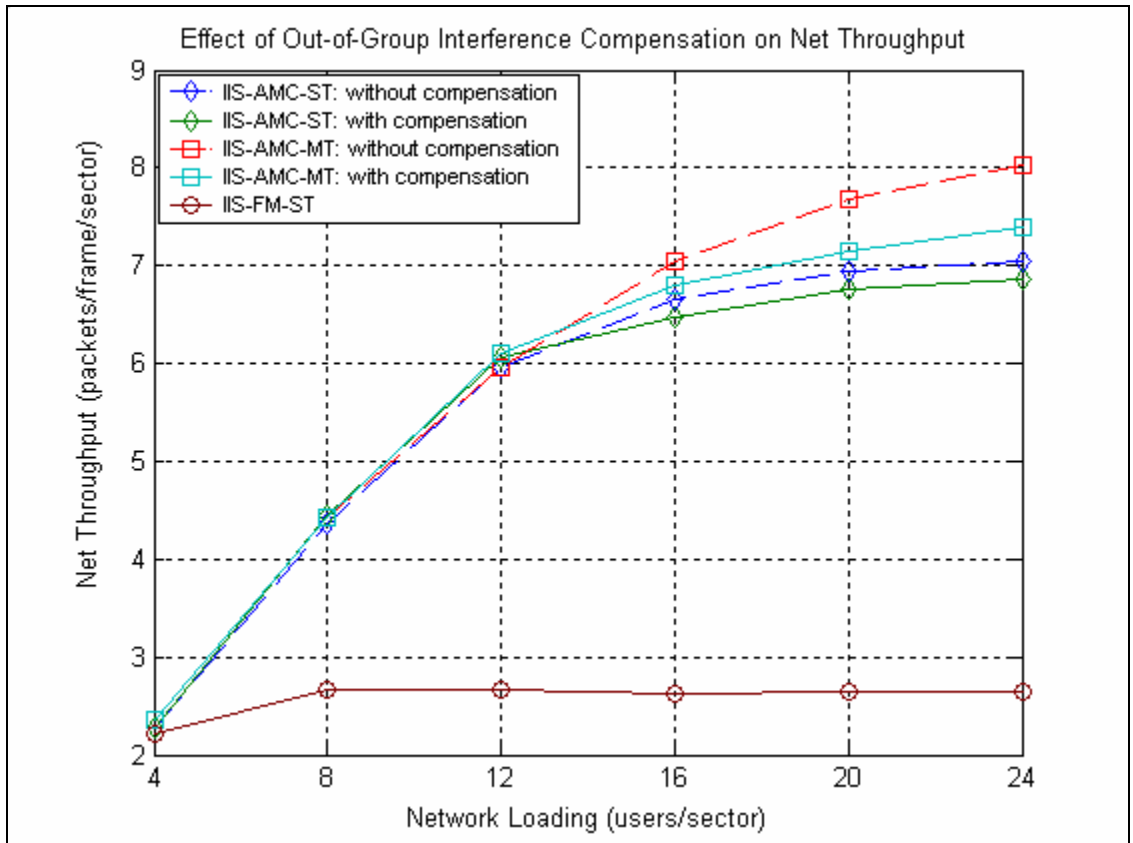


Figure 5.20: Effect of out-of-group compensation on net throughput

Figure 5.21 shows the effect of compensation on dropped packets. Because of the conservative AMC modes, less number of packets is transmitted when compensation is used. As a result, queue drop increases. For the same reason, the queuing delay also rises. The effect on end-to-end delay is plotted in Figure 5.22.

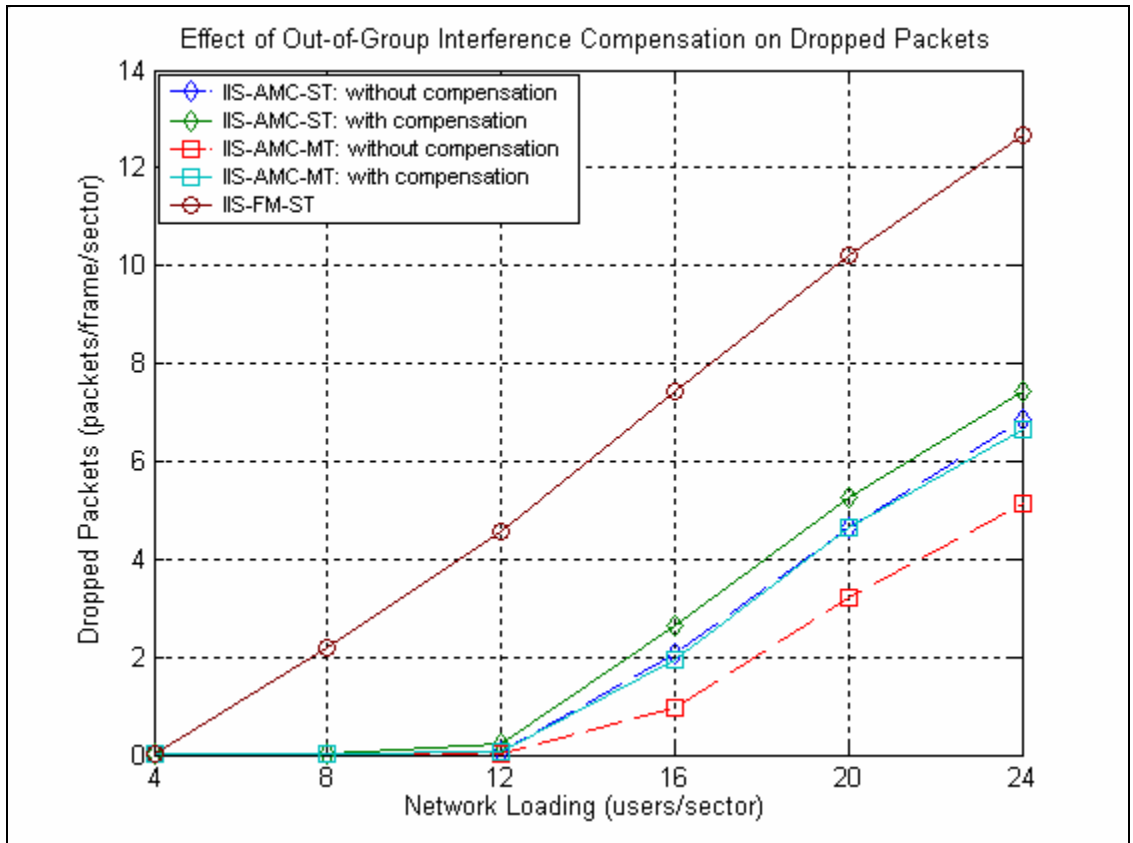


Figure 5.21: Effect of out-of-group compensation on dropped packets

Now, we have observed that compensation improves PER while degrades other network performance such as net throughput, area spectral efficiency, end-to-end delay and queue dropped packets. Therefore, employing out-of-group compensation is a tradeoff between PER and other performance metrics.

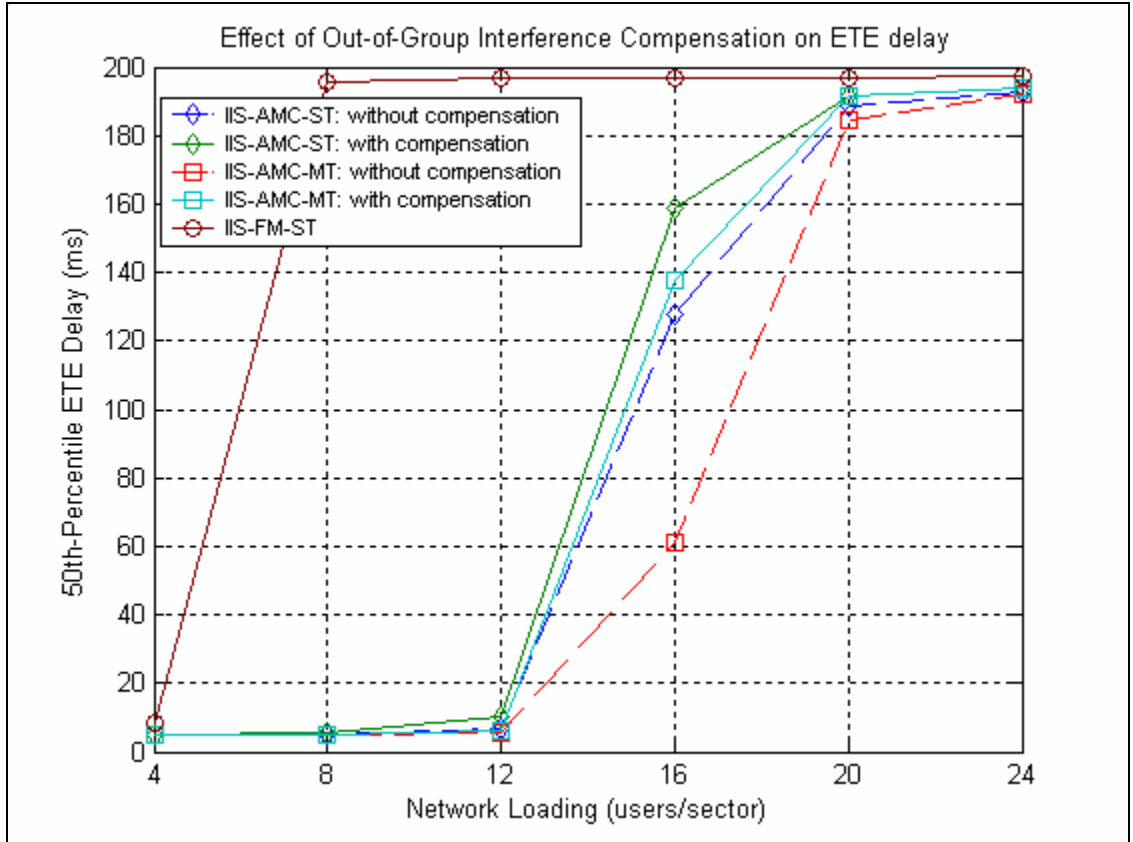


Figure 5.22: Effect of out-of-group compensation on packet delay

5.7 Exclusive Comparison between IIS-AMC-ST and IIS-AMC-MT

In the previous sections of this chapter, we have seen that IIS-AMC-ST performs significantly better than IIS-FM-ST in any simulation scenarios. However, performance enhancements in IIS-AMC-MT are not found to be very significant in comparison to IIS-AMC-ST. The reason is that system parameters considered in these simulations result in highly interference limited system which are purposely taken so that interference management/avoidance issues are justified. Figure 5.23 shows CDF of received interference for the system considered in previous simulations ($n = 3.0$ in the legend) in IIS-AMC-MT when user loading is 12 users per sector. We observe from the Figure that the received interference is higher than the average background noise (-134.06 dBW)

around 65% of the time. We should note that these statistics have been taken from the system when IIS-AMC-MT algorithm is in place to avoid/minimize in-group interference. If avoidance is not performed we would expect even higher interference in the system. Readers are referred to Figure A.4 to have an idea of the severity of the in-group interference when IIS-AMC-MT is not employed. We can see from Figure A.4 that the 50th-percentile interference received from the most dominant in-group interferer is -123.20 dBW. While the 50th-percentile interference received with IIS-AMC-MT in the system is -131.35 dBW (Figure 5.23). If the algorithm is not in place, the received interference would have been much higher. Therefore, the simulated system is indeed highly interference limited system.

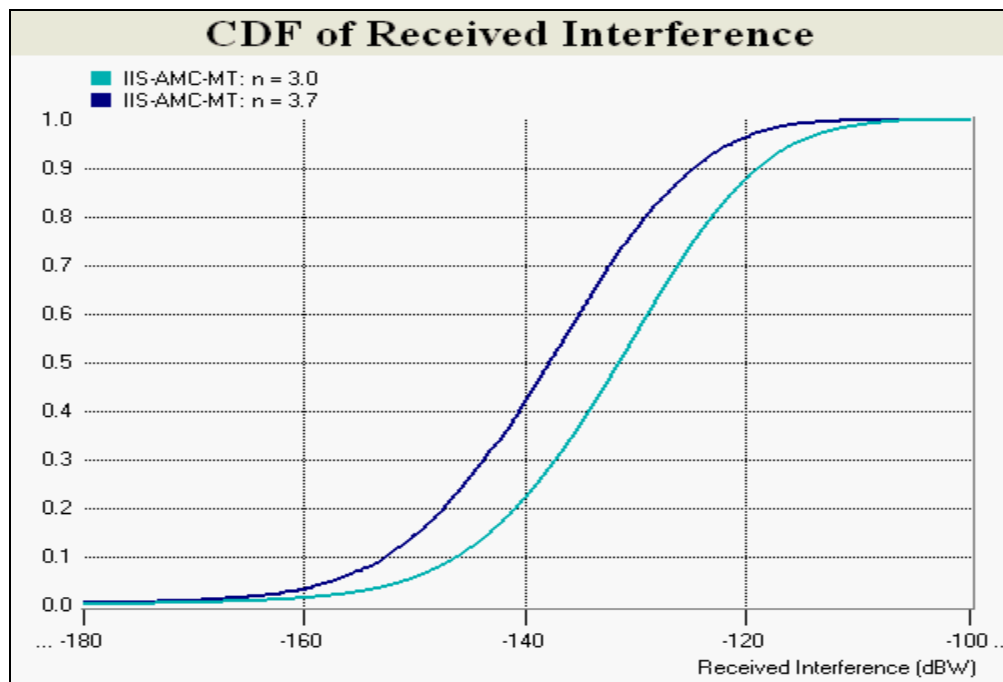


Figure 5.23: Comparison of CDF of received interference in IIS-AMC-MT (12 users per sector, 60⁰ sector antenna, 30⁰ sector antenna, and no compensation)

Now, it is obvious that a highly interference limited system will limit the number of multi-transmission decisions in IIS-AMC-MT as the high in-group interference tends to lead IIS-AMC-MT decision to single transmission decision. Therefore, we investigate a less interference limited scenario where propagation exponent is changed from 3.0 to 3.7. For comparison, the CDF of received interference when $n = 3.7$ is also shown in Figure 5.23.

The transmit power is adjusted (50.0 Watts) accordingly so that the link budget provides similar percentage of availability ($\approx 92.5\%$) to a user placed at cell boundary as in Appendix B. An exact 95% availability requires 85.0 Watts of transmit power which is very high, therefore 92.5% availability is considered in this scenario. Discussions in this section are limited to analysis of IIS-AMC-ST and IIS-AMC-MT to present further comparative study between these schemes employing AMC. We use 30° beamwidth user antennas (gains remain same), 60° beamwidth sector antennas (gains remain same) and, out-of-group interference compensation is not considered in the schedulers.

Figure 5.24 shows packet error rate performance for this new scenario. We see that packet error rates are improved (reduced by factor of 1/2 in both schemes) compared to those presented in similar scenario in Figure 5.10 (30° beamwidth cases) in Section 5.5 for $n = 3.0$. These improvements are realized due to reduced intensity of out-of-group interference.

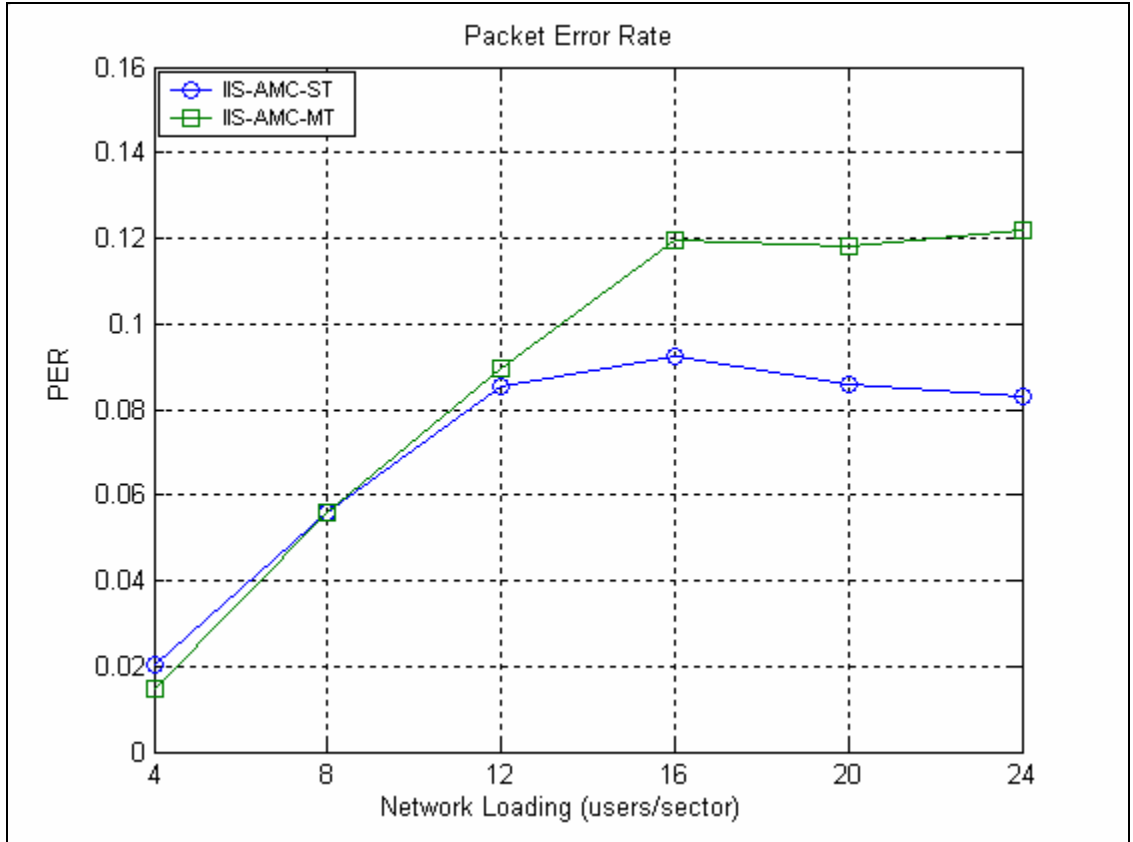


Figure 5.24: Packet error rate in IIS-AMC-ST and IIS-AMC-MT for $n = 3.7$

Area spectral efficiency and net throughput for this scenario is shown in Figure 5.25 and 5.26, respectively. The IIS-AMC-MT achieves 26% (compared to around 14% for $n = 3.0$) better spectral efficiency and net throughput than those of IIS-AMC-ST at network loading of 24 users per sector. This performance difference is around twice as much as obtained in the previous simulations with propagation exponent of 3.0. We should note that these performance improvements in IIS-AMC-MT are resulted from higher percentage of multiple transmissions decisions as shown in Figure C.1 in Appendix C (compared with Figure 5.12, 30° beamwidth case). The PMFs of AMC modes used by IIS-AMC-ST and IIS-AMC-MT at a loading of 12 users per sector are provided in Figure C.2 in Appendix C for reference.

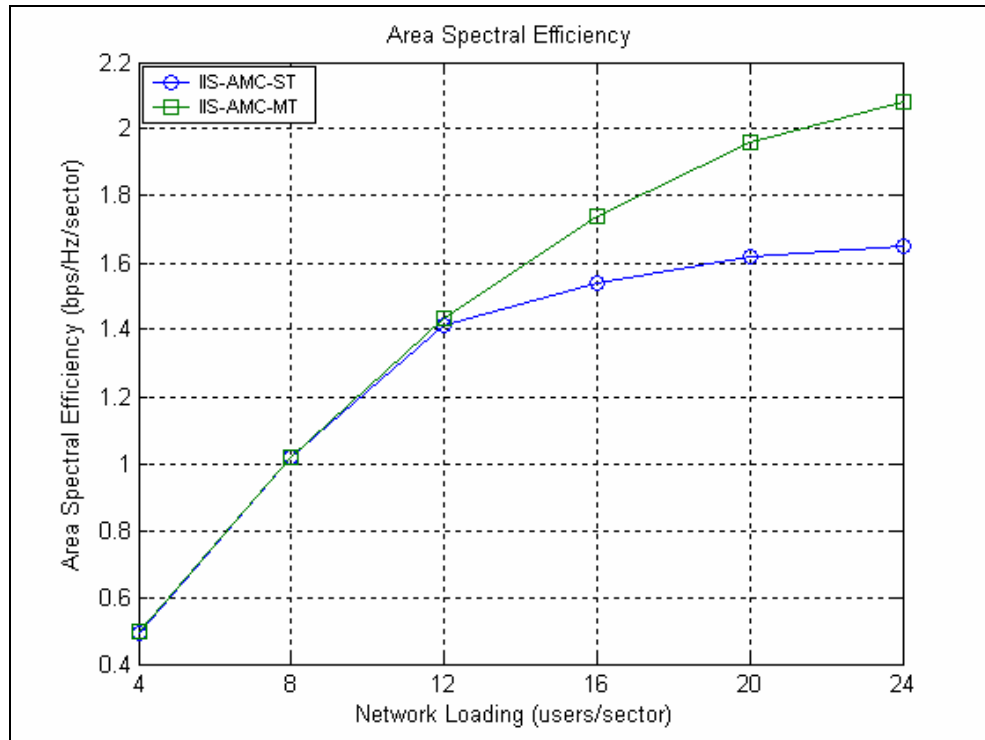


Figure 5.25: Area spectral efficiency in IIS-AMC-ST and IIS-AMC-MT for $n = 3.7$

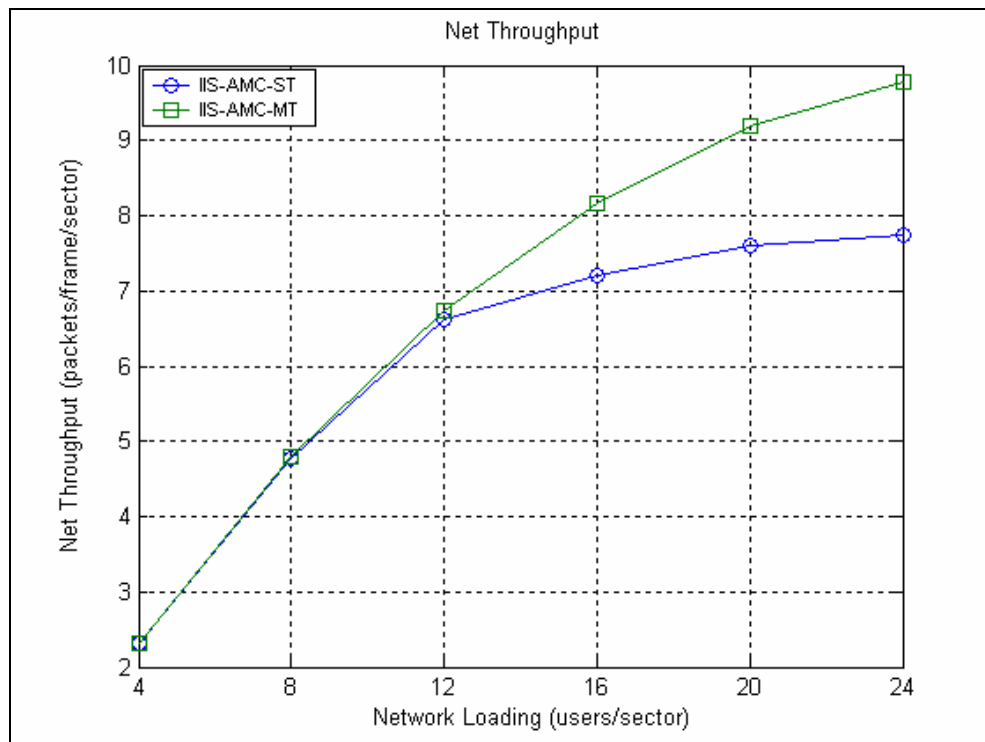


Figure 5.26: Net throughput in IIS-AMC-ST and IIS-AMC-MT for $n = 3.7$

The difference in ETE packet delay and packet dropping rates performance between IIS-AMC-MT and IIS-AMC-ST are also more significant for $n = 3.7$ resulted from increased throughput as shown in Figure 5.27 and 5.28, respectively (compared with Figure 5.14 and 5.15, respectively; 30^0 beamwidth cases).

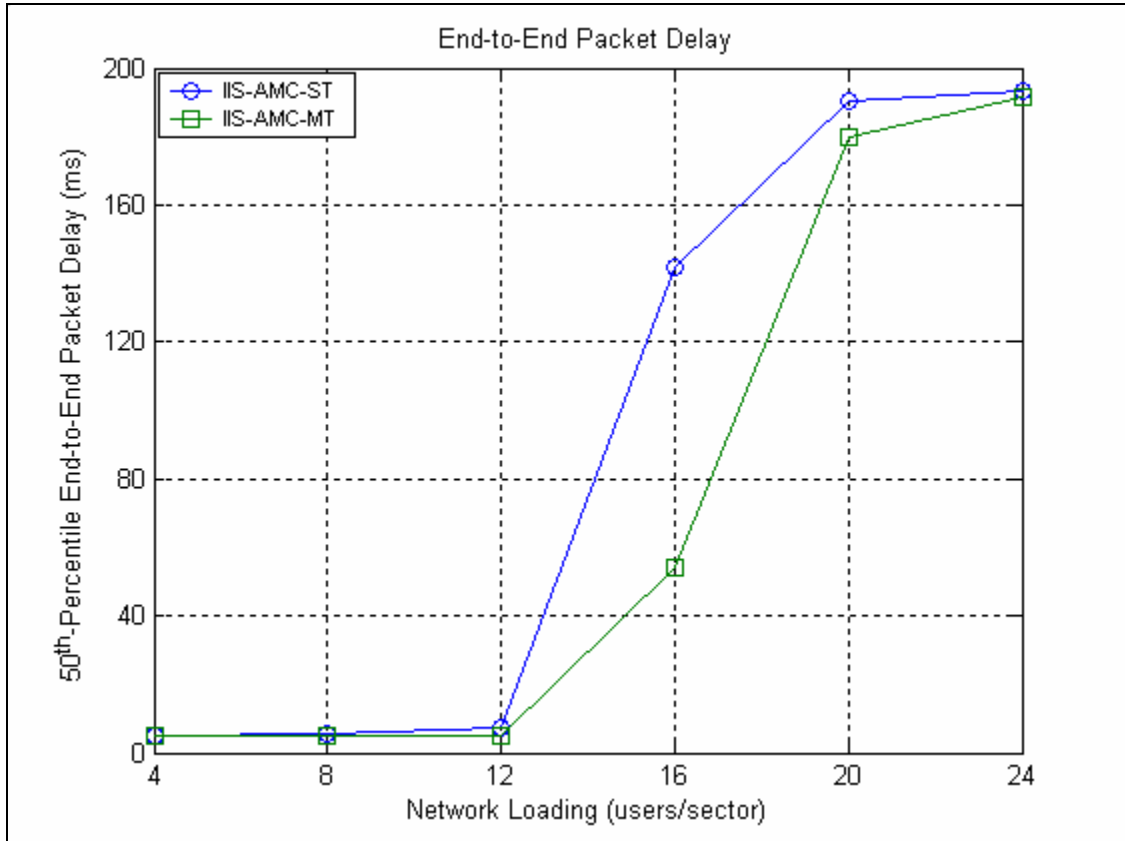


Figure 5.27: ETE delay in IIS-AMC-ST and IIS-AMC-MT for $n = 3.7$

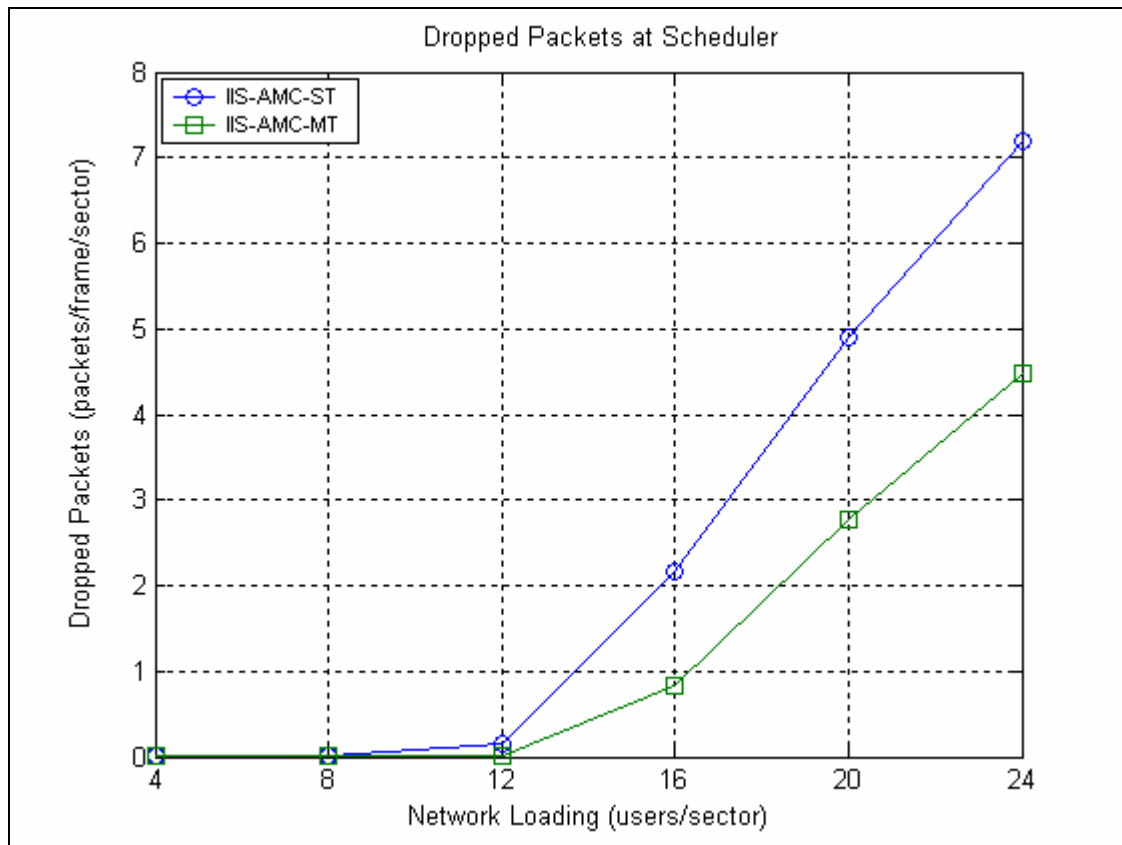


Figure 5.28: Queue dropped packets in IIS-AMC-ST and IIS-AMC-MT for $n = 3.7$

Chapter 6

Conclusions and Future Works

6.1 Summary on Findings

The benefits of combining AMC with scheduling techniques in fixed broadband wireless access networks have been investigated extensively in this research. We also have examined performance enhancements when controlled multiple transmissions in the interferer group are permitted.

It has been observed that even when schedulers perform conservatively such that only one sector transmits in an interferer group, scheme employing AMC performs much more efficiently than the scheme with fixed modulation. This can be concluded by comparing the presented results for IIS-FM-ST and IIS-AMC-ST in Section 5.4. We have observed that more than 150% spectral efficiency and throughput gain can be achieved due to the integration of AMC with scheduling. Moreover, higher throughput results in significant improvements in end-to-end delay and number of dropped packets.

Increased performance gain is achieved when restriction on multiple transmissions in the interferer group is relaxed. We have evaluated IIS-AMC-MT against IIS-AMC-ST to quantify the advantages of multiple transmissions. It has been found that multiple in-group transmissions yield up to 14% throughput and efficiency gain compared to single transmission adaptive modulation case when 30^0 directional user antennas are used. As packet delay is related to throughput, better end-to-end packet delay and lower dropped packets are observed in IIS-AMC-MT. We also have observed that better performances are expected from IIS-AMC-MT when interference level is less ($n = 3.7$ case).

While schemes incorporating AMC show performance improvements in terms of area spectral efficiency, throughput, delay, and dropped packets, they experience higher PER due to the fact that increased packets on the air results in increased number of interferers.

We have shown that narrow beamwidth user antenna helps improve PER for all simulated schemes. We have further shown that when out-of group interferers are taken into account and AMC modes are used conservatively, improvements in PER are achieved in case of the scheduling schemes that employ AMC. However, degradations in throughput, area spectral efficiency, end-to-end delay, and packet dropping rate are noted as consequences of using out-of-group interferer guards. Nevertheless, IIS-AMC-MT is proven to be an efficient scheduling scheme that exhibits enormous gain in network performance.

6.2 Thesis Contributions

We summarize the following contributions achieved throughout the course of this thesis study:

- First, we have employed AMC in a scheduling scheme which takes scheduling decisions based on the channel conditions and performs orthogonal transmissions in the interferer group (IIS-AMC-ST). We have observed enhanced performance of IIS-AMC-ST compared to a similar scheme that takes delay based scheduling decisions (IIS-FM-ST). The benefits of AMC and channel condition dependent scheduling decisions result in significantly higher spectral efficiency and net throughput, and lower delay as well as number of dropped packets.
- Secondly, we have evaluated IIS-AMC-MT scheme, where channel dependent multiple concurrent transmissions are allowed. We have observed from simulation

results that IIS-AMC-MT performs better than IIS-AMC-ST. The novel algorithm for scheduling decision in IIS-AMC-MT is designed to provide better performance than IIS-AMC-ST.

- A novel slot allocation strategy that suits for variable length packets using different AMC modes, which facilitates accurate packet network simulation and eliminates the need for assuming traditional fixed time-slot assignments. We should note that fixed time-slot strategy might not accurately match with traffic model, and might not represent accurate interference pattern resulted from a network where variable length packets are transmitted with different AMC.
- Effective interference power is largely dependent on user antenna beamwidth. The influence of beamwidth on network performance has been investigated.
- We have found that out-of-group interference is the primary cause for packet errors (especially in the schemes employing AMC) and have observed that out-of-group interference compensation improves PER, but degrades other observed performance parameters such as net throughput, spectral efficiency, ETE delay, packet dropping rate etc. We have investigated the effect of this guard on network performance.

6.3 Recommended Future Works

The ideas and algorithms developed in this thesis can be extended further to carry out following investigations:

- In this study, the simulations have been carried out for a single class of traffic (real-time video). However, future work can be recommended to investigate into performance when different classes of services are used in the network.

- The focus of this research is to evaluate the advantages of combining AMC with scheduling schemes and therefore a simple queuing discipline such as FCFS is used for intra-sector scheduling throughout the thesis. However, when several classes of service is offered in the network, other complex packet fair queuing schemes such as WFQ or it's variants can be employed to observe the fairness and other network performances of the network.
- In this thesis, the throughput optimization is performed based on the HOL packets in three sectors in the group at the decision instants over the decision region. This idea can be extended to perform optimization over the whole frame instead of decision region.
- Although IIS-AMC-ST and IIS-AMC-MT assure long-term fairness among users, a deeply shadowed distant user might have fewer service opportunities over a short interval of time than a user located at close proximity of the serving base station with good shadowing parameter. Future research can be recommended to evaluate such fairness among users.
- It would be interesting to observe the performance when more sectors are taken in the interferer group instead of three considered in this thesis. More coordinated transmissions would be realized with the expense of increased signaling overhead. However, the performance is expected to improve.
- The IIS-AMC-MT can be employed in a multi-hop fixed relay networks because of its feature to improve end-to-end packet delay. Transmission delay accumulates in every hop in such network; therefore, IIS-AMC-MT could be a good choice to alleviate delay issues.

References

- [1] IEEE802.16a Standard for Local and Metropolitan Area Networks, “Part 16: Air interface for fixed broadband wireless access systems”, April 2003.
- [2] H. Bölcskei, A.J. Paulraj, K.V.S. Hari, R.U. Nabar, and W.W. Lu, “Fixed broadband wireless access: State of the art, challenges, and future directions”, *IEEE Communications Magazine*, pp. 100-108, January 2001.
- [3] D.L. Waring, “The ssymmetric digital subscriber line (ADSL): A new transport technology for delivering wideband capabilities to the residence”, *Global Telecommunications Conference (GLOBECOM'91)*, vol. 3, pp. 1979-1968, December 1991.
- [4] K. Maxwell, “Asymmetric digital subscriber line (ADSL): Interim technology for the next forty years”, *IEEE Communications Magazine*, pp. 100-106, October 1996.
- [5] C. Bisdikian, K. Maruyama, D.I. Seidman, and D.N. Serpanos, “Cable access beyond the hype: On residential data services over HFC networks”, *IEEE Communications Magazine*, pp.128-135, November 1996.
- [6] M. Katevenis, S. Sidiropoulos, and C. Courcoubetis, “Weighted round-robin cell multiplexing in a general purpose ATM switch chip”, *IEEE Journal on Selected Areas in Communications*, vol. 9, no. 8, pp. 1265-1279, October 1991.
- [7] M. Shreedhar and G. Verghese, “Efficient fair queuing using deficit round-robin”, *IEEE/ACM Transaction on Networking*, vol. 4, no. 3, pp. 375-385, June 1996.
- [8] A. Demers, S. Keshav, and S. Shenker, “Analysis and simulation of a fair queuing algorithm”, *Proceedings of ACM SIGCOM'89*, pp. 1-12, 1989.
- [9] J.C.R. Bennett and H. Zhang, “WF²Q: Worst-case fair weighted fair queuing”, *IEEE INFOCOM'96*, vol. 1, pp. 120-128, March 1996.
- [10] S.J. Golestani, “A self-clocked fair queuing scheme for broadband applications”, *IEEE INFOCOM'94*, vol. 2, pp. 636-646, June 1994.
- [11] H. Zhang, “Service disciplines for guaranteed performance service in packet-switching networks”, *Proceedings of the IEEE*, vol. 83, no. 10, pp. 1374-1396, October 1995.
- [12] P. Bhagwat, P. Bhattacharya, A. Krishna, and S.K. Tripathi, “Enhancing throughput over wireless LANs using channel state dependent packet scheduling”, *IEEE INFOCOM'96*, vol. 3, pp. 1133-1140, March 1996.

- [13] S. Desilva and S.R. Das , “Experimental evaluation of channel state dependent scheduling in an in-building wireless LAN”, *7th International Conference on Computer Communications and Networks*, pp. 414-421, October 1998.
- [14] C. Fragouli, V. Sivaraman, and M.B. Srivasta, “Controlled multimedia wireless link sharing via enhanced class based queuing with channel-state-dependent packet scheduling”, *IEEE INFOCOM’98*, pp. 572-580, April 1998.
- [15] S. Floyd and V. Jacobson, “Link-sharing and resource management models for packet networks”, *IEEE/ACM Transactions on Networking*, vol. 3, no. 4, pp. 365-386, August 1995.
- [16] S. Lu, V. Bharagavan, and R. Srikant, “Fair scheduling in wireless packet networks”, *IEEE/ACM Transaction on Networking*, vol. 7, no. 4, pp. 473-489, August 1999.
- [17] T.S.E. Ng, I. Stoica, and H. Zhang, “Packet fair queuing algorithms for wireless networks with location-dependent errors”, *IEEE INFOCOM’98*, pp. 1103-1111, March 1998.
- [18] Y. Cao and V.O.K. Li, “Scheduling algorithms in broadband wireless networks”, *Proceedings of the IEEE*, vol. 89, no. 1, pp. 76-87, January 2001.
- [19] T.K. Fong, P.S. Henry, K.K. Leung, X. Qiu, and N.K. Shankaranarayan, “Radio resource allocation in fixed broadband wireless networks”, *IEEE Transactions on Communications*, vol. 46, no. 6, pp. 806-818, June 1998.
- [20] K.K. Leung and A. Srivastava, “Dynamic allocation of downlink and uplink resource for broadband services in fixed wireless networks”, *IEEE Journal on Selected Areas in Communications*, vol. 17, no. 5, pp. 990-1006, May 1999.
- [21] F. Borgonovo, M. Morzi, L. Fratta, V. Trecordi, and G. Bianchi “Capture division packet access for wireless personal communications”, *IEEE Journal on Selected Areas in Communications*, vol. 14, pp. 609-622, May 1996.
- [22] K. Chawla and X. Qiu, “Quasi-Static resource allocation with interference avoidance for fixed wireless systems”, *IEEE Journal on Selected Areas in Communications*, vol. 17, no. 3, pp. 493-504, March 1999.
- [23] M.H. Ahmed, H. Yanikomeroglu, S. Mahmoud, and D. Falconer, “Scheduling multimedia traffic in interference-limited broadband wireless access networks”, *The 5th International Symposium on Wireless Personal Multimedia Communications (WPMC’02)*, Honolulu, Hawaii, USA, October 2002.
- [24] M.H. Ahmed, H. Yanikomeroglu, and S. Mahmoud, “Comparing the performance of inter-sector/intra-sector scheduling and ARQ for multimedia traffic in wireless

- access networks”, *IEEE Newfoundland Electrical and Computer Engineering Conference (NECE'03)*, November 2003.
- [25] M.H. Ahmed, H. Yanikomeroglu, and S. Mahmoud, “Interference management using packet scheduling in broadband wireless access networks”, *Wiley Wireless Communications and Mobile Computing Journal*, November 2003.
- [26] X. Qiu, K. Chawla, J.C.-I. Chuang, and N. Sollenberger, “Network-assisted resource management for wireless data networks”, *IEEE Journal on Selected Areas in Communications*, vol. 19, no. 7, pp. 1222-1234, July 2001.
- [27] L. Mailaender, H. Huang, and H. Viswanathan, “Simple inter-cell coordination schemes for high speed CDMA packet downlink”, *IEEE Vehicular Technology Conference (VTC'98)*, vol. 3, pp. 1680 – 1684, May 1998.
- [28] E. Armanious, “Link adaptation techniques for cellular fixed broadband wireless access systems”, *Master's Thesis, Carleton University*, Co-supervisors: H. Yanikomeroglu and D.D. Falconer, January 2003.
- [29] A.J. Goldsmith and P.P. Varaiya, “Capacity of fading channels with channel side information”, *IEEE Transactions on Information Theory*, vol. 43, no. 6, pp. 1986-1992, November 1997.
- [30] M.-S. Alouini and A.J. Goldsmith, “Capacity of Nakagami multipath fading channels”, *IEEE 47th Vehicular Technology Conference (VTC)*, vol. 1, pp. 358-362, May 1997.
- [31] A.J. Goldsmith and S.-G. Chua “Adaptive coded modulation for fading channels”, *IEEE Transactions on Communications*, vol. 46, no. 5, pp. 595-602, May 1998.
- [32] V. Erceg, L.J. Greenstein, S.Y. Tjandra, S.R. Parkoff, A. Gupta, B. Kulic, A.A. Julius, and R. Bianchi, “An empirically based path loss model for wireless channels in suburban environments”, *IEEE Journal on Selected Areas in Communications*, vol. 17, no. 7, pp. 1205-1218, July 1999.
- [33] V. Erceg, K.V. S. Hari, M.S. Smith, D.S. Baum, K.P. Sheikh, C. Tappenden, J.M. Costa, C. Bushue, A. Sarajedini, R. Schwartz, D. Branlund, T. Kaitz, and D. Trinkwon, “Channel models for fixed wireless applications”, *IEEE 802.16 work-in-progress document # 802.16.3c-01/29r4*, July 2001.
- [34] T.S. Rappaport, *Wireless Communications: Principles & Practice*, Prentice Hall, 1st Edition, 1996.
- [35] R.J. Pannoose, P.V. Nikitin, and D.D. Stancil, “Efficient simulation of Ricean fading within a packet simulator”, *IEEE Vehicular Technology Conference (VTC'00)*, pp. 764-767, September 2000.

- [36] C.R. Baugh and Jun Huang, “Traffic model for 802.16 TG3 MAC/PHY simulations”, *IEEE 802.16 work-in-progress document # 802.16.3c-01/30r1*, March 2001.
- [37] G. Caire, G. Taricco, and E. Biglieri, “Bit-interleaved coded modulation”, *IEEE Transaction on Information Theory*, vol. 44, pp. 927-946, May 1998.

Appendix A

Finding Wraparound Interference Positions

The following steps are followed to find the wraparound position of BS7 when interference power is needed to be calculated for users in sector 1 of BS3, as shown in Figure A.1.

- Define all possible wraparound positions of BS7 as shown in Figure A.1. BS7 drawn with solid line is the original BS7 and other 8 dotted line locations show the wraparound positions of BS7.
- Now, the interference powers from each of these BS7 locations to the user in BS3 are computed. For simplicity, fading and shadowing effects are neglected in these calculations to find interferer position as the relative position will depend on the distance attenuation and antenna direction. However, shadowing and fading are considered in the interference calculation in the simulation of the scheduling schemes.
- To consider the directivity of the antenna in calculations, user is placed at four different locations as shown by four black dots at BS3. User antennas (as well as sector antennas) are assumed to be ideal and are pointing to respective base stations. BS3 is zoomed at the top-right corner of Figure A.1 to show the antenna directivity for user at topmost black dot.
- We find the interference pattern for following operating parameters (link budget is given in Appendix B):
 - o Transmit power: 2.2 Watts

- Base station antenna: 60° directional with effective gain of 20 dB (10 dB front lobe and -10 dB back lobe)
- User antenna: 60° directional with effective gain of 10 dB (5 dB front lobe and -5 dB back lobe)
- Large scale path-loss model is used as described in Section 3.2.1.

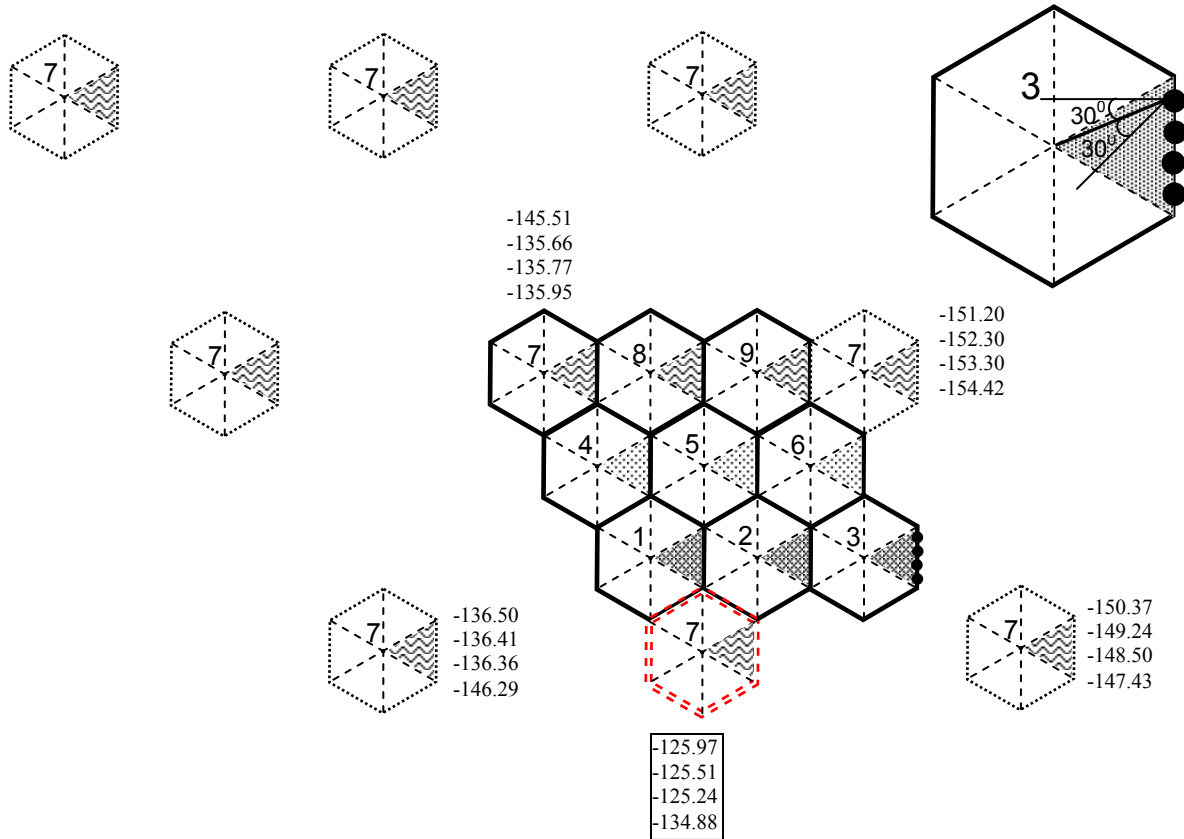


Figure A.1: Finding BS7 interferer location for users in BS3

- In Figure A.1, the numbers beside BS7 locations correspond to the interference power in dBW from that location to the user in BS3. The number on the top corresponds to user position shown by topmost black dot in BS3, and so on.

- The most dominant position for BS7 on users in BS3 is shown by double dotted hexagon, and interference values for different user positions are shown inside a rectangle beside the location.

Similarly, interferer locations for other seven BSs can be found. Figure A.2.a shows all eight interferer positions with corresponding interference power for user locations in BS3.

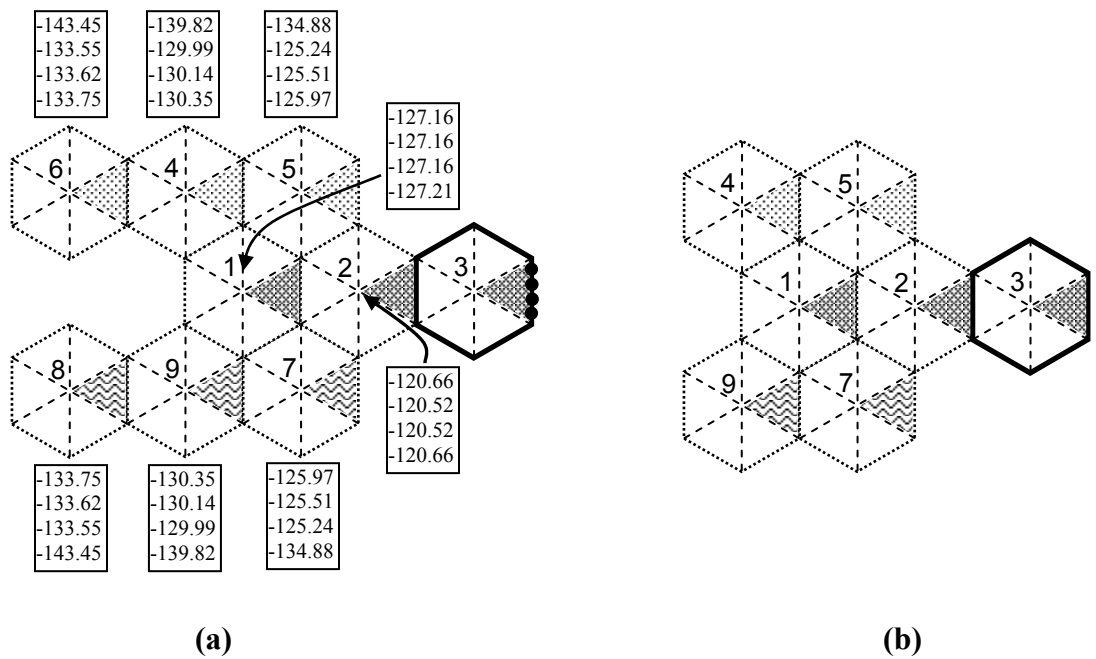


Figure A.2: Wraparound interferer positions for users in BS3

From Figure A.2.a it is observed that for certain user positions in BS3 interference from BS5 and BS7 locations are stronger than from interference BS1 position. We are presenting a more rigorous interference study, where a 2-tier interference pattern is obtained for 20 users placed in the sector of interest uniformly.

It is observed that BS1 and BS2 are two most dominant interferers for users in BS3. The interference from BS6 and BS8 are negligible compared to other dominant interferers,

therefore they are omitted in the simulation. Figure A.2.b shows the resulting interferers for users in BS3 and their relative positions. It can be shown that among BS1, BS2 and BS3, two always be the dominant interferers for the third. Therefore, these three BSs form an *interferer group*.

2-tier interference patterns are obtained for two different cases. A total of 19 BSs have been considered where the BS of interest (BS10) is surrounded by other 18 BSs. Twenty users are placed uniformly in the shown sector of BS10.

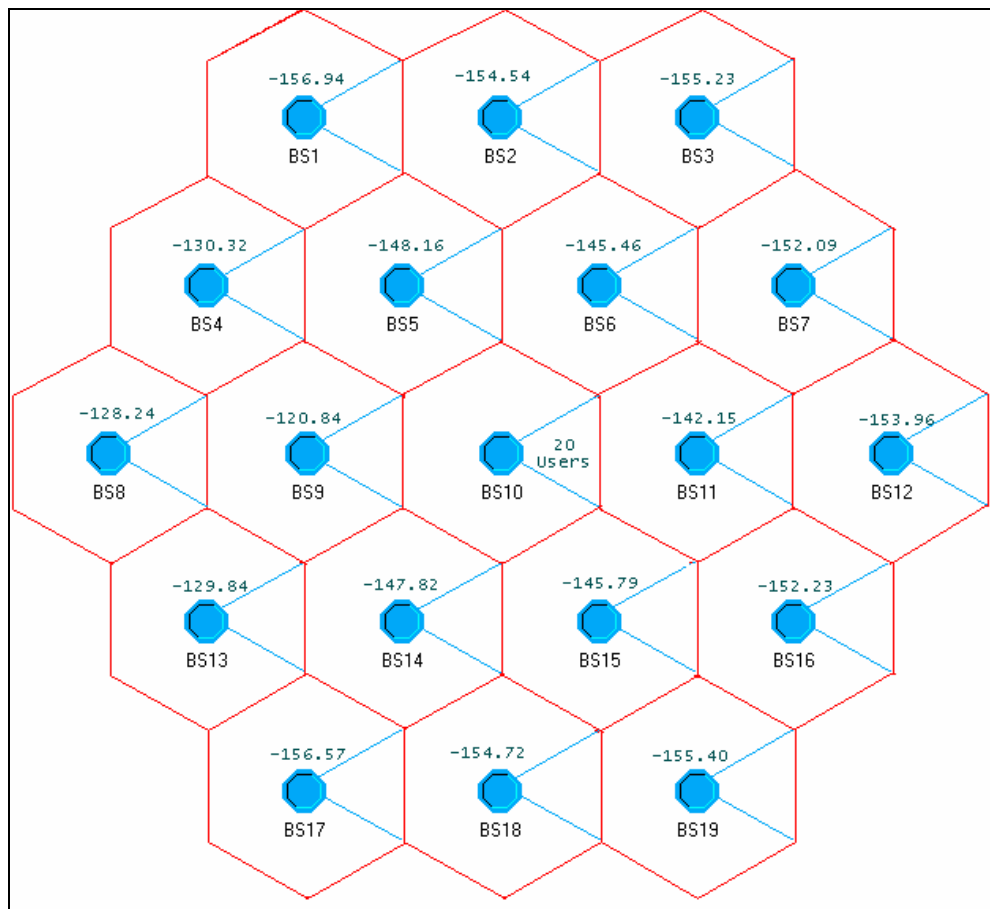


**Figure A.3: 2-Tier interference pattern for users in BS10
(60° beamwidth user antenna)**

User's directional antennas are pointing towards BS10. Sector antenna is 60° directional assumed to be uniform to cover the whole sector. Effective sector antenna gain is 20 dB with 10 dB front lobe and -10 dB back lobe. The user antenna is 60° directional in the first case and 30° directional in the second case with effective antenna gain of 10 dB, 5 dB front lobe and -5 dB back lobe. The transmit power is 2.2 Watts. Independent shadowing of 8 dB standard deviation and correlated fading as illustrated in Chapter 3 are used.

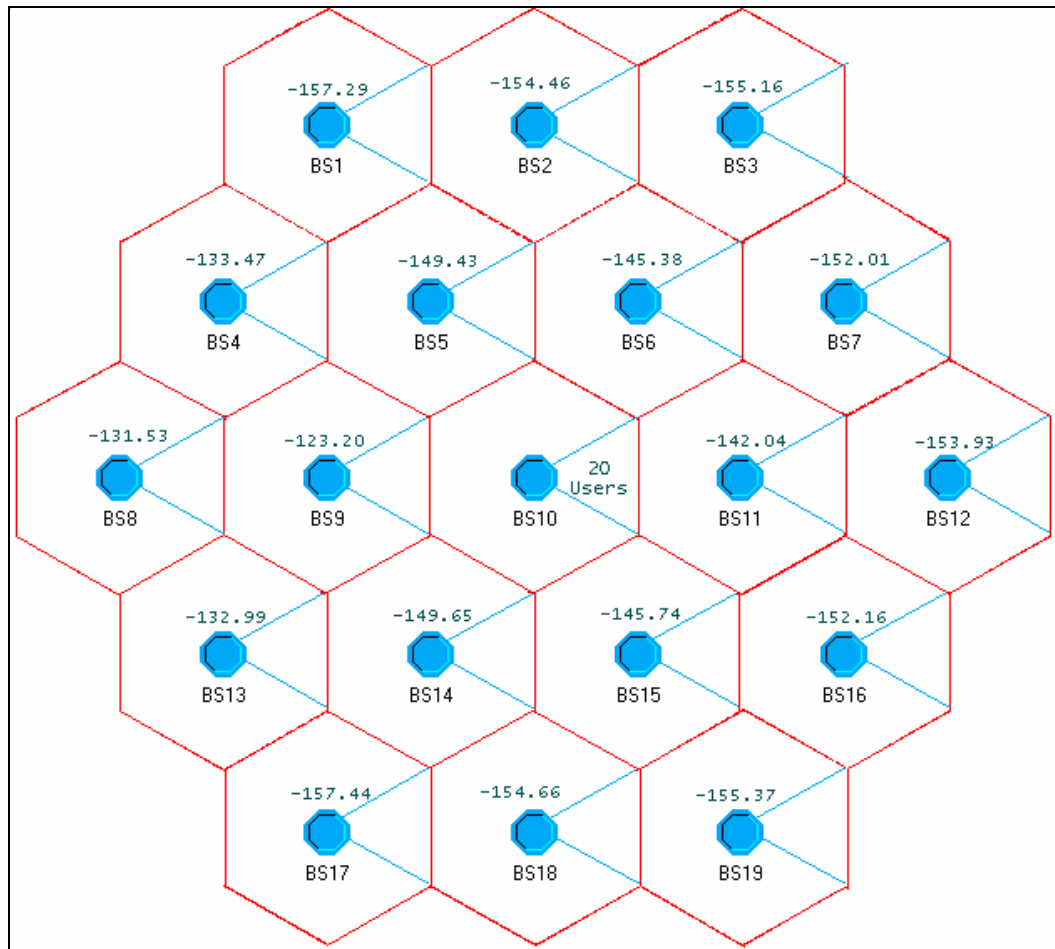


Figure A.4: 2-Tier interference pattern for users in BS10 (30° beamwidth user antenna)

Figure A.3 and A.4 show the interference patterns for 60° and 30° beamwidth user antenna, respectively. The numbers written near BSs correspond to 50th-percentile interference received by all randomly placed 20 users from these BSs. Statistics are collected at every user to obtain averaging over different antenna directivity and distance attenuation. It is seen that the most dominant interferer is BS9, and BS8 is the second strongest. They both reside on the left of BS10. Thus the 2-tier interference pattern cross-validate the method for finding wrap around interference pattern shown in Figure A.2.

Appendix B

Link Budget Calculation

Link budget is calculated for the reference scheme IIS-FM-MT, where 16-QAM rate $\frac{1}{2}$ BICM modulation scheme is used. The calculated power budget will assure a user placed at cell boundary (2.0 km) 95% availability for its packets to be received with this modulation scheme.

Background noise floor for 3.0 MHz channel and 5 dB noise figure, as per (3.12), is

$$P_N = -134.06 \text{ dBW.}$$

Large-scale path-loss for 2.0 km T-R separation is given by (3.6) as follows,

$$PL = 126.49 \text{ dB.}$$

Now for 16-QAM rate $\frac{1}{2}$ scheme, the minimum required SINR to achieve 1.0×10^{-4} bit error rate is (found from Table 3.2),

$$\gamma_{req} = 9.23 \text{ dB.}$$

Therefore, minimum required received power,

$$\begin{aligned} P_{r(min)} &= P_N + \gamma_{req} \\ &= -124.83 \text{ dBW} \end{aligned}$$

With 95% availability, the average received power P_r considering a long-normal shadowing with 8 dB standard deviation can be found by solving the following equation [34],

$$\frac{P_r + 124.83}{8} = Q^{-1}(0.05)$$

which yields,

$$P_r = -111.65 \text{ dBW}$$

Note that the BS antenna gains G_t are 10 dB for the front lobe and -10 dB for the back lobe, and the user antenna gains G_r are 5 dB for the front lobe and -5 dB for the back lobe.

Therefore, required transmission power can be calculated as,

$$P_t = P_r + PL - G_{t_f} - G_{r_f} + \text{Fade Margin}$$

Assuming 3.5 dB *Fade Margin*, the required transmit power would be 3.34 dBW or 2.2 Watts. Fade margin is required as above calculations do not account for fading, while fading is used in simulations.

The above power calculation is verified by placing a user at the cell boundary. Shadowing and fading are used as described in Chapter 3. To achieve averaging for shadowing we assume that the shadowing is changing from packet to packet, although the user is fixed at that particular location. Figure B.1 shows simulated PER, which agrees with the link budget calculations.

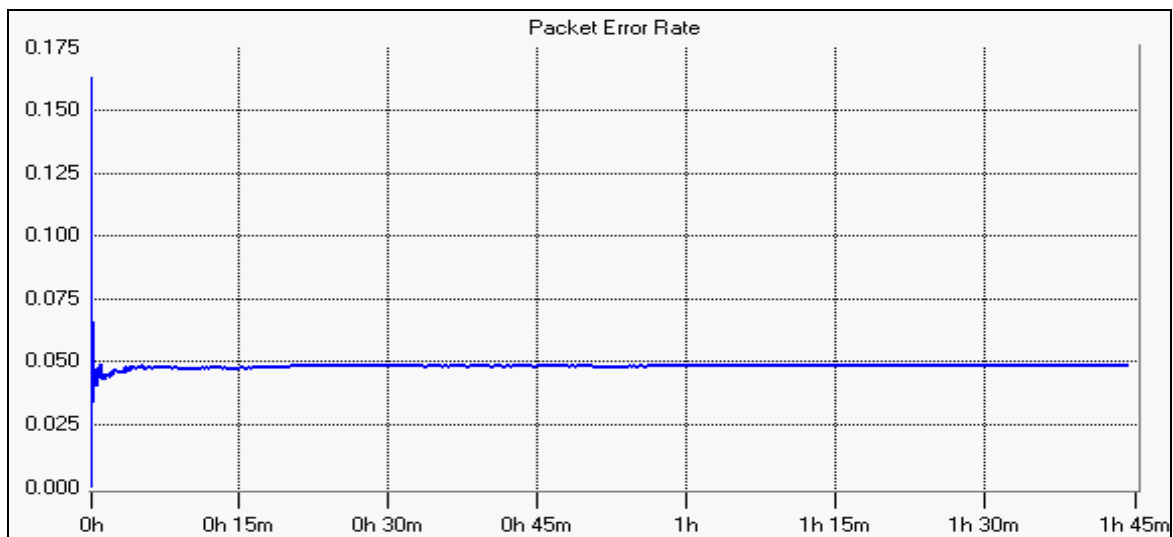


Figure B.1: Packet error rate for a user at cell boundary against simulation time (No interferer is present)

Appendix C

Additional Curves for the System with Propagation Exponent of 3.7

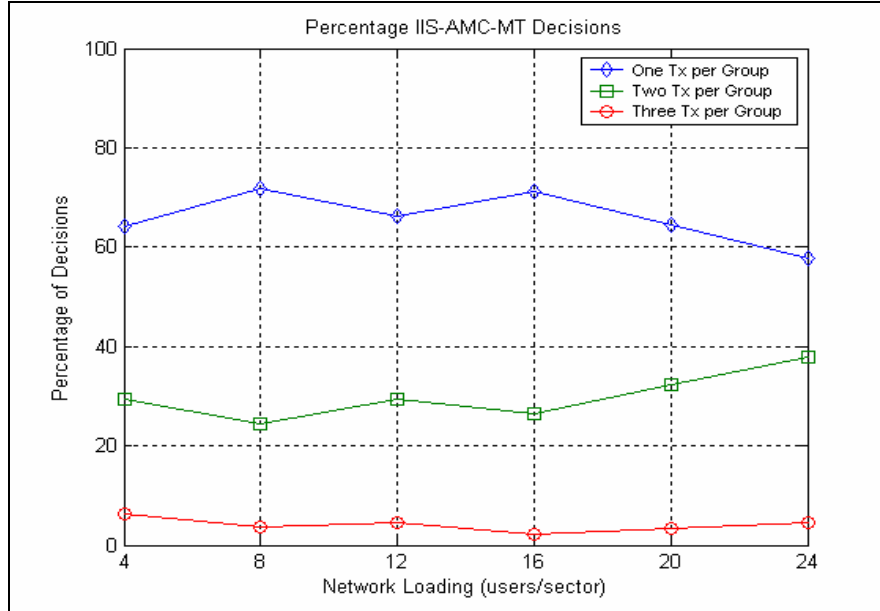


Figure C.1: Percentage of multiple transmissions decisions in IIS-AMC-MT ($n = 3.7$)

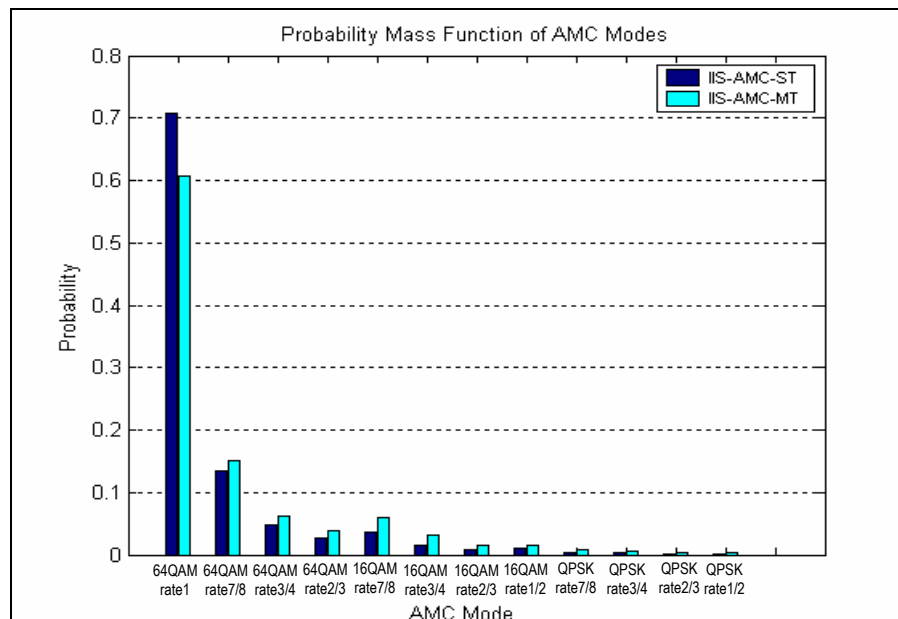


Figure C.2: PMF of AMC modes in IIS-AMC-ST and IIS-AMC-MT (12 users per sector, $n = 3.7$)